

pro:Holz

Information

Cross-Laminated Timber Structural Design Volume 2

proHolz Austria
January 2018

Applications

Cross-laminated timber has conquered new markets since the publication of volume I *Basic design and engineering principles according to Eurocode*. The present volume II describing Applications provides the designer of timber structures on the one hand with basics for design factors, mechanical properties and modelling with finite element method. On the other hand it describes in detail the design of floors, ribbed plates and walls e.g. by design approaches regarding forces in joints of plates and diaphragms, concentrated loads, openings, effective width and compression perpendicular to grain. Current scientific knowledge as well as experience from practical engineers is taken into account. 15 examples demonstrate the design approaches as references for practitioners. Closing background information for the shear correction coefficient, deformations due to concentrated loads and the modelling of cross-laminated timber as general grillage will illuminate the background and facilitate deeper understanding of the design with cross-laminated timber.

Markus Wallner-Novak
Manfred Augustin
Josef Koppelhuber
Kurt Pock

Publication details

Owner and publisher
proHolz Austria

Working group of the Austrian
timber industry for promotion of
the application of timber

Chairman Christoph Kulterer
Managing Director Georg Binder
Project Management
Ulrich Hübner
Am Heumarkt 12
1030 Vienna/Austria
T + 43 (0)1/712 04 74
info@proholz.at, www.proholz.at

Financial support by

Binderholz Bausysteme GmbH
Solvay-Halvic-Straße 46
A-5400 Hallein
T + 43 (0)6245/70 500
bbs@binderholz.com
www.binderholz.com

Mayr-Melnhof Holz Holding AG
Turmgasse 67
A-8700 Leoben
T + 43 (0)3842/300 -0
brettsperrholz@mm-holz.com
www.mm-holz.com

HASSLACHER NORICA TIMBER
Feistriz 1
A-9751 Sachsenburg
T + 43 (0)4769/2249 - 0
info@hasslacher.at
www.hasslacher.at

KLH Massivholz GmbH
Gewerbestraße 4
A-8842 Teufenbach-Katsch
T + 43 (0)3588/8835
office@klh.at
www.klh.at

Stora Enso
Building and Living
Wisperndorf 4
A-9462 Bad St. Leonhard
T + 43 (0)4350/2301 - 3207
buildingsolutions@
storaenso.com
www.clt.info

Fachverband der Holz-
industrie Österreichs
Schwarzenbergplatz 4
A-1037 Wien
T + 43 (0)1/712 26 01
office@holzindustrie.at
www.holzindustrie.at

Design: Cover Atelier Gassner, Schlins (AT)
Reinhard Gassner, Marcel Bachmann

Print: Eberl Print, Immenstadt (DE)

Translation: ALLESPRACHEN.AT-ISO 9001 GmbH

1st edition english 2018, 800 copies
Price per copy 35 Euros, incl. VAT, excl. shipment
ISBN 978-3-902320-96-4
ISSN 1680-4252



Printed on PEFC-certified paper. This product
originates from sustainably managed forests and
controlled sources. www.pefc.at

Copyright 2017 by proHolz Austria and the
authors. The publication and any contributions
and figures contained therein are copyrighted.
Any use beyond the limits of copyright without
the publisher's approval is inadmissible and
punishable. proHolz Austria and the authors
endeavour to research or state, respectively,
information correctly and completely. However,
we ask for your understanding that no liability
can be assumed for the contents.

My first encounter with cross-laminated timber was more than 25 years ago. In the course of our civil engineering studies at Graz University of Technology, we completed an internship with the company Stingl in Trofaiach/AT. In the factory workshop, we saw novel structural elements – panels of crosswise glued lamellas. At that time, these wooden elements did not have an official name in the German-speaking region yet, at first, they were called glued board stack elements.

"I love fools experiments. I am always making them."
Charles Darwin, British natural scientist (1809 – 1882)

An intensive research and development period concerning the load-bearing and deformation behaviour of these structural timber elements started, wherein it should be noted here, that the research achievements in Austria played an essential role for the development of the structural elements – now designated as cross-laminated timber. Based on these experimental analyses, technical approvals, guidelines and standards were compiled, on the basis of which calculation and dimensioning of components made of cross-laminated timber can be undertaken.

"The book of nature is written in the language of mathematics."
Galileo Galilei, Italian philosopher, mathematician, physicist (1564–1642)

In 2013, the team of authors M. Wallner-Novak, J. Koppelhuber and K. Pock compiled the structural design guideline "Cross-Laminated Timber Structural Design – Basic design and engineering principles according to Eurocode" and made it available for practical application. This book is very well received by engineering consultants as well as during training and is appreciated as practice-oriented support. It was translated into English and Italian. The structural design guideline is now being continued with the present second volume: "Cross-Laminated Timber Structural Design – Applications" by the authors M. Wallner-Novak, M. Augustin, J. Koppelhuber and K. Pock. New subject areas and open questions for practical dimensioning are described, basic principles explained, and engineering models for calculation presented. The numerous examples assist the engineer in applying and implementing the calculation models. Following the steps of comprehensive research and development work and composing of the approvals, guidelines and standards, the present book "Cross-Laminated Timber Structural Design – Applications" represents a sensible and necessary contribution to the third step – the practice-oriented application of cross-laminated timber.

I would like to thank the members of the team of authors and the staff at *holz.bau forschung gmbh*. In numerous meetings, we discussed various questions on building with cross-laminated timber at a high scientific and engineering level. In that, we always pursued the objective of getting to the heart of the relations as practical, concise and simple as possible. As representatives of the academic-scientific level, Manfred Augustin and Alexandra Thiel contributed to an enhanced understanding of the load-bearing performance of cross-laminated timber. The numerous structural element tests confirmed the results in an impressive manner. Josef Koppelhuber and Kurt Pock, as experienced timber construction engineers, were able to contribute their knowhow on the engineeringbased approach and the structural implementation and to check and critically assess the newly processed subjects with regard to the appropriateness of their presentation. I would also like to thank Maria Almer for the EDP implementation of the sketches and drawings.

Markus Wallner-Novak

Contents

1 Introduction	7
2 Symbols	8
2.1 Uppercase letters.....	8
2.2 Lowercase letters.....	8
2.3 Greek letters	10
2.4 Legend for the plan view of floors.....	10
3 Basic design principles	11
3.1 Characteristic building material values.....	11
3.1.1 Weight ratios.....	11
3.1.2 System strength	11
3.1.3 Characteristic stiffness and strength values	12
3.1.4 Buckling coefficients	13
3.1.5 Partial safety factor.....	14
3.1.6 Creep coefficient	14
4 Floors	15
4.1 Vibration of CLT floors.....	17
4.2 Openings in floors.....	24
4.3 Vertical forces transverse to the direction of span.....	30
4.3.1 Compatibility forces.....	31
4.3.2 Lateral joint forces	32
4.4 Joint forces from plate effect.....	38
4.4.1 Shearing forces of the joint	40
4.4.2 Normal forces of the joint.....	41
4.4.3 Joints with joint cover strip	47
4.5 Concentrated loads	50
4.5.1 Load distribution.....	50
4.5.2 Load-bearing effect of panels.....	51
4.5.3 Compression perpendicular to grain	59
5 Ribbed plate	69
5.1 Pre-design	69
5.1.1 Recommendations for roofs.....	70
5.1.2 Recommendations for floors.....	71
5.2 Effective widths	72
5.2.1 Bending	73
5.2.2 Shear	74
5.3 Modelling	75
5.3.1 Rib cross-section as shear-flexible beam.....	75
5.3.2 Rib cross-section as flexibly connected beam.....	75
5.4 Screw-press gluing.....	75
5.5 Local loads	77
6 Walls	89
6.1 Buckling of walls.....	89
6.1.1 Cross-laminated timber as shear-flexible buckling beam	89

6.1.2 Influence of openings.....	93
6.2 Application of local loads.....	95
6.2.1 Practical estimate for concentrated loads.....	97
6.2.2 Practical estimate for partial line loads and low wall heights.....	98
6.3 Sill pressing.....	101
7 Finite element modelling.....	103
7.1 Calculation sequence	103
7.2 Finite element models	104
7.2.1 Shell elements for diaphragm and plate effect	104
7.2.2 Internal forces.....	105
7.2.3 Stiffnesses.....	107
7.2.4 Cross-sectional load-bearing capacity	108
7.2.5 Load application problems.....	109
7.2.6 Singularities	109
7.3 CLT as an orthotropic finite element	110
8 Erratum and amendments to Volume 1	131
8.1 Erratum	131
8.1.1 Design value of action (load-bearing capacity)	131
8.1.2 Withdrawal of screws	131
8.1.3 Horizontal acceleration earthquake.....	132
8.1.4 General gamma method according to Schelling	132
8.2 Standard adjustments and new findings	133
8.2.1 Minimum distances of self-tapping woodscrews	133
8.2.2 Verification of vibration	133
8.2.3 Fire dimensioning	133
8.2.4 Lateral pressure	133
8.2.5 Load distribution at the panel strip.....	134
8.2.6 Local load application into walls.....	134
9 In-depth considerations.....	135
9.1 Determination of the shear correction coefficient.....	135
9.2 Deformation with local loads	140
9.2.1 Compression upon general stress distributions	140
9.2.2 Deformation of panel due to load transfer column-panel-column	142
9.2.3 Deformation of panel due to load transfer wall-panel-wall.....	143
9.3 Modelling as general grillage	144
9.3.1 Comparison of differential equations.....	145
9.3.2 Model for the calculation as a grid of members.....	146
9.3.3 Panels supported on three sides.....	147
10 Sources.....	149
10.1 Standards	149
10.2 Literature.....	150

List of examples

Example 4.1	Verification of vibration of an apartment floor.....	15
Example 4.2	Panel with opening.....	20
Example 4.3	Floor span with vertical loads.....	32
Example 4.4	Diaphragm with horizontally and vertically acting loads.....	39
Example 4.5	Screw connection for a joint with recessed top layer.....	44
Example 4.6	Panel strip with point load.....	52
Example 4.7	Load passages of supports.....	62
Example 5.1	Ribbed panel.....	74
Example 6.1	Wall as shear-flexible member.....	87
Example 6.2	Application of local loads into a wall.....	95
Example 6.3	Sill pressing.....	97
Example 7.1	Characteristic values for the FEM calculation.....	106
Example 7.2	Linearly supported roofing slab with bilateral overhang.....	112
Example 7.3	Canopy with point support.....	121
Example 9.1	Tabular calculation of the shear correction coefficient.....	132

1 Introduction

Based on the basic structural design principles of cross-laminated timber elements according to the model of the Eurocodes compiled in Volume 1, in the present volume, important applications are discussed and processed as numerical examples. For that, firstly, frequent questions of the cross-laminated timber industry were addressed.

The objective, on the one hand, is the application of the calculation model for cross-laminated timber for the shear-flexible panel or the shear-flexible beam according to Timoshenko, resp. The simpler, from an engineering point of view, and in Volume 1 predominantly applied extended gamma method according to Schelling is well suited for uniaxially acting systems, for use as a spatial load-bearing structure or for a slenderness, deviating from the standard, however, the model of the shear-flexible beam, generally explained in the annex of Volume 1, is to be preferred.

For the elaboration of the examples it was necessary, on the one hand, to process the basic structural mechanics principles and, on the other hand, to consider the comprehensive research results of *holz.bau forschung gmbh*, Graz, in the basic principles for cross-laminated timber.

In order to be able to use the high potential of cross-laminated timber as a load-bearing plain, in some cases, the mathematically complex relations shall be processed such that they are easy to apply by an engineer.

*'Designing' means deciding*¹. For structural design, this means that the criteria for decision-making by the architect or engineer are not to be impeded by unnecessarily complicating things, but rather to be simplified by simple basic principles. The authors pursued this objective in extensive discussions, hoping to suitably present the complex material behaviour for everyday engineering work. In that, the requirements to technical correctness of the models, appropriateness of the means and plausibility of structural element verifications shall be unified.

¹ Lecture at ETH Zurich in Polónyi, 1987

2 Symbols

2.1 Uppercase letters

A_{90}	Pressing area
D	Lehr's damping factor
$D_{xy} = GI_T = K_{xy}$	Torsional stiffness
$E_{0,mean}$	Mean modulus of elasticity in the direction of the top layer
$E_{0.05}$	5 th percentile of the modulus of elasticity in the direction of the top layer for stability analyses
$E_{90,mean}$	Mean modulus of elasticity in the thickness direction
$G_{0,mean}$	Mean shear modulus for shear stress in the longitudinal and radial direction with regard to the position of the annual rings
$G_{0.05}$	5 th percentile of the shear modulus
$G_{r,mean}$	Mean rolling shear modulus for shear stress in the tangential direction with regard to the position of the annual rings
$K_y = EI_{90}$	Bending stiffness for bending about one axis in parallel to the top layer
$K_x = EI_0$	Bending stiffness for bending about one axis transverse to the top layer
K_{xy}	Torsional stiffness
M^*	Modal (actively vibrating) mass
M_d	Design value of the bending moment
$S_{xy}^* = GA_{S,xy}$	Shear stiffness as a plate

2.2 Lowercase letters








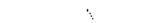
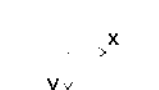



a	Mean board width
$a_{90,d}$	Design value of a compatibility force
a_{rms}	Assessed acceleration value for verification of vibration
$b_{90,ef}$	Effective width for compression perpendicular
$b_{ef}, b_{M,ef}, b_{V,ef}$	effective width
e_x	Distance of the fasteners along the joint
f_1	First natural frequency

$f_{m,k}$	Characteristic bending strength
$f_{t,0,k}$	Characteristic tension strength parallel to the grain of a lamination
$f_{c,0,k}$	Characteristic compression strength along the grain
$f_{c,90,k}$	Characteristic value of compression strength perpendicular to grain
$f_{v,k}$	Characteristic shear strength
$f_{v,T,k}$	Characteristic torsional shear strength
$f_{v,S,k}$	Characteristic shear strength of the plate – Mechanism 1: shear strength of the individual boards
$f_{v,T,k}$	Characteristic shear strength of the plate – Mechanism 2: Torsional shear strength of the glued joints
$f_{v,k}$	Characteristic value of shear strength of the plate – Mechanism 3: Shear strength gross cross-section
k_S	Factor for shear stiffness
ℓ_x	Span in the main load-bearing direction
$n_{xy,d}$	Shear force of the joint, shear force of the plate (design value)
$n_{y,d}$	Design value of the axial force of the joint
$v_{y,d}$	Design value of the lateral force of the joint
n_d	Design value of live loads
k_c	Buckling coefficient
$k_{c,90}$	Lateral pressure coefficient for consideration of the type of action, the risk of splintering and the degree of deformation under pressure
k_{cs}	Factor for consideration of the shear flexibility in case of buckling
k_{def}	deformation modification factor for service classes
k_{mod}	strength modification factor for service classes and load-duration classes
k_{ortho}	Orthotropy factor
k_{sys}	Coefficient for system strength for consideration of the parallel load distribution on laminations with an assumed reference width of 150 mm
$n_{xy,d}$	Design value of shear force of the joint
$n_{y,d}$	Design value of axial force of the joint
$v_{y,d}$	Design value of lateral force of the joint
w_{stat}	Static deflection for verification of the stiffness criterion upon vibration of CLT floors
x_D	Length of the pressure zone

2.2.1 Greek letters

α	Load propagation angle, Factor for consideration of the frequency action by walking
β_c	Straightness factor
γ_k	Characteristic weight per unit of volume (density)
γ_M	Partial safety factor for building material properties
ν or κ	Shear correction factor
λ	Slenderness
ρ_k	Characteristic density
ρ_{mean}	Mean density

2.3 Legend for the plan view of floors

	Edge of a ceiling span
	Edge with vertical support
	Edge with horizontal support
	Edge with vertical and horizontal support
	Restrained edge
	Joint (articulated)
	Main direction of load-bearing capacity (x, 0°)
	Ancillary direction of load-bearing capacity (y, 90°)
	Local coordinate system x-axis in parallel to the top layer (main direction of load-bearing capacity)
	Opening
	Point support
	Point load

3 Basic design principles

3.1 Characteristic building material values

The characteristic values system of Volume 1 was adjusted according to ÖNORM B 1995-1-1:2015. Therefore, this volume is based on the characteristic values for CLT according to these determinations stated in this chapter. Laminations of strength class T14 or C24 are assumed as initial material.

All calculation models established in the present volume apply independently of the material system. Therefore, adjustments of the characteristic values to manufacturer-specific approvals or new determinations in the standards are possible anytime.

At the European level, the working group 'CEN TC250 SC5 WG1' is working on the inclusion of cross-laminated timber into Eurocode 5 (EN 1995-1-1). Here, the development points in the direction of a higher evaluation of the rolling shear properties of the transverse layers, with respect to their strength as well as their stiffness. From today's perspective, standard adjustments of further characteristic values or verification models are not foreseeable in detail. Generally speaking, a slight increase of individual strength values shall be assumed.

3.1.1 Weight ratios

Table 3-1 General characteristic building material values

Density (for load assumptions acc. to EN 1991-1-1)	γ_k	5.50	kN/m ³
Characteristic minimum density	ρ_k	385	kg/m ³
Mean density	ρ_{mean}	420	kg/m ³

3.1.2 System strength

The characteristic strength values of cross-laminated timber may be calculated increased by the coefficient for system strength k_{sys} , when, upon stressing, several laminations are equally stressed in parallel. This applies to all bending, tensile and compressive stresses in the direction of the board of CLT panels. The reason for that is a statistic effect, since defects can be compensated over several parallel structural elements. If CLT elements are stressed by upright bending, as is the case with a lintel, then only few longitudinal layers act in parallel and the system coefficient k_{sys} shall not be applied.

Common – and frequently anchored in technical approvals – is the determination of a constant coefficient: $k_{sys} = 1.1$.

In ÖNORM B 1995-1-1:2015, the general determination for the system strength from Eurocode 5 is also taken over for cross-laminated timber. As the standard width for a board, $b = 15$ cm is determined, and the system strength coefficient is upwardly limited with $k_{sys} \leq 1.2$. For narrow structural elements made of cross-laminated timber with a width of less than 30 cm, according to this standard determination, the system strength

coefficient is to be reduced to $k_{sys} = 0.9$, since the characteristic strength values were determined with wider specimens.

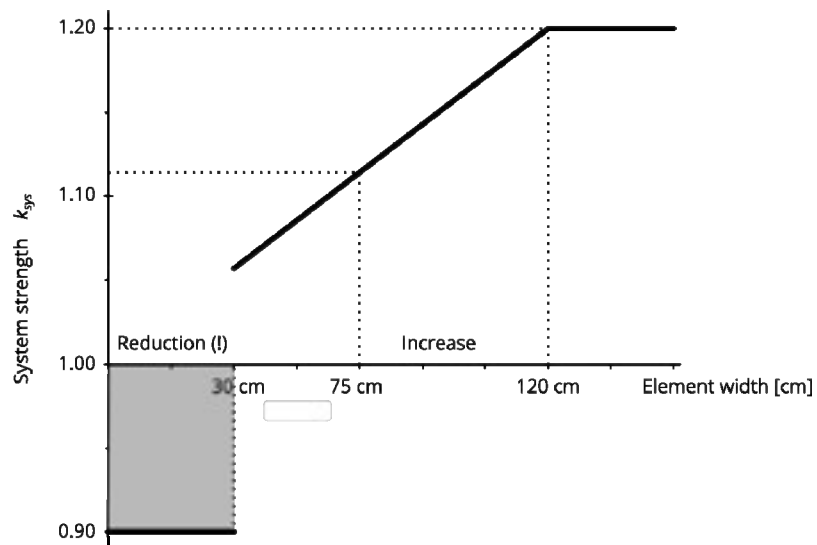


Figure 3.1 Suggestion for the system strength of CLT according to ÖNORM

Figure 3.1 shows the determinations according to ÖNORM B 1995-1-1:2015 described in the form of a diagram. It shows that for standard elements with more than 75 cm in width, the coefficient $k_{sys} = 1.1$ is on the safe side.

$$k_{sys} = 1.1 \tag{3.1}$$

For constructional reasons, wall columns should not be executed narrower than 30 cm.

For structural elements narrower than 60 cm – as for example wall columns – it is recommended to assume $k_{sys} = 1.0$ and not to execute these, for constructional reasons, narrower than 30 cm.

For verifications on the basis of calculations with the finite element method, $k_{sys} = 1.0$ is to be applied, if the distribution of the stresses onto parallel layers is not analysed in greater detail.

3.1.3 Characteristic stiffness and strength values

Table 3-2 Characteristic stiffness values for cross-laminated timber

Modulus of elasticity (normal stresses)	$E_{0,mean}$	11 550	N/mm ²
	$E_{0.05}$	9 625	N/mm ²
Modulus of elasticity (in direction of thickness)	$E_{90,mean}$	450	N/mm ²
Shear modulus	$G_{0,mean}$	690	N/mm ²
	$G_{0.05}$	570	N/mm ²
Rolling shear modulus	$G_{r,mean}$	65	N/mm ²

Table 3-3 Characteristic strength values for cross-laminated timber

Bending strength (panel)	$f_{m,k}$	24.00	N/mm ²
Tensile strength	$f_{t,0,k}$	14.00	N/mm ²
Compressive strength parallel to grain	$f_{c,0,k}$	21.00	N/mm ²
compressive strength perpendicular to grain	$f_{c,90,k}$	3.00	N/mm ²
Shear strength	$f_{v,k}$	2.50	N/mm ²
Rolling shear strength	$f_{v,R,k}$	1.10	N/mm ²
Shear strength torsion	$f_{v,T,k}$	2.50	N/mm ²
Strength for shearing off of the individual boards (plate – mechanism 1)	$f_{v,S,k}$	5.00 ¹	N/mm ²
Torsional strength of the glued joints (plate – mechanism 2)	$f_{v,T,k}$	2.50	N/mm ²
Shear strength gross cross-section (plate – mechanism 3)	$f_{v,k}$	2.50	N/mm ²

3.1.4 Buckling coefficients

Deviating from the suggestion in ÖNORM B 1995-1-1:2015, Annex K, K.6.3, the following determinations are made: the coefficient of imperfection for cross-laminated timber – due to the production conditions comparable to glued-laminated timber – is assumed as $\beta_c = 0.1$. For that, the buckling analysis is undertaken considering the shear flexibility. This results in verifications at an approximately equal safety level. This determination of the coefficient of imperfection was confirmed by measurements in Augustin et al., 4/2017.

¹ The thickness of individual layers or the sum of directly adjacent layers parallel in fibre must not exceed 40 mm. If this thickness is exceeded, then $f_{v,S,k} = 3.5 \text{ N/mm}^2$ must be assumed.

Table 3-4 Buckling coefficients k_c for cross-laminated timber

Slenderness λ		Unit									
		0	1	2	3	4	5	6	7	8	9
Hundreds and tens	10	1.000	1.000	1.000	1.000	1.000	1.000	1.000	1.000	1.000	1.000
	20	1.000	0.999	0.997	0.995	0.994	0.992	0.990	0.988	0.986	0.984
	30	0.982	0.980	0.978	0.976	0.973	0.971	0.968	0.966	0.963	0.960
	40	0.957	0.954	0.951	0.947	0.944	0.940	0.936	0.932	0.927	0.922
	50	0.917	0.912	0.906	0.900	0.894	0.887	0.880	0.872	0.864	0.855
	60	0.846	0.837	0.827	0.816	0.806	0.794	0.783	0.771	0.759	0.747
	70	0.734	0.721	0.709	0.696	0.683	0.670	0.658	0.645	0.633	0.621
	80	0.609	0.597	0.585	0.574	0.563	0.552	0.541	0.530	0.520	0.510
	90	0.500	0.491	0.481	0.472	0.463	0.455	0.446	0.438	0.430	0.422
	100	0.414	0.407	0.399	0.392	0.385	0.379	0.372	0.366	0.359	0.353
	110	0.347	0.341	0.336	0.330	0.325	0.319	0.314	0.309	0.304	0.299
	120	0.295	0.290	0.285	0.281	0.277	0.272	0.268	0.264	0.260	0.257
	130	0.253	0.249	0.245	0.242	0.238	0.235	0.232	0.228	0.225	0.222
	140	0.219	0.216	0.213	0.210	0.208	0.205	0.202	0.199	0.197	0.194
	150	0.192	0.189	0.187	0.185	0.182	0.180	0.178	0.175	0.173	0.171
	160	0.169	0.167	0.165	0.163	0.161	0.159	0.157	0.156	0.154	0.152
	170	0.150	0.149	0.147	0.145	0.144	0.142	0.140	0.139	0.137	0.136
	180	0.134	0.133	0.132	0.130	0.129	0.127	0.126	0.125	0.123	0.122

Based on the characteristic building material values:

$$E_{0,mean} = 11\,550 \text{ N/mm}^2; E_{0.05} = 9\,620 \text{ N/mm}^2; f_{c,0,k} = 21 \text{ N/mm}^2; \beta_c = 0.1$$

3.1.5 Partial safety factor

$\gamma_M = 1.25$ according to ÖNORM B 1995-1-1:2015

3.1.6 Creep coefficient

The deformation coefficient k_{def} for calculation of the creep deformations of cross-laminated timber is determined – as already in Volume 1 – with the following values:

Utilisation class (NKL)	1	2
Deformation coefficient	$k_{def} = 0.8$	$k_{def} = 1.0$

Consequently, the creep deformation results from the quasi-permanent portions (qp) of the initial deformation ($inst$) to

$$w_{creep} = k_{def} \cdot w_{inst,qp} \tag{3.2}$$

4 Floors

Cross-laminated timber as a large-format and panel-shaped timber-based material is well suited as a floor element. The crosswise layup and the large format enable using the load-bearing effect of panels in the main direction of load-bearing capacity as well as in the ancillary direction of load-bearing capacity. While in the main direction of load-bearing capacity, loads are distributed between the support axes, smaller spans in the ancillary direction of span can be spanned without additional structural elements. Likewise, openings floor do not need additional reinforcing elements and local loads distributed to a larger effective panel width.

The interlocked layup of the floor elements results in a very favourable swelling and shrinking behaviour without significant deformations in plane.

Due to the mostly very pronounced main direction of load-bearing capacity of the panels, the preferred model for the static analysis of floors is the uniaxially stressed beam of imaginary "one-metre strips" of the panel, as described in Volume 1 and shown in Figure 4.1 a). The load-bearing capacity in the ancillary direction of load-bearing capacity is completely neglected in this simple structural model.

For the calculation of deflections of CLT floors, the shear deformation shall be considered in addition to the bending deformation. As suitable methods for beams, the gamma method is applied in Volume 1 and the shear-flexible beam according to Timoshenko is presented. While the simple, from an engineering point of view, gamma method considers the shear portions by increasing the bending deformation, in the shear-flexible beam according to Timoshenko, these are considered via the shear stiffness of the cross-section and the shear deformation portions resulting therefrom.

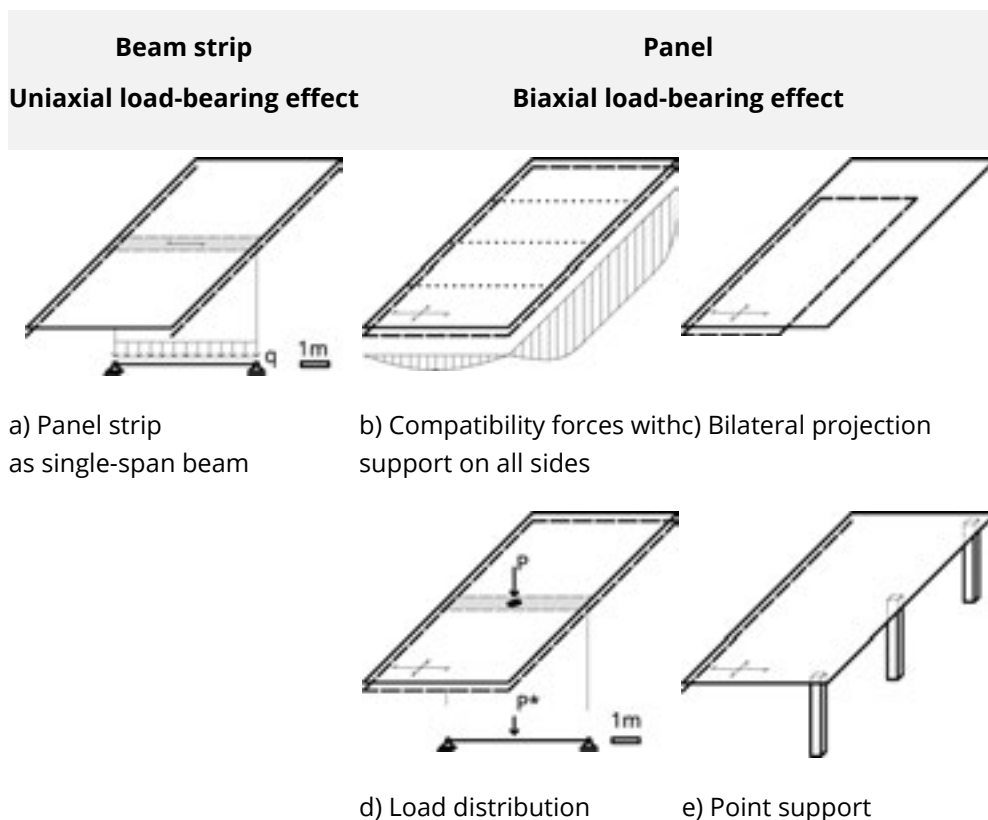


Figure 4.1 Load-bearing effect of floors

The present chapter describes cases, which cannot be solved by the one-dimensional examination of the one-metre strip alone and require examinations on the biaxial load distribution.

First, the current state of the verification of vibration of floors is summarised, in which the biaxial load-distributing effect is considered. Then, vertical forces occurring transverse to the direction of span are being dealt with. These are, on the one hand, reaction forces on lateral supporting walls and, on the other hand, lateral joint forces (Figure 4.1 b). In most cases CLT floor members act as a diaphragm and additional forces in plane shall be considered for the design of joints. Their determination is discussed in the subsequent section and the load-bearing capacity of the two most frequent joint designs analysed on the basis of examples.

Concludingly, the load-bearing performance with concentrated loads is examined, as can be seen in Figure 4.1 d).

Applications exceeding the cases presented in this chapter can be examined with models of finite elements and EDP-based calculations, as presented in Chapter 1 (Figure 4.1 c and e).

4.1 Vibration of CLT floors

The verification of the deflection and vibration is foreseen in the course of examinations in the serviceability limit state design, for apartment floors and similarly utilised floors, in EN 1995-1-1:2015. The basic principles on that were described in Chapter 6.3 of Volume 1. Originally, the verification procedure aimed at exceeding a minimum natural frequency of 8 Hz. Every day use in residential buildings lead to excitation frequencies in the range of about 4 Hz and resonance should be avoided. Further criteria for the perception of floor vibrations are the quantity of deformation – the stiffness of the floor is used as a measure for that – and the acceleration caused by the vibration. On the basis of the publications of Hamm and Richter as well as further measurements, associated verification criteria and limits were compiled in ÖNORM B 1995-1-1:2015. In the following, these newer limit values are stated for the various floor classes (DKL - *Deckenklassen*).



Figure 4.2 Vibration of a floor panel

$$f_1 \geq \begin{cases} 8 \text{ Hz} & \text{for DKL1} \\ 6 \text{ Hz} & \text{for DKL2} \\ - & \text{for DKL3} \end{cases} \quad (4.1)$$

For verifications of vibration, the stiffness of the screed in both directions of load-bearing capacity may be considered in addition to the bending stiffness of the CLT panels, when it is ensured that the relevant standard provisions were complied with.

The influence of joists or other structural components susceptible to vibration was described in Volume 1 in Section 6.3.2.

The limits of the stiffness criterion, i.e. the admissible deflections due to a point load of 1 kN at the most unfavourable location, were regulated more strictly according to Formula (4.2), compared to the limit values in Volume 1.

$$w_{stat} \leq \begin{cases} 0.25 \text{ mm} & \text{for DKL1} \\ 0.50 \text{ mm} & \text{for DKL2} \\ - & \text{for DKL3} \end{cases} \quad (4.2)$$

The acceleration criterion was adjusted with respect to the effective force.

$$a_{rms} = \frac{0.4 \cdot \alpha \cdot F_0}{2 \cdot D \cdot M^*} \leq a_{limit} \quad (4.3)$$

In that, the term $0.4 \cdot \alpha \cdot F_0$ in the numerator represents the force effective for vibration. The factor 0.4 originates from the fact that the action upon walking is variable in position as well as limited in its duration.

The factor α considers the dependence of the force emitted upon walking from the step frequency. In the literature, this dependence from the frequency is defined as constant

in certain areas, while in ÖNORM B 1995-1-1:2015 it was considered via a formula. F_0 is the weight force of a person: $F_0 = 700 \text{ N}$.

$$\alpha = e^{-0.4f_1} \tag{4.4}$$

The modal degree of damping, which is also designated as Lehr’s damping factor, is in ÖNORM B 1995-1-1:2015 designated with ζ instead of here with D .

Compared to the statement in Volume 1, the maximum damping factor of cross-laminated timber floors was increased to 0.04, as stated in Table 4-1.

The modal damping factor of cross-laminated timber floors is 0.04.

Table 4-1 Benchmarks for the modal degree of damping according to ÖNORM B 1995-1-1:2015, NA.7.2-E5

Type of floor structure	Modal degree of damping D
Floor structures without or with, resp., light floor structure	0.01
Floor structures with floating screed	0.02
Cross-laminated timber floors without or with, resp., light floor structure	0.025
Timber beam floors and mechanically connected board stack floors with floating screed	0.03
Cross-laminated timber floors with floating screed and heavy floor structure	0.04

The limit accelerations for floors, in which the demanded limit frequency is undercut, remain unchanged and, upon compliance with the demanded minimum frequency of $f_{1,min} = 4.5 \text{ Hz}$, are

$$a_{rms} \leq \begin{cases} 0.05 \text{ m/s}^2 & \text{for DKL1} \\ 0.10 \text{ m/s}^2 & \text{for DKL2} \\ - & \text{for DKL3} \end{cases} \tag{4.5}$$

Example 4.1 Verification of vibration of an apartment floor

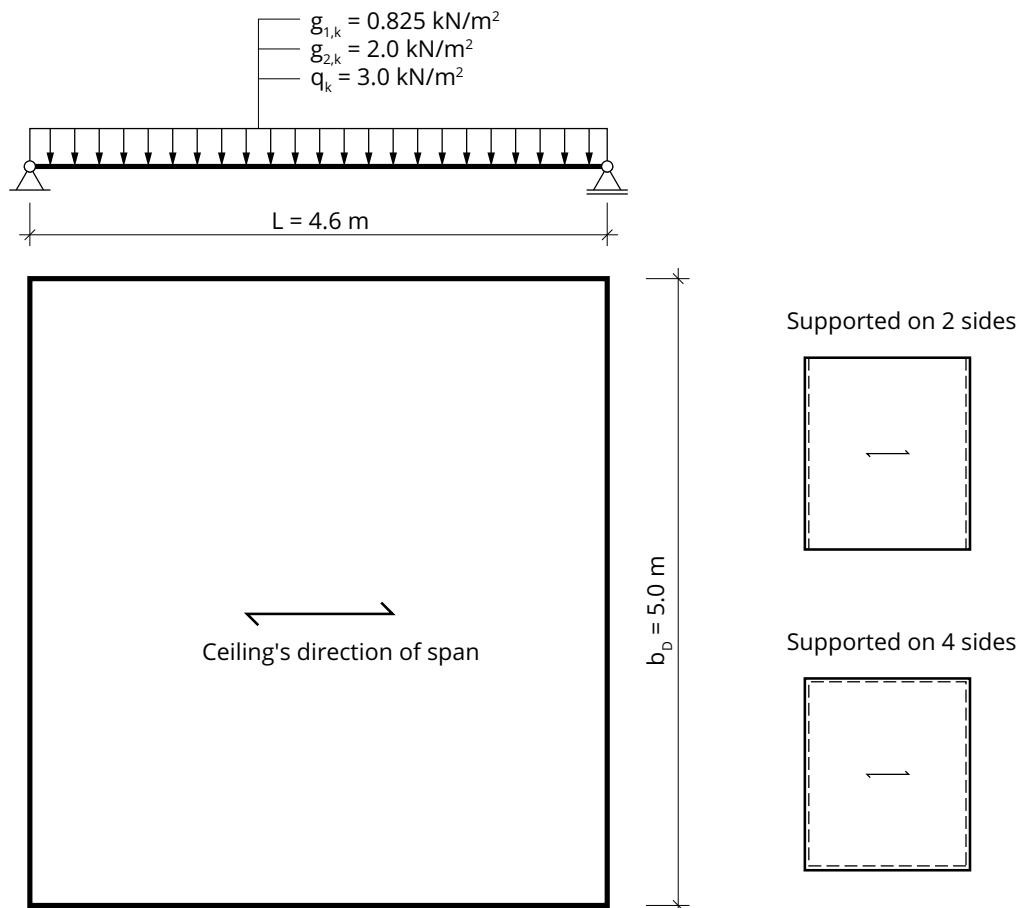
Apartment floor across one span with heavy floor structure.

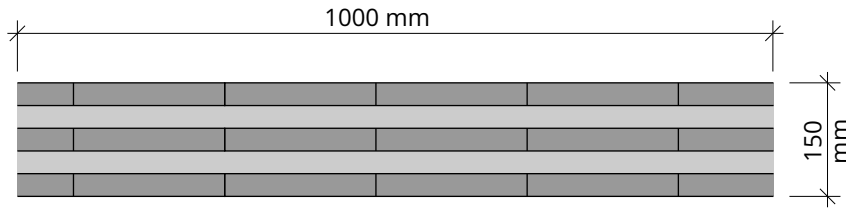
The span of the apartment floor is $L = 4.6$ m. The floor element is a CLT 150-L5s (30l-30w-30l-30w-30l). The characteristic building material values correspond to the determinations in Chapter 1. The width of the floor span is $b_D = 5.0$ m.

The verification of vibration for the apartment floor shall be undertaken according to ÖNORM B 1995-1-1:2015. In that, the two variants of bilateral support and support on all sides are analysed.

Actions

- Dead weight of the CLT panel: $g_{1,k} = 0.15 \cdot 5.5 = 0.825$ kN/m²
- Permanent loads - floor structure: $g_{2,k} = 2.0$ kN/m²
- Live load of category B: $q_k = 3.0$ kN/m²





Assumptions for vibration calculation

- Vibration requirement: Floor class I
- Damping factor: $D = \zeta = 4.0\%$ according to Table 4-1
- Concrete screed ($E = 25,000 \text{ N/mm}^2$); thickness: 50 mm

Bending stiffness of the CLT panel in the floor's direction of span

$$EI_{CLT,0} = 11,550 \cdot 10^6 \cdot \left(3 \cdot \frac{1.0 \cdot 0.03^3}{12} + 0.03 \cdot 1.0 \cdot 0.06^2 + 0.03 \cdot 1.0 \cdot (-0.06)^2 \right)$$

$$EI_{CLT,0} = 2.57 \cdot 10^6 \text{ Nm}^2/\text{m}$$

Bending stiffness of the CLT panel at right angles to the floor's direction of span

$$EI_{CLT,90} = 11,550 \cdot 10^6 \cdot \left(2 \cdot \frac{1.0 \cdot 0.03^3}{12} + 0.03 \cdot 1.0 \cdot 0.03^2 + 0.03 \cdot 1.0 \cdot (-0.03)^2 \right)$$

$$EI_{CLT,90} = 6.76 \cdot 10^5 \text{ Nm}^2/\text{m}$$

Extract from ÖNORM B 1995-1-1:2015:

The bending stiffness of screeds may, generally without statement of the compound effect, be considered in the calculation, when these correspond to the applicable standards with respect to properties and requirements as well as the manufacture of screeds (according to ÖNORM EN 13813 and ÖNORM B 2232).

Overall bending stiffness in the floor's direction of span

$$(EI)_\ell = EI_{CLT,0} + EI_{Screed} = 2.57 \cdot 10^6 + 25,000 \cdot 10^6 \cdot \frac{1.0 \cdot 0.05^3}{12} = 2.57 \cdot 10^6 + 2.60 \cdot 10^5$$

$$(EI)_\ell = 2.83 \cdot 10^6 \text{ Nm}^2/\text{m}$$

Overall bending stiffness transverse to the floor's direction of span

$$(EI)_b = EI_{CLT,90} + EI_{Screed} = 6.76 \cdot 10^5 + 25,000 \cdot 10^6 \cdot \frac{1.0 \cdot 0.05^3}{12} = 6.76 \cdot 10^5 + 2.60 \cdot 10^5$$

$$(EI)_b = 9.36 \cdot 10^5 \text{ Nm}^2/\text{m}$$

Verification

Frequency criterion

Natural frequency upon support on 2 sides (without transverse distribution effect)

$$f_1 = \frac{\pi}{2 \cdot l^2} \cdot \sqrt{\frac{(EI)_l}{m}} = \frac{\pi}{2 \cdot 4.6^2} \cdot \sqrt{\frac{2.83 \cdot 10^6}{825 + 2000}} = 7.36 \text{ Hz}$$

$$f_1 = 7.36 \text{ Hz} < f_{gr,l} = 8.00 \text{ Hz}$$

The demanded limit frequency for DKL1 is not being complied with. Consequently, in addition to the verification of deflection as a consequence of a point load at the most unfavourable position, the verification of acceleration is required. Prerequisite for the acceleration criterion is compliance with a minimum frequency of $f_{1,min} \geq 4.5 \text{ Hz}$.

Natural frequency upon support on 4 sides (with transverse distribution effect)

$$f_1 = \frac{\pi}{2 \cdot l^2} \cdot \sqrt{\frac{(EI)_l}{m}} \cdot \sqrt{1 + \left(\frac{l}{b}\right)^4 \cdot \frac{(EI)_b}{(EI)_l}}$$

$$f_1 = \frac{\pi}{2 \cdot 4.6^2} \cdot \sqrt{\frac{2.83 \cdot 10^6}{825 + 2000}} \cdot \sqrt{1 + \left(\frac{4.6}{5.0}\right)^4 \cdot \frac{9.36 \cdot 10^5}{2.83 \cdot 10^6}} = 7.36 \cdot 1.11$$

$$f_1 = 8.19 \text{ Hz} \geq f_{gr,l} = 8.00 \text{ Hz}$$

The demanded limit frequency for DKL1 is being complied with. But additionally, the stiffness criterion (deflection as a consequence of a point load) has to be fulfilled.

Stiffness criterion

Effective width b_F

Due to the load-distributing effect of cross-laminated timber floorfloors, the actions of concentrated loads may be applied to larger widths. The origin of this effective load distribution width is described in Section 4.5.2 and is accordingly applied for the deflection calculation as a consequence of a unit load.

The load distribution width b_F applies to the internal area of simply supported floor spans and is to be considered conservative for floor spans supported on four sides. For floors with free and non-reinforced edges, the effective load distribution width should be reduced according to the statements on free edges in Section 4.5.2.

In the present example, the vibration within the floor span is analysed and the free edge is not being considered. Then, the effective load distribution width for both support cases is:

$$b_F = \frac{l}{1.1} \cdot \sqrt[4]{\frac{(EI)_b}{(EI)_l}} = \frac{4.6}{1.1} \cdot \sqrt[4]{\frac{9.36 \cdot 10^5}{2.83 \cdot 10^6}} = 3.17 \text{ m}$$

Deflection as a consequence of a vertically acting static point load $F = 1 \text{ kN}$

$$w(1\text{kN}) = \frac{F \cdot \ell^3}{48 \cdot (EI)_I \cdot b_F} = \frac{1.0 \cdot 10^3 \cdot 4.6^3}{48 \cdot 2.83 \cdot 10^6 \cdot 3.17} = 2.26 \cdot 10^{-4} \text{ m} = 0.23 \text{ mm} < w_{gr,I} = 0.25 \text{ mm}$$

The stiffness criterion for DKL1 is being complied with.

Acceleration criterion

If the frequency criterion cannot be fulfilled, then a floor is present, the natural frequency of which is closer to the excitation frequency. In these cases, for the verification of vibration, the verification of acceleration shall be additionally fulfilled, as long as the minimum frequency is being complied with.

Minimum frequency

$$f_1 = 7.36 \text{ Hz} \geq f_{min} = 4.5 \text{ Hz}$$

The minimum frequency is being complied with.

Modal mass

$$M^* = m \cdot \frac{l}{2} \cdot b_F = \frac{(825 + 2000)}{9.81} \cdot \frac{4.6}{2} \cdot 3.17 = 2100 \text{ kg}$$

Vibration acceleration for the bilaterally supported case

Fourier coefficient

$$\alpha = e^{-0.4 \cdot f_1} = e^{-0.4 \cdot 7.36} = 0.053$$

Effective value of acceleration

$$a_{rms} = \frac{0.4 \cdot \alpha \cdot F_0}{2 \cdot D \cdot M^*} = \frac{0.4 \cdot 0.053 \cdot 700}{2 \cdot 0.04 \cdot 2100} = 0.09 \text{ m/s}^2 > a_{gr,I} = 0.05 \text{ m/s}^2$$

The acceleration criterion for the bilaterally supported floor is not fulfilled.

Summary of results

Bilateral support

Frequency criterion	$f_1 = 7.36 \text{ Hz} < f_{gr,I} = 8.00 \text{ Hz}$	X
Stiffness criterion	$w(1\text{kN}) = 0.23 \text{ mm} < w_{gr,I} = 0.25 \text{ mm}$	✓
Acceleration criterion	$f_1 = 7.36 \text{ Hz} > f_{min} = 4.5 \text{ Hz}$	✓
	$a_{rms} = 0.09 \text{ m/s}^2 > a_{gr,I} = 0.05 \text{ m/s}^2$	X
Verification not fulfilled X		

Upon bilateral support, especially the frequency criterion cannot be fulfilled. Since the limit acceleration in the acceleration criterion cannot be complied with, the verification of vibration as a whole is not fulfilled.

Support on all sides

Frequency criterion	$f_1 = 8.19 \text{ Hz} > f_{gr,I} = 8.00 \text{ Hz}$	✓
Stiffness criterion	$w(1\text{kN}) = 0.23 \text{ mm} < w_{gr,I} = 0.25 \text{ mm}$	✓
Acceleration criterion	Not required, since frequency criterion fulfilled.	
Verification fulfilled ✓		

With the transverse load-bearing effect upon support on all sides, the frequency criterion as well as the stiffness criterion can be complied with. Thus, the verification of vibration is fulfilled.

4.2 Openings in floors

Openings with their largest dimension below ten percent of the span are considered small openings and normally can be executed without verification.

Systems with larger openings should be analysed using a general grillage model or a suitable finite element model. In practical analyses of a number of floors with an opening inside the floor elements – i.e. without cut edges – a simple grillage of individual substitute beams along the edges of the rectangular opening proved to be expedient.

In that, the grillage of transverse and longitudinal beams is selected from cross-sections with a strip width of $b_x = b_y = \ell_x/10$. The residual cross-sections of the panel remaining beside the opening should, according to this assumption, provide at least ten percent of the span.

Example 4.2 Panel with opening

Given:

Roofing panel with an opening for a light dome according to Figure 4.3. Cross-section layout of the panel: CLT 150 L5s (30l-30w-30l-30w-30l).

The load from the load combination of permanent loads and snow loads is given as a design value of action. The calculation is undertaken under the conservative assumption, that loads due to the light dome are distributed exclusively in the x-direction.

Design value of action:

$$q_d = 4 \text{ kN/m}^2$$

The associated k_{mod} value is

$$k_{mod} = 0.9$$

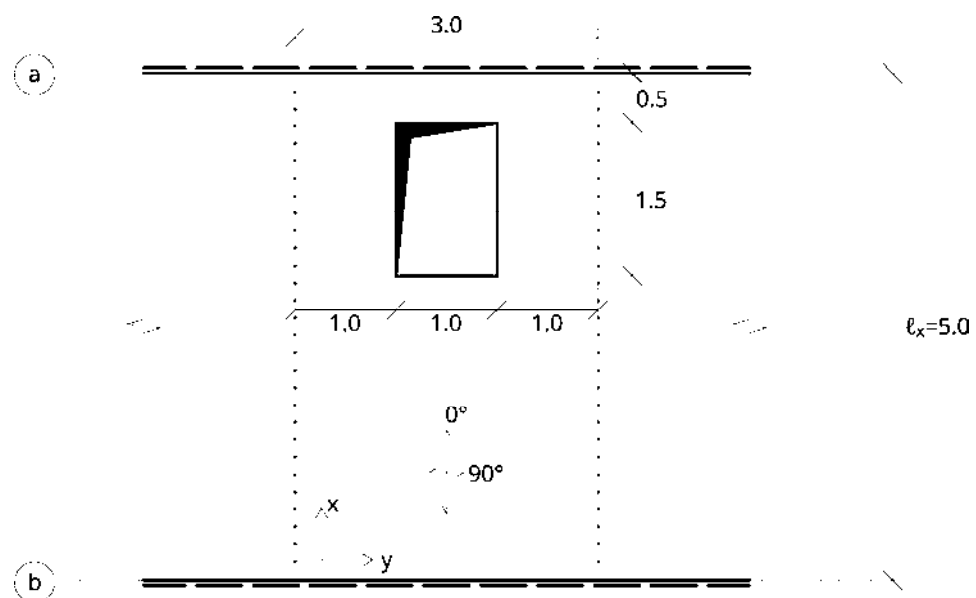


Figure 4.3 Panel with opening

Sought:

Internal forces and required verifications of the load-bearing capacity

Estimation by a grillage model

Comparative calculations showed that a substitute model of suspended beams can be applied for the manual calculation according to Figure 4.4. In that, it is assumed that at the panel edges, strips with the width of at least one tenth of the span remain. If the remaining width of the edge strip is larger, then a maximum of one beam with the width $\ell/10$ next to the opening should be applied.

General calculations with panel models (e.g. with the finite element method), as presented in Chapter 1, naturally result in more exact results.

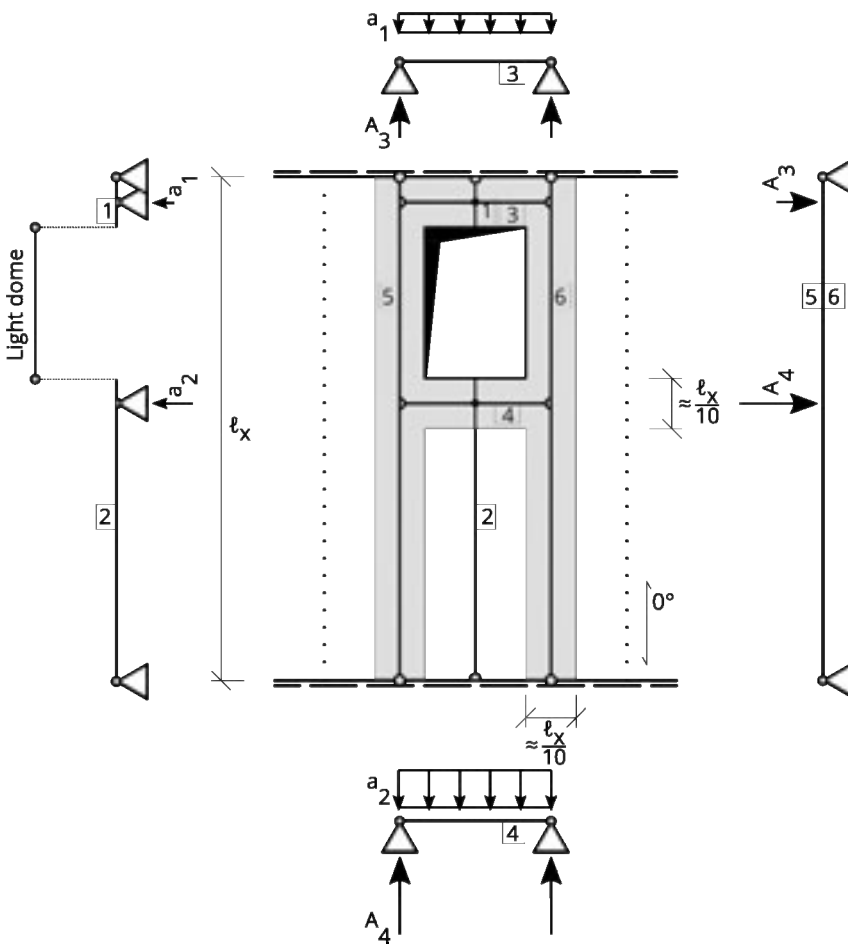


Figure 4.4 Simple grillage as substitute system

Applied beam widths:

$$\frac{\ell}{10} = \frac{500 \text{ cm}}{10} = 50 \text{ cm}$$

Substitute beam 1

Cantilever $c_1 = 0.25 \text{ m}$

Span $\ell_1 = 0.25 \text{ m}$

Beam width $b_1 = 1 \text{ m}$

Load:

At the cantilever tip from the surface load on half the opening

$$F_{1,d} = q_d \cdot \frac{1.5 \text{ m}}{2} \cdot 1 \text{ m} = 4 \text{ kN/m}^2 \cdot 0.75 \text{ m}^2 = 3.0 \text{ kN}$$

from the surface load

$$q_{1,d} = 4 \text{ kN/m}$$

reaction force for load transfer to beam 3

$$a_{1,d} = \frac{q_{1,d}}{2} \cdot \left(\ell_1 + \frac{c_1^2}{\ell_1} + 2 \cdot c_1 \right) + F_{1,d} \cdot \frac{\ell_1 + c_1}{\ell_1}$$

$$a_{1,d} = \frac{4}{2} \cdot \left(0.25 + \frac{0.25^2}{0.25} + 2 \cdot 0.25 \right) + 3.0 \cdot \frac{0.25 + 0.25}{0.25} = 8 \text{ kN}$$

Substitute beam 2

Cantilever $c_2 = 0.25 \text{ m}$

Span $\ell_2 = 2.75 \text{ m}$

Beam width $b_2 = 1 \text{ m}$

Load: at the cantilever tip from half the opening

$$F_{2,d} = 0.75 \cdot 4 = 3.0 \text{ kN}$$

from the surface load

$$q_{2,d} = 4 \text{ kN/m}$$

reaction force for load transfer to beam 4

$$a_{2,d} = \frac{q_{2,d}}{2} \cdot \left(\ell_2 + \frac{c_2^2}{\ell_2} + 2 \cdot c_2 \right) + F_{2,d} \cdot \frac{\ell_2 + c_2}{\ell_2}$$

$$a_{2,d} = \frac{4}{2} \cdot \left(2.75 + \frac{0.25^2}{2.75} + 2 \cdot 0.25 \right) + 3.0 \cdot \frac{2.75 + 0.25}{2.75} = 9.82 \text{ kN}$$

Substitute beam 3Span $\ell_3 = 1.50 \text{ m}$ Beam width $b_3 = \frac{\ell}{10} = 0.5 \text{ m}$

Load from beam 1:

$$a_{1,d} = 8 \text{ kN/m}$$

Bending moment of the beam

$$M_{3,d} = \frac{a_{1,d} \cdot \ell^2}{8} = \frac{8.0 \cdot 1.5^2}{8} = 2.25 \text{ kNm}$$

Design moment of panel strip 3

$$m_{3,y,d} = \frac{M_{3,d}}{b_3} = \frac{2.25}{0.5} = 4.50 \text{ kNm/m}$$

Reaction force for load transfer to beams 5 and 6

$$A_{3,d} = \frac{a_{1,d} \cdot \ell}{2} = \frac{8 \cdot 1.5}{2} = 6.00 \text{ kN}$$

 $x_{A,3} = 0.25 \text{ m}$ from the edge of beam 5 or 6, resp.

Lateral design force of panel strip 3

$$v_{3,y,d} = \frac{A_{3,d}}{b_4} = \frac{6.00}{0.5} = 12.00 \text{ kN/m}$$

Substitute beam 4Span $\ell_3 = 1.50 \text{ m}$ Beam width $b_3 = \frac{\ell}{10} = 0.5 \text{ m}$

Load from beam 2:

$$a_{2,d} = 9.82 \text{ kN/m}$$

Bending moment of the beam

$$M_{4,d} = \frac{a_{2,d} \cdot \ell^2}{8} = 2.76 \text{ kNm}$$

Design moment of panel strip 4 for the

Verification of the bending load-bearing resistance in the ancillary direction of load-bearing capacity:

$$m_{4,y,d} = \frac{M_{4,d}}{b_4} = \frac{2.76}{0.5} = 5.52 \text{ kNm/m}$$

Reaction force for the load transfer at beams 5 and 6

$$A_{4,d} = \frac{a_{1,d} \cdot \ell}{2} = \frac{9.82 \cdot 1.5}{2} = 7.37 \text{ kN}$$

 $x_{A,4} = 2.25 \text{ m}$ from the edge of beam 5 or 6, resp.

Lateral design force of panel strip 4 for the

Verification of the shear load-bearing resistance in sections transverse to the ancillary direction of load-bearing capacity:

$$v_{4,y,d} = \frac{A_{4,d}}{b_4} = \frac{7.36}{0.5} = 14.73 \text{ kN/m}$$

Calculation of the substitute beams 5 or 6, resp.

Span $\ell_5 = 5.00 \text{ m}$

Beam width $b_5 = \frac{\ell}{10} = 0.5 \text{ m}$

Load from beams 3 and 4:

$$A_{3,d} = \frac{a_{1,d} \cdot \ell}{2} = \frac{8 \cdot 1.5}{2} = 6.00 \text{ kN}$$

$x_{A,3} = 0.25 \text{ m}$ from the edge of beam 5 or 6, resp. (upper edge)

$$A_{4,d} = \frac{a_{1,d} \cdot \ell}{2} = \frac{9.82 \cdot 1.5}{2} = 7.4 \text{ kN}$$

$x_{A,4} = 2.25 \text{ m}$ from the edge of beam 5 or 6, resp. (upper edge)

Reaction force on the side of the opening

$$A_{5,d} = q_d \cdot b_5 \cdot \frac{\ell_5}{2} + A_{3,d} \cdot \frac{(\ell_5 - x_{A,3})}{\ell_5} + A_{4,d} \cdot \frac{(\ell_5 - x_{A,4})}{\ell_5}$$

$$A_{5,d} = 4 \cdot 0.5 \cdot \frac{5.00}{2} + 6.00 \cdot \frac{(5.00 - 0.25)}{5.00} + 7.4 \cdot \frac{(5.00 - 2.25)}{5.00} = 14.75 \text{ kN}$$

Bending moment of the beam at position $x_{A,4}$

$$M_{5,max,d} = A_{5,d} \cdot x_{A,4} - \frac{q_d \cdot b_5 \cdot x_{A,4}^2}{2} - A_{3,d} \cdot (x_{A,4} - x_{A,3}) = 16.13 \text{ kN}$$

Design moment of panel strip 5 for the

Verification of the bending load-bearing resistance in the main direction of load-bearing capacity:

$$m_{5,x,d} = \frac{M_{5,max,d}}{b_5} = \frac{16.13}{0.5} = 32.25 \text{ kNm/m}$$

Lateral design force of panel strip 5 for the

Verification of the shear load-bearing resistance in sections transverse to the main direction of load-bearing capacity:

$$v_{5,x,d} = \frac{A_{5,d}}{b_5} = \frac{14.75}{0.5} = 29.5 \text{ kN/m}$$

Dimensioning in the ultimate limit states is undertaken by comparison of the design values of the internal forces from the actions with the design values of the load-bearing capacity. For the given element CLT 150 L5s, the following characteristic values of load-bearing capacity (R) result according to Section 7.3, pages 113 cont.

$$m_{R,x,k} = 78.4 \text{ kNm/m}$$

$$v_{R,x,k} = 136.1 \text{ kN/m}$$

$$m_{R,y,k} = 34.3 \text{ kNm/m}$$

$$v_{R,y,k} = 71.5 \text{ kN/m}$$

Thus, the verifications of the load-bearing capacity are as follows:

Bending load-bearing capacity in the main direction of load-bearing capacity x

$$m_{5,x,d} = 32.26 \text{ kNm/m} \leq m_{R,x,d} = k_{mod} \cdot \frac{m_{R,x,k}}{\gamma_m} = 0.9 \cdot \frac{78.4}{1.25} = 56.5 \text{ kNm/m}$$

Verification fulfilled (57 %) ✓

Lateral force load-bearing capacity in the main direction of load-bearing capacity x

$$v_{5,x,d} = 29.5 \text{ kN/m} \leq v_{R,x,d} = k_{mod} \cdot \frac{v_{R,x,k}}{\gamma_m} = 0.9 \cdot \frac{136.1}{1.25} = 98 \text{ kN/m}$$

Verification fulfilled ($\eta = 30\%$) ✓

Bending load-bearing capacity transverse to the main direction of load-bearing capacity y

$$m_{4,y,d} = 5.52 \text{ kNm/m} \leq m_{R,y,d} = k_{mod} \cdot \frac{m_{R,y,k}}{\gamma_m} = 0.9 \cdot \frac{34.3}{1.25} = 24.7 \text{ kNm/m}$$

Verification fulfilled (22 %) ✓

Lateral force load-bearing capacity transverse to the main direction of load-bearing capacity y

$$v_{4,y,d} = \frac{A_{4,d}}{b_4} = \frac{7.36}{0.5} = 14.73 \text{ kN/m} \leq v_{R,y,d} = k_{mod} \cdot \frac{v_{R,y,k}}{\gamma_m} = 0.9 \cdot \frac{71.5}{1.25} = 51.5 \text{ kN/m}$$

Verification fulfilled ($\eta = 29\%$) ✓

Deflections

The entire deflection can be determined and verified by addition of the deflections of beams 4 and 5 at the level of the characteristic actions. The deformations can be determined with beam formulas and the bending stiffnesses EI_x or EI_y , resp. The influence of the shear stiffnesses can be estimated in a simplified fashion by increasing these deformations by about 20 %.

4.3 Vertical forces transverse to the direction of span

For rectangular floors simply supported on all four sides and outer layers in the direction of the short span, loads are predominantly transferred in x-direction and only low stresses in y-direction. In cross-laminated timber, this effect is enhanced due to its orthotropy – i.e. the differences in stiffness of main and ancillary direction of span. Consequently, a conservative static calculation can be undertaken as a uniaxially stressed panel strip. The vertical forces in sections parallel to the y-axis shown in Figure 4.5 are of interest for the verification of the lateral walls and joints.

Compatibility forces are reaction forces of walls in parallel to the direction of span of floors.

For dimensioning of the lateral walls, the reaction forces from the floor panel's transverse to the main direction of load-bearing capacity $a_{90,d}$ are of interest. These are also designated as compatibility forces and can be determined from the floor load via an influencing effective width b_y .

The design of butt joints longitudinal to the x-axis follows ÖNORM B 1995-1-1:2015 and takes place with a standard screw connection with crossed, self-tapping partially threaded screws (TGS – *Teilgewindeschrauben*) or fully threaded screws (VGS – *Vollgewindeschrauben*) Ø 8 mm every 50 cm as usual for CLT constructions.

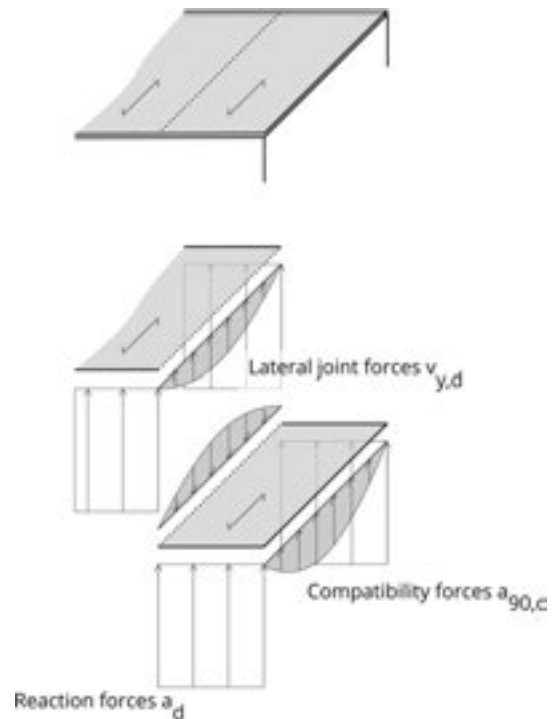


Figure 4.5 Lateral joint forces and compatibility forces

For more accurate analyses and in case of high live loads, the more exact knowledge of the lateral force in the joints is of interest for dimensioning of the connection. The lateral joint forces can likewise be determined from the live load via effective widths.

As a model for simple calculation of the compatibility forces and lateral joint forces, an analogy of the orthotropic panel strip to the embedded beam can be used, as shown in Figure 4.6. Due to the pronounced load distribution in the direction of span, the type of butt joint design has no significant effect on the size of the compatibility forces.

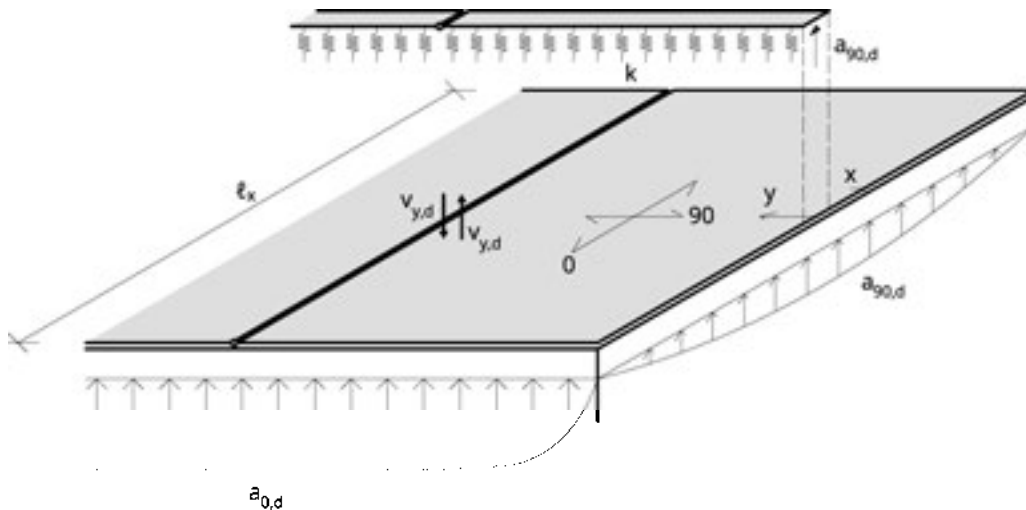


Figure 4.6 Compatibility forces and lateral joint forces of floor spans

4.3.1 Compatibility forces

The reaction forces $a_{90,d}$ per running metre in walls in parallel to the direction of span for two-dimensional loads q_d are:

$$a_{90,d} = b_y \cdot q_d \quad (4.6)$$

with q_d as the design value of the entire floor load

For the orthotropic panel strip supported on three sides, the influence width b_y results with consideration of the stiffness ratios in a simplified fashion as follows¹:

$$b_y = k_{ortho} \cdot 0.2855 \cdot \ell \quad (4.7)$$

$$k_{ortho} = \sqrt[4]{\frac{EI_y}{EI_x}} \quad (4.8)$$

with ℓ as the span in the main direction of load-bearing capacity

The relation of the influence width b_y with regard to the span ℓ and the ratio of longitudinal to transverse stiffness is shown in Figure 4.7.

¹ For derivation via the model of an embedded beam, see Winter, 2008 p. 48 cont.

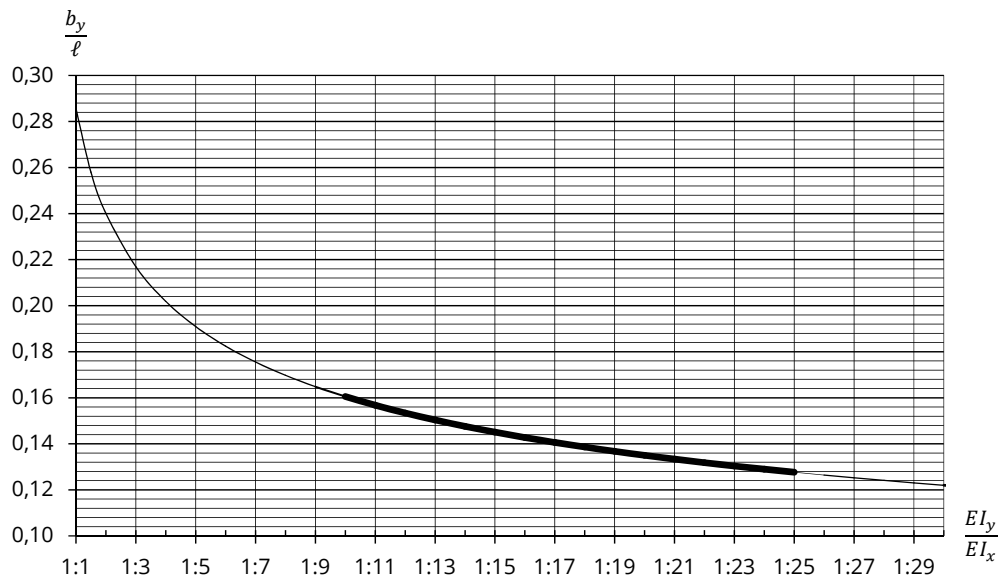


Figure 4.7 Determination of the influence width for compatibility forces

CLT panels normally have stiffness ratios EI_y/EI_x in the range from 1:10 to 1:25. For floor spans up to about $l = 6$ m, influence widths of a maximum of $b_y = 1$ m are obtained.

Consequently, the assumption of one metre of load influence width for compatibility forces according to Figure 4.8 represents a sensible assumption for the estimation of compatibility forces. The actual distribution of the compatibility forces corresponds to the shape of the bending curve, which would occur with a free edge and is approximately parabolic.

For pre-designs, compatibility forces can be determined with one metre of influence width

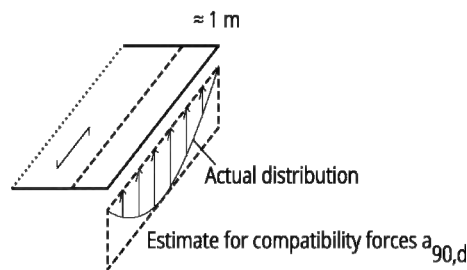


Figure 4.8 Estimation of the compatibility forces

4.3.2 Lateral joint forces

Longitudinal joints shall be designed such that edges of floor elements touching one another have the same deformation. Thus, lateral joint forces occur by compensation of possible relative displacements of the edges in case of different loads or different support of the adjacent floor elements. Their distribution corresponds to the shape of the bending curve and is approximately parabolic.

The most unfavourable load situation results from live loads alternating from span to span n_d . Snow loads on roofs are considered stationary and, in principle, don't have to

be applied as unfavourable. Applying ÖNORM EN 1990¹, as the most unfavourable load position, snow loads can be alternately applied full and at 85 %. Independent of the snow load, for flat roofs with up to 15° pitch it is recommended to apply the live load from repair work on roofs (Category H) of $q_k = 1 \text{ kN/m}^2$.

Joint forces from differently supported adjacent floor elements, as for example an element supported on three sides next to its neighbour supported on two sides, can be considered via the difference of deformation Δw at the centre of the joint. Therefrom, the lateral forces to be transferred in the joint can be determined.

¹ In ÖNORM EN 1991-1-3:2003, Paragraph 2.1, snow loads are defined as *fixed variable actions*. According to ÖNORM EN 1990:2013, Section 1.5.3.8, fixed actions are *action that has a fixed distribution and position over the structure or structural member such that the magnitude and direction of the action are determined unambiguously for the whole structure or structural member if this magnitude and direction are determined at one point on the structure or structural member*. ÖNORM EN 1990:2003, Paragraph 3.5.7 further describes that *load cases should be selected, identifying compatible load arrangements, sets of deformations and imperfections that should be considered simultaneously with fixed variable actions and permanent actions*.

Thus, according to Eurocodes, with respect to their arrangement, snow loads are equated with permanent loads. Consequently, snow loads are not to be treated as free variable impacts and generally not to be applied unfavourably in a span by span fashion. According to ÖNORM EN 1991-1-3 and ÖNORM B 1991-1-3, however, snow loads must be considered for the non-drifted and the drifted case. In that, however, drifts refer to roof shapes with luv and lee roofages (e.g. shed roofs) or obstacles (as layups at the roof) and are not described for smooth roof surfaces.

For the determination of internal forces from an unfavourable load position of snow loads, the following approach is suggested for further considerations. According to EN 1990:2013, Table A.1.2(A), for equilibrium considerations, permanent loads with an unfavourable effect must be multiplied with the factor $\gamma_{G,\text{sub}} = 1.35$ and permanent loads with a favourable effect with the factor $\gamma_{G,\text{inf}} = 1.15$. If the stationary snow loads are treated like that for verifications of the load-bearing capacity, like permanent loads for verifications against the loss of equilibrium, then a span-wise alternating load position of 100 % and 85 % of the snow load on the roof results therefrom.

Shading or drifts can result in higher differences of the snow load in adjacent spans and must be applied respectively.

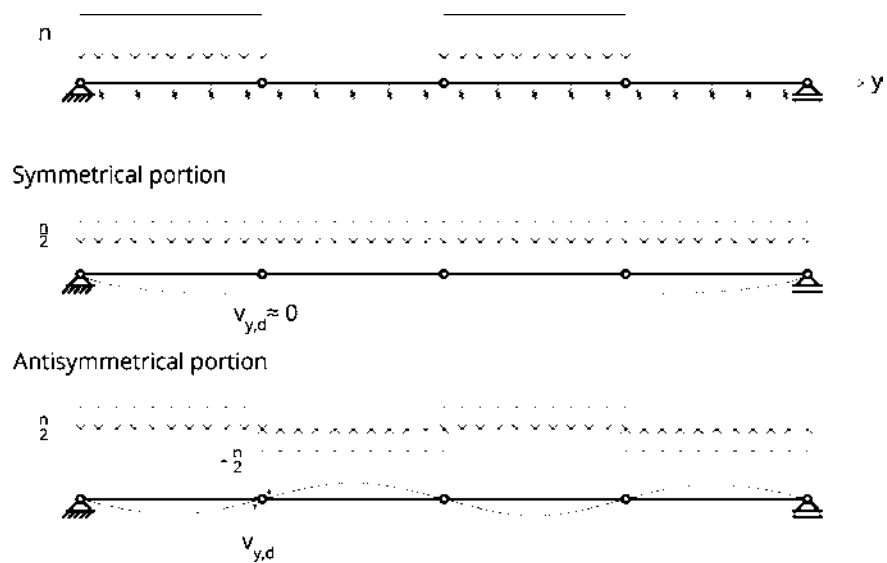


Figure 4.9 Unfavourable load position with symmetrical and antisymmetrical portion

The lateral joint forces are determined analogous to the compatibility forces. The most unfavourable load image is split into a symmetrical and an antisymmetrical portion. As shown by the deformation image in Figure 4.9, only the antisymmetrical portion $q_{as,d}$ results in lateral joint forces. Therefore, only half of the live loads n_d are applied, and snow loads s_d are only applied with half of the load differences between the spans. For the selected approach for snow loads, this results in a portion of $(100\% - 85\%)/2 = 7.5\%$. As for the compatibility forces, the load influence width b_y can be applied for this antisymmetrical load portion. The second portion of lateral joint forces according to the Formula (4.9) results from a possible differential deformation at the centre of the floor Δw . For floor elements supported at three edges, this portion amounts to 20 % to 50 % of the first term in Equation (4.9) originating from the load, depending on the ratio of longitudinal to transverse stiffness. Thus, the simplified Equation (4.10) can be applied for a practice-oriented estimation of the lateral joint forces of floor spans.

$$v_{y,d} = b_y \cdot q_{as,d} + \Delta w \cdot k_{ortho} \cdot \frac{\pi^3 \cdot EI_x}{2^{1.5} \cdot \ell^3} \quad (4.9)$$

$$v_{y,d} \approx b_y \cdot q_{as,d} \cdot 1.50 \quad (4.10)$$

$$q_{as,d} = \frac{n_d}{2} \quad \text{for live loads } n_d$$

$$q_{as,d} = \frac{s_{max,d} - s_{min,d}}{2} = 0.075 s_d \quad \text{for snow loads } s_d \quad (4.11)$$

The model stated considers the ratios of bending stiffnesses, while the influence of shear and torsional stiffnesses of the cross-laminated timber elements is neglected. For practical construction ratios and common dimensions, the formulas stated are to be considered sufficiently accurate.

For simple estimation of the lateral joint forces in usual buildings, for live loads, a load influence of 0.75 m can be assumed for the entire live load and for snow loads of only 0.12 m for the entire snow load.

Estimate of lateral joint forces from live loads

$$v_{y,d} \approx 0.75 \cdot n_d \quad (4.12)$$

Estimate of lateral joint forces from snow loads

$$v_{y,d} \approx 0.12 \cdot s_d \quad (4.13)$$

Example 4.3 Floor with vertical loads

Determination of compatibility forces and lateral joint forces

Details:

A rectangular floor spans over $\ell = 5$ m and is $b = 9.6$ m wide.

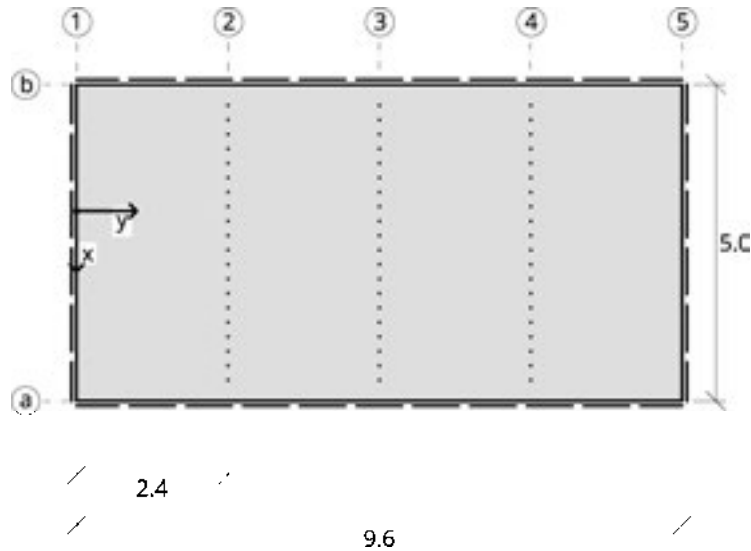


Figure 4.10 Floor span

The CLT floor elements have the layup

CLT 220 – L7s2 (30l – 30l – 30w – 40l – 30w – 30l – 30l)

The characteristic values of action are:

Permanent loads, total: $g_k = 3.5$ kN/m²,

Live load (Category A): $n_k = 2.5$ kN/m²

Sought:

The compatibility forces and the lateral joint forces are to be determined.

Stiffness ratios

$$I_x = 2 \cdot \left(100 \cdot \frac{6^3}{12} + 100 \cdot 6 \cdot 8^2 \right) + 100 \cdot \frac{4^3}{12} = 80\,933 \text{ cm}^4$$

$$I_y = 2 \cdot \left(100 \cdot \frac{3^3}{12} + 100 \cdot 3 \cdot 3.5^2 \right) = 7\,800 \text{ cm}^4$$

$$\frac{EI_x}{EI_y} = \frac{80\,933}{7\,800} = 10.38$$

Compatibility force on the walls in parallel to the outer layers (axes 1 and 5)

$$q_d = \gamma_G \cdot g_k + \gamma_Q \cdot n_k = 1.35 \cdot 3.5 + 1.50 \cdot 2.5 = 8.48 \approx 8.5 \text{ kN/m}^2$$

$$k_{ortho} = \sqrt[4]{\frac{EI_y}{EI_x}} = \sqrt[4]{\frac{7800}{80933}} = 0.557$$

$$b_y = 0.557 \cdot 0.2855 \cdot \ell = 0.159 \cdot 5 = 0.795 \approx 0.8 \text{ m}$$

The compatibility force on the wall in parallel to the main direction of load-bearing capacity is:

Formulas (4.6) and (4.7)

$$a_{90,d} = b_y \cdot q_d = 0.8 \cdot 8.5 = 6.8 \text{ kN/m}$$

Lateral force in the butt joints (axes 2 and 4)

$$n_d = \gamma_Q \cdot n_k = 1.5 \cdot 2.5 = 3.75 \approx 3.8 \text{ kN/m}^2$$

Formula (4.10)

The largest lateral force in the butt joint is:

$$v_{y,d} \approx b_y \cdot \frac{n_d}{2} \cdot 1.50 = 0.8 \cdot \frac{3.8}{2} \cdot 1.50 = 2.28 \approx 2.3 \text{ kN/m}$$

The lateral joint force in axis 3 is lower by about the factor 1.5.

4.4 Joint forces from plate effect

In floor, wall or roof diaphragms, used for bracing of the structure, axial joint forces and longitudinal shearing forces of the joint occur beside the lateral joint forces from vertical actions, as shown in Figure 4.11.

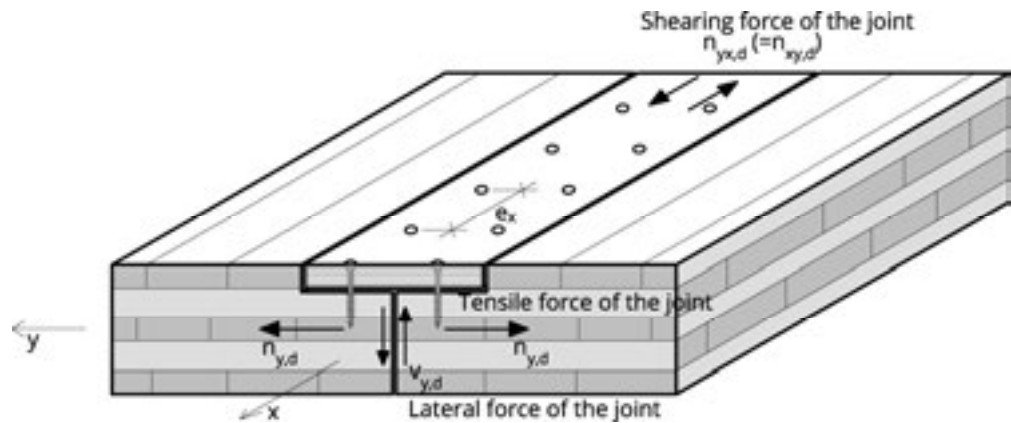


Figure 4.11 Designation of the internal joint forces

Depending on the load level, butt joint with milled-in cover strips, rebated joint or butt joint with crossed fully threaded screws are possible as connections, as shown in Figure 4.12.

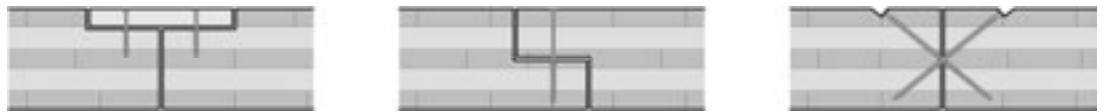


Figure 4.12 Frequently executed joint designs (a) butt joint with milled-in cover strips, b) rebated joint, c) butt joint with fully threaded screws)

Horizontally acting wind or earthquake loads shall be transferred from the diaphragm into the bracing walls or cores, as shown in Figure 4.13.

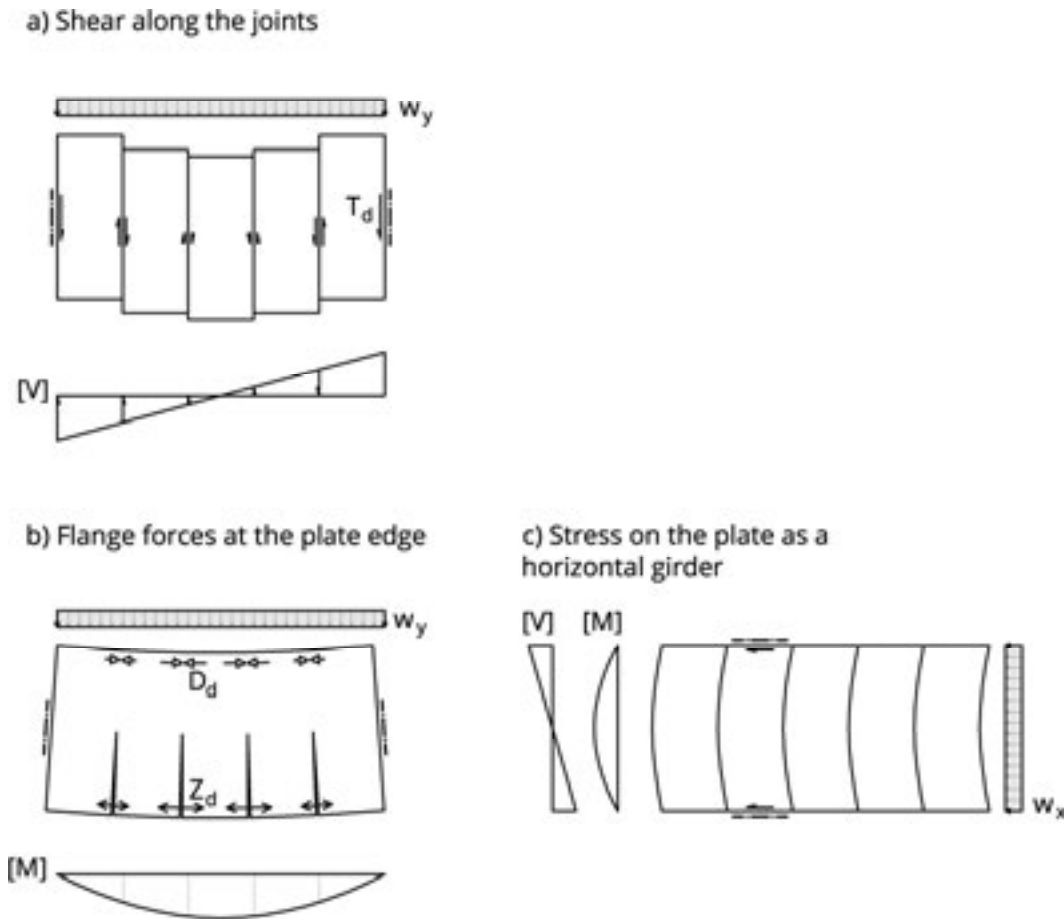


Figure 4.13 diaphragms and types of stresses

In that, the diaphragm can be modelled as a substitute beam in the horizontal plane between the bracing walls, as shown, in principle, in Figure 4.14. Offset joints in at least one direction are recommended in the arrangement of CLT panels for better load distribution. The lateral force V_d in a section of the substitute beam is equal to the resultant of the joint's shear forces $n_{xy,d}$ and the bending moment M_d of the substitute beam corresponds to the resultant of the joint's axial forces $n_{y,d}$ in this section.

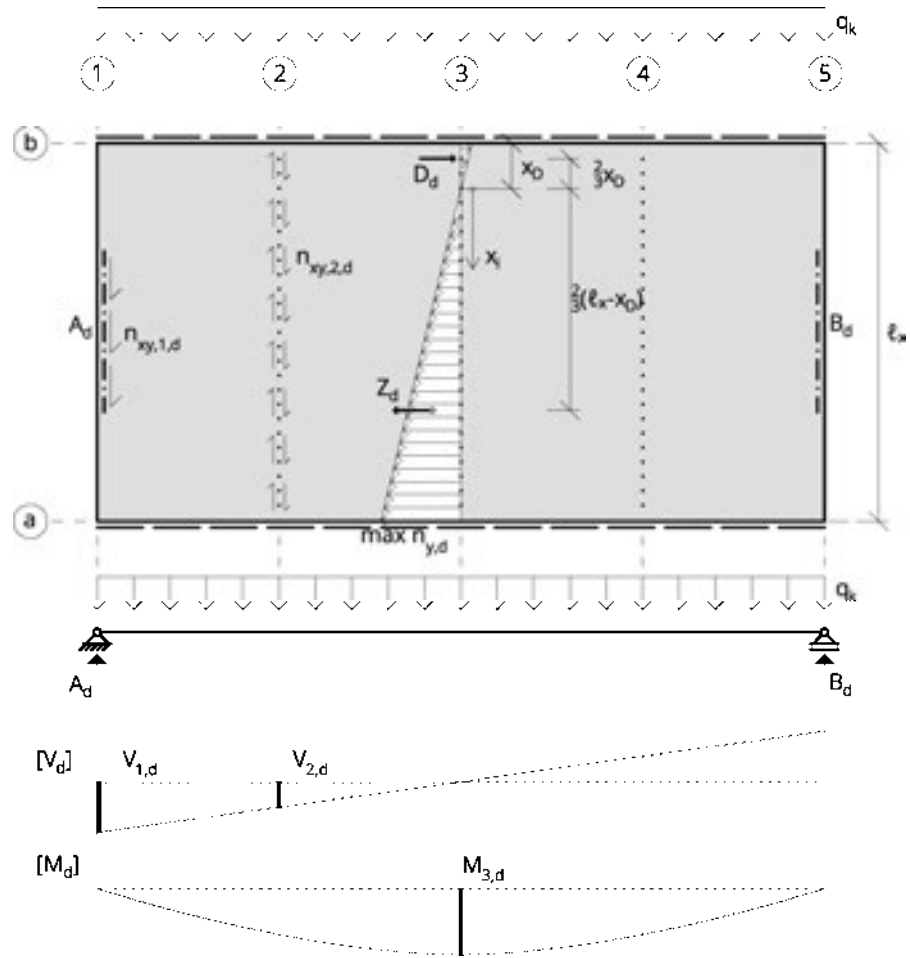


Figure 4.14 Diaphragm with internal forces in the joints and substitute beam

For dimensioning of the fasteners in the joints it is assumed that the shear flow along the joint is constant and axial forces are linear distributed. Possible connections at the longitudinal edges a and b are considered non-effective and frictionless joints are assumed.

4.4.1 Shearing forces of the joint

With a continuous connection of the elements using screws, the shearing force over the entire joint length can be assumed as uniformly distributed.

The longitudinal shearing force of the joint constant over the entire joint per running metre of joint then is

$$n_{xy,d} = \frac{V_d}{l_x} \quad (4.14)$$

The force per fastener consequently is

$$F_{xy,i,d} = n_{xy,d} \cdot e_x = \frac{V_d}{\ell_x} \cdot e_x \quad (4.15)$$

with

- V_d Lateral force of the substitute beam at the position of the joint considered
- e_x Distance of the fasteners along the joint
- ℓ_x Span in the main direction of load-bearing capacity

4.4.2 Normal forces of the joint

Normal forces of the joint in the respectively considered section can be determined from the associated internal moment M_d of the substitute beam.

For simpler calculation, a linear distribution of the joint's normal stresses per unit of length of the joint is assumed, without mapping the exact positions of the individual screws, since normally continuous screw connections of the joint with constant distance are undertaken. From the load-bearing capacity of a fastener, the statically required minimum distance of the fasteners can ultimately be calculated from the stress on the joint.

In case of a relatively low load level, the compression as well as the tension zone will respectively extend over half the joint length. With an increase in load, the compression zone will considerably decrease due to the higher stiffness parallel to grain, while the tension zone increases due to the ductile screws connection and extends over almost the entire joint length, as shown in Figure 4.14. Upon reaching the load capacity – with sufficient screw connections – the timber strength in the pressure zone is reached.

With this assumption, the maximum compression force with an initially still unknown length of the pressure zone x_D is:

$$D_d = \frac{f_{c,0,d} \cdot \sum d_{90} \cdot x_D}{2} \quad (4.16)$$

By establishing the equilibrium of forces from tensile and compressive forces and the equilibrium of moments with the internal moment of the substitute beam M_d , the following results

$$Z_d = D_d \quad (4.17)$$

$$M_d = D_d \cdot \left(\frac{2x_D}{3} + \frac{2(\ell_x - x_D)}{3} \right) = D_d \cdot \frac{2}{3} \ell_x \quad (4.18)$$

Therefrom, the following is obtained for the length of the compression zone x_D .

$$x_D = \frac{3M_d}{f_{c,0,d} \cdot \sum d_{90} \cdot \ell_x} \quad (4.19)$$

The length x_D is small compared to the length ℓ_x and can, in good approximation, be assumed with $x_D = 0$. With this assumption, the expansion baseline of the joint moves right up to the compressed edge and the compression zone becomes a compressive force.

With the simplification of a tension wedge and a compressive force, the following results for the axial force of the joint at the tension edge:

$$\max n_{y,d} = \frac{3 M_d}{\ell_x^2} \quad (4.20)$$

with

M_d Design value of the moment of the substitute beam
in the section considered

The triangular course of the joint's tensile forces has to be covered by fasteners, as initially described. This can be undertaken by continuous screw connections or by individual fasteners allocated to this task, as for example fully nailed perforated plates arranged in the proximity of the floor edges.

Upon assumption of a constant fastener distance e_x , the following results for the fastener force $F_{y,i,d}$ at position x_i

$$F_{y,i,d} = \max n_{y,d} \frac{x_i}{\ell_x} e_x = \frac{3 M_d e_x x_i}{\ell_x^3} \quad (4.21)$$

and for the most highly stressed fastener at the edge

$$\max F_{y,i,d} = \max n_{y,d} \cdot e_x = \frac{3 M_d e_x}{\ell_x^2} \quad (4.22)$$

From the load-bearing capacity of a fastener $F_{R,d}$, the statically required fastener distance can be determined:

$$\text{req } e_x = \frac{F_{y,R,d} \ell_x^2}{3 M_d} \quad (4.23)$$

with

$F_{y,R,d}$ Design value of the resistance of a fastener
 M_d Moment of the substitute beam in the section considered
 ℓ_x Span in the main direction of load-bearing capacity

If only a connection with punctiform effect, like an perforated plate, is arranged, then this should absorb the entire tensile force Z_d .

$$Z_d = \frac{M_d}{z} = \frac{3 M_d}{2 \ell_x} \quad (4.24)$$

with

z Internal lever arm between tension and pressure resultant.
Conservatively, a triangular course with $z = \frac{2}{3} \cdot \ell_x$ can be assumed.

Example 4.4 Diaphragm with horizontally and vertically acting loads

Determination of the joint forces in a diaphragm

Details:

Rectangular Floor with the dimensions 6 x 14.4 m consisting of 6 elements CLT 150 – L5s (30l – 30w – 30l – 30w – 30l) with a width of $b = 2.4$ m each.

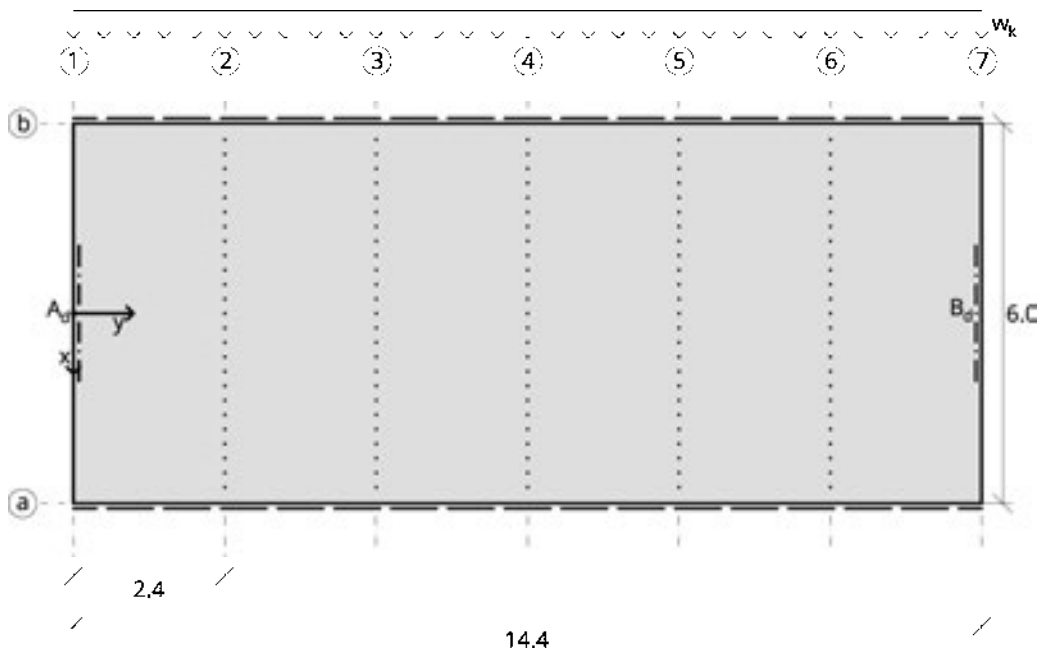


Figure 4.15 Layout of the diaphragm

As loads act a horizontal wind action: $w_k = \pm 3$ kN/m (load duration short-term/ instantaneous) and the live load on the floor: $n_d = 2.0$ kN/m² (load duration medium-term).

The design of the joint is undertaken with crossed fully threaded screw pairs in the vertical plane.

Sought:

Dimensioning and verification of the joint connection (crossed screws).

The load-bearing capacity of a screw VGS 8 × 200 mm, $\ell_{ef} = 100$ mm is:

$F_{ax,k} = 6.7$ kN for axial stress (tension and compressive forces)

$F_{v,k} = 4.3$ kN for shear stress

Determination of the lateral joint forces by live loads on the diaphragm

$$I_x = 22\,275 \text{ cm}^4$$

$$I_y = 5\,850 \text{ cm}^4$$

Formulas (4.7) and (4.10)

Load influence width

$$k_{\text{ortho}} = \sqrt[4]{\frac{EI_y}{EI_x}} = \sqrt[4]{\frac{5 \cdot 850}{22 \cdot 275}} = 0.716$$

$$b_y = k_{\text{ortho}} \cdot 0.2855 \cdot \ell = 0.716 \cdot 0.2855 \cdot 6 = 1.227 \text{ m} \approx 1.2 \text{ m}$$

Design value of the live load

$$n_d = \gamma_Q \cdot n_k = 1.5 \cdot 2.0 = 3.0 \text{ kN/m}^2$$

Lateral joint force in joint 2 ($y = 2.4 \text{ m}$) and in an approximate fashion in the same size in the further joints

$$v_{y,d} = b_{90} \cdot \frac{n_d}{2} \cdot 1.50 = 1.2 \cdot \frac{3.0}{2} \cdot 1.50 = 2.7 \text{ kN/m}$$

Determination of the joint forces from plate effect

Internal forces at the substitute beam

Design value of the wind load

$$w_d = \gamma_Q w_k = 1.5 \cdot 3 = 4.5 \text{ kN/m}$$

Reaction force at the substitute beam

$$A_d = \frac{w_d \ell_y}{2} = \frac{4.5 \cdot 14.4}{2} = 32.4 \text{ kN}$$

Internal forces in joint 2 ($y = 2.4 \text{ m}$)

$$V_{2,d} = A_d - w_d y = 32.4 - 4.5 \cdot 2.4 = 21.6 \text{ kN}$$

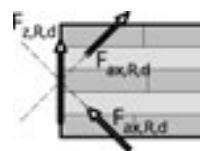
$$M_{2,d} = A_d y - \frac{w_d y^2}{2} = 32.4 \cdot 2.4 - \frac{4.5 \cdot 2.4^2}{2} = 64.8 \approx 65 \text{ kNm}$$

Internal forces in joint 4 in the centre of the diaphragm ($y = 7.2 \text{ m}$)

$$V_{4,d} = 0$$

$$M_{4,d} = \frac{w_d \ell_y^2}{8} = \frac{4.5 \cdot 14.4^2}{8} = 117 \text{ kNm}$$

Design values of resistances



Force diagram



Figure 4.16 Resistances of the crossed screws upon vertical load

Resistance of a screw upon axial stress (tension and pressure, load duration brief/very brief)

$$F_{ax,R,d} = k_{mod} \frac{F_{t,R,k}}{\gamma_M} = 1.0 \cdot \frac{6.70}{1.3} = 5.15 \text{ kN}$$

Resistance of the crossed screws upon vertical or horizontal load, resp. (load duration medium-term) according to Figure 4.16:

$$F_{z,R,d} = F_{y,R,d} = \sqrt{2} F_{ax,R,d} = k_{mod} \sqrt{2} \frac{F_{t,R,k}}{\gamma_M} = 0.8 \cdot \sqrt{2} \cdot 5.15 = 5.83 \text{ kN}$$

Resistance of the crossed screws upon shear out of the screw plane (load duration short-term):

$$F_{v,R,d} = k_{mod} \frac{2 F_{v,R,k}}{\gamma_M} = 1.0 \cdot \frac{2 \cdot 4.3}{1.3} = 6.62 \text{ kN}$$

Verification for joint 4 in the centre of the plate ($y = 7.2 \text{ m}$)

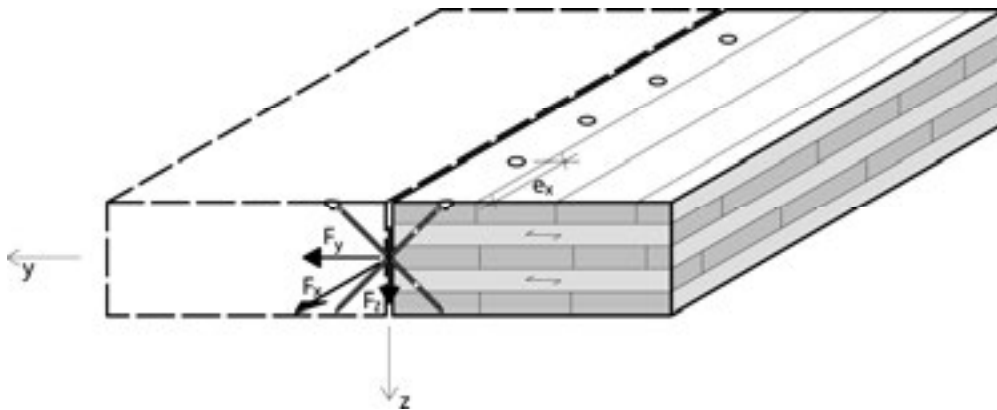


Figure 4.17 Forces at the crossed screws

Pre-design of the screw distance for the joint's tensile force ($k_{mod} = 1.0$)

$$\text{req } e_x = \frac{F_{y,R,d} \cdot l_x^2}{3 M_{4,d}} = \frac{\sqrt{2} \cdot 5.15 \cdot 6^2}{3 \cdot 117} = \frac{7.29 \cdot 6^2}{3 \cdot 117} = 0.74 \text{ m}$$

selected: $e_x = 50 \text{ cm}$

Tensile force of the joint in the outermost set of crossed screws

$$\max F_{y,i,d} = \frac{3 M_{4,d} e_x}{\ell_x^2} = \frac{3 \cdot 117 \cdot 0,5}{6^2} = 4.88 \text{ kN}$$

Lateral joint force per set of crossed screws:

On the safe side, the maximum lateral joint force $F_{z,d}$ between first and second floor span is also applied in the joint in the centre of the plate. The load-bearing capacity of possibly existing floating screed is not considered.

$$F_{z,d} = v_{2,y,d} \cdot e_x = 2.7 \cdot 0.5 = 1.35 \text{ kN}$$

Verification upon combined effect of tensile joint force and lateral joint force:

$$\frac{F_{y,d} + F_{z,d}}{\sqrt{2} F_{ax,R,d}} = \frac{4.86 + 1.35}{7.29} = \frac{6.21}{7.29} = 0.85 \leq 1$$

Verification fulfilled

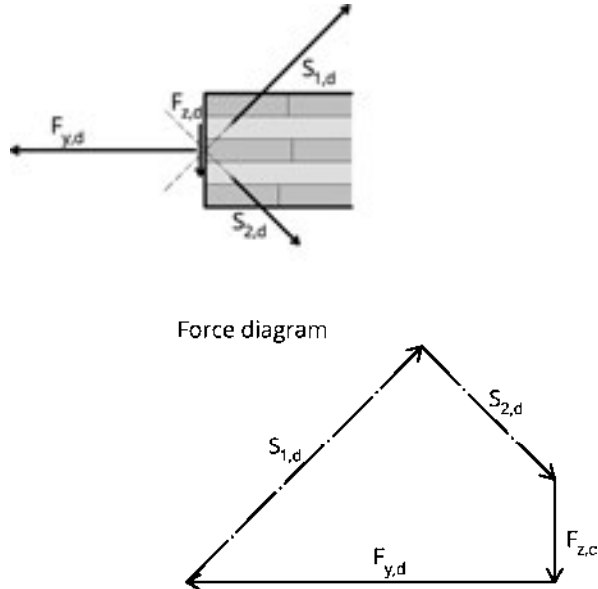


Figure 4.18 Effect of the joint forces on screws S_1 and S_2

Verification for joint 2 ($y = 2.4 \text{ m}$)

Joint 2 is stressed by tensile joint forces, lateral joint forces and shearing joint forces

Shearing joint force per set of crossed screws

$$F_{xy,d} = \frac{V_{2,d}}{\ell_x} \cdot e_x = \frac{21.6}{6} \cdot 0.5 = 1.80 \text{ kN}$$

Tensile joint force in the outermost set of crossed screws

$$\max F_{y,d} = \frac{3 M_{2,d} e_x}{\ell_x^2} = \frac{3 \cdot 65 \cdot 0.5}{6^2} = 2.71 \text{ kN}$$

Lateral joint force per set of crossed screws

$$F_{z,d} = 1.35 \text{ kN}$$

Verification (load duration short-term)

$$\left(\frac{F_{xy,d}}{F_{v,R,d}} \right)^2 + \left(\frac{F_{y,d} + F_{z,d}}{\sqrt{2} F_{ax,R,d}} \right)^2 = \left(\frac{1.80}{6.62} \right)^2 + \left(\frac{2.71 + 1.35}{7.29} \right)^2 = 0.074 + 0.31 = 0.39 \leq 1$$

Verification fulfilled.

Verification for lateral force from live load alone (load duration medium-term)

$$\frac{F_{z,d}}{F_{z,R,d}} = \frac{2.71}{5.83} = 0.46 \leq 1$$

Verification fulfilled.

Verification for the support joint ($y = 0 \text{ m}$)

The vertical compatibility forces are transferred to the wall via support pressure. The shearing forces of the joint shall be applied into the bracing shear wall with the length $\ell_W = 3 \text{ m}$.

Shearing force of the joint for connection of the floor with the wall

$$n_{xy,1,d} = \frac{A_d}{\ell_W} = \frac{32.4}{3} = 10.8 \text{ kN/m}$$

Shearing force of the joint per set of crossed screws

$$F_{xy,d} = n_{xy,1,d} \cdot e_x = 10.8 \cdot 0.5 = 5.4 \text{ kN}$$

Verification

$$\frac{F_{xy,d}}{F_{v,R,d}} = \frac{5.4}{6.62} = 0.82 \leq 1$$

✓Verification fulfilled ($\eta = 82 \%$).

4.4.3 Joints with joint cover strip

Beside the joint design with crossed fully threaded screws stated above, designs with rebated joint and designs with butt joint with milled-in cover strips – i.e. recessed top layers of wood-based panels – are common. In the following, static models for the transfer of the joint's internal forces with a recessed top layer are presented, in order to explore the limits of their load-bearing capacity.

Due to lateral joint forces $v_{y,d}$ the screws in the joint cover strip are subject to withdrawal stress, while they are predominantly subject to shear stress by axial joint forces $n_{y,d}$ and joint shear force $n_{xy,d}$. For the proper transfer of higher lateral joint forces, rebated joints

are to be preferred; in case of higher axial forces, designs with crossed screw pairs or nailed sheets are more effective.

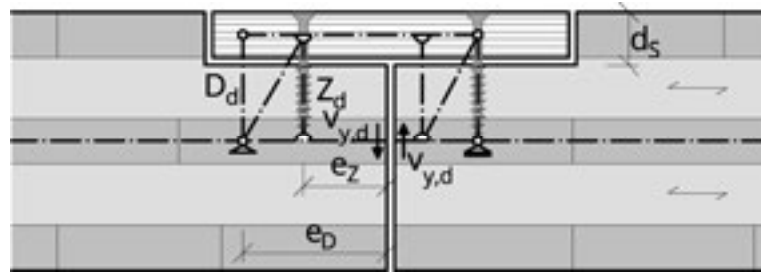


Figure 4.19 Static model for the transfer of lateral joint forces

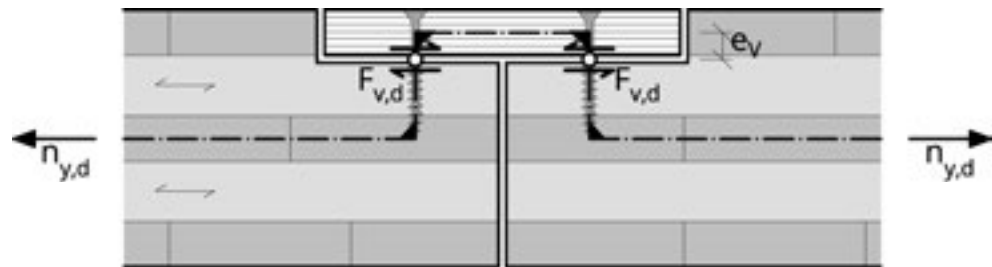


Figure 4.20 Static model for the transfer of tensile joint forces

According to the static models from Figure 4.19 and Figure 4.20, the screw forces result as follows:

Tensile force per screw from lateral joint forces

$$Z_d = v_{y,d} \cdot e_x \cdot \frac{e_D}{e_D - e_Z} \quad (4.25)$$

Withdrawal force per screw from tensile joint forces and shearing joint forces

$$F_{v,d} = \sqrt{n_{y,d}^2 + n_{xy,d}^2} \cdot e_x \quad (4.26)$$

with

- e_x Distance of the screw in the joint's longitudinal direction
- e_Z Distance of the screw from the panel edge
- e_D Distance of the resulting compressive force from the panel edge

The required screw distance in the direction of the joint for an impacting lateral joint force and a given tensile load-bearing capacity of the screw $F_{ax,d}$ can be determined as follows:

$$req\ e_x = F_{ax,d} \frac{e_D - e_Z}{v_{y,d} \cdot e_D} = k_{mod} \frac{F_{ax,k}}{\gamma_m} \frac{e_D - e_Z}{v_{y,d} \cdot e_D} \quad (4.27)$$

Example 4.5 Screw connection for a joint with recessed top layer

Determination of the required screw connection distances

Details:

The joint is executed with a rabbet dimension of 27×80 mm. The top layer is a three-layered solid wood panel with a thickness $t = 27$ mm and a width $b = 160$ mm.

Screw connections are to be undertaken with partially threaded screws (TGS – *Teilgewindeschrauben*) with countersunk head. The outer thread diameter is $d = 8$ mm, the screw length $l_g = 120$ mm. The head's resistance against pulling through, and thus the maximum tensile force of the screw, is $F_{ax,k} = 2.25$ kN.

The distance of the screw or the pressure resultant, resp., is $e_Z = 40$ mm or $e_D = 40 + \frac{2}{3} \cdot 40 = 67$ mm, resp., from the edge of the panel.

As an action, a lateral joint force $v_{y,d} = 2.0$ kN/m is given.

Sought

Determination of the required screw connection distance e_x

Design value of the head's resistance against pulling through

$$F_{ax,d} = k_{mod} \frac{F_{ax,k}}{\gamma_m} = 0.8 \frac{2.25}{1.3} = 1.38 \text{ kN}$$

Required distance

$$req\ e_x = F_{ax,d} \frac{e_D - e_Z}{v_{y,d} \cdot e_D} = 1.38 \cdot \frac{1}{2.0} \cdot \frac{67 - 40}{67} = 1.38 \cdot 0.5 \cdot 0.403 = 0.278 \text{ m}$$

Selected distance

$$sel.\ e_x = 0.25 \text{ m} = 25 \text{ cm}$$

Screw connection of the butt joints: TGS 8×120 mm every 25 cm per panel edge

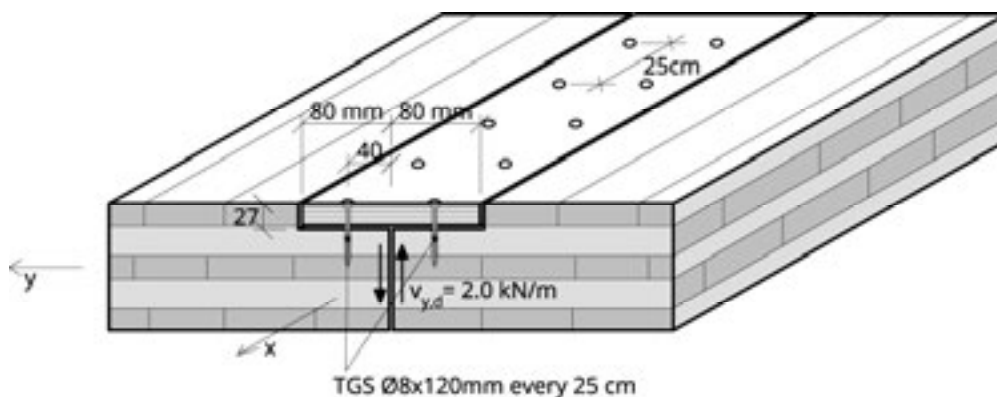


Figure 4.21 Selected screw connections

4.5 Concentrated loads

Concentrated loads, and likewise punctiform supports, result in local stress concentrations in CLT elements. Beside the direct local stress from compression perpendicular to grain, which is being dealt with in Section 6.2, the stresses from bending moments and lateral forces as a consequence of concentrated loads occurring in CLT panels are of interest.

Concentrated loads can originate from local live loads or supports and other rod-shaped structural elements. For calculation, these shall be related to the centre plane of the load-bearing panels, as described in 4.5.1.

Due to the biaxial load-bearing performance of CLT panels, stresses from local loads can also be related to a larger load distribution width for panels supported on two sides, due to the transverse load-bearing effect. This results in considerable reductions of the stress compared to the uniaxial consideration as a beam strip.

4.5.1 Load distribution

Local loads are related to a load distribution width c_y at the centre plane of the CLT panel. Load propagation takes place, on the one hand, through possibly existing screeds, and on the other hand, in the CLT panel itself.

As possible actions, concentrated live loads for multi-storey buildings normally occur in the quantity of $Q_k = 2$ to 4 kN. Their contact area is assumed with a square of 5×5 cm. Supports and other rod-shaped elements normally act directly on the CLT panel.

Q_k according to
ÖNORM EN 1991-1-1,
Table 6.2

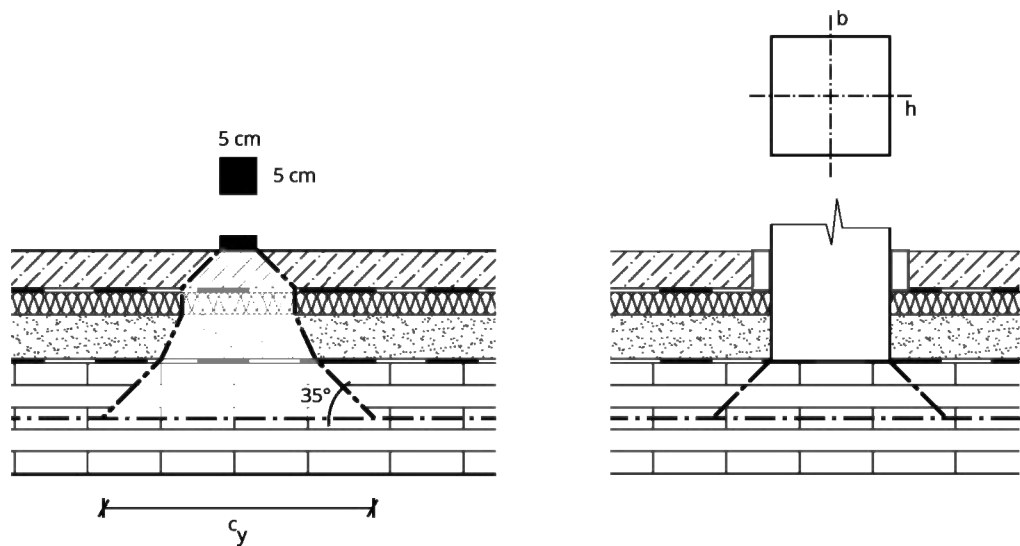


Figure 4.22 Load distribution of live loads and supports

The load-distributing effect up to the centre plane of the CLT panel can be determined by application of propagation angles for each of the layers of the floor structure up to the centre plane. The load width at the height of the centre plane then is c_y . In accordance with Figure 4.22, typical load propagation angles for floating screeds are

45°, for CLT simplified 35° (45° for longitudinal layers and 15° for transverse layers), for fills about 15° and for insulations 0°. In the main direction of load-bearing capacity, concentrated loads can likewise be related to the centre plane in the described manner. The respective load length is then designated with c_x and is shown in Figure 4.23.

4.5.2 Load-bearing effect of panels

The load distribution by the load-bearing effect of panels was not considered in Section 11.2.3 of Volume 1 as a conservative assumption.

Due to the biaxial load-bearing effect of panels of CLT floors, as a consequence of concentrated loads Q_d or linear loads q_d acting along the main direction of load-bearing capacity, the plate's bending moment $m_{y,d}$ is lower than the internal moment M_d of a panel strip exclusively acting in one direction. By introducing a calculated load distribution width $b_{M,ef}$ the internal moment of the panel can be recalculated from that of the panel strip.

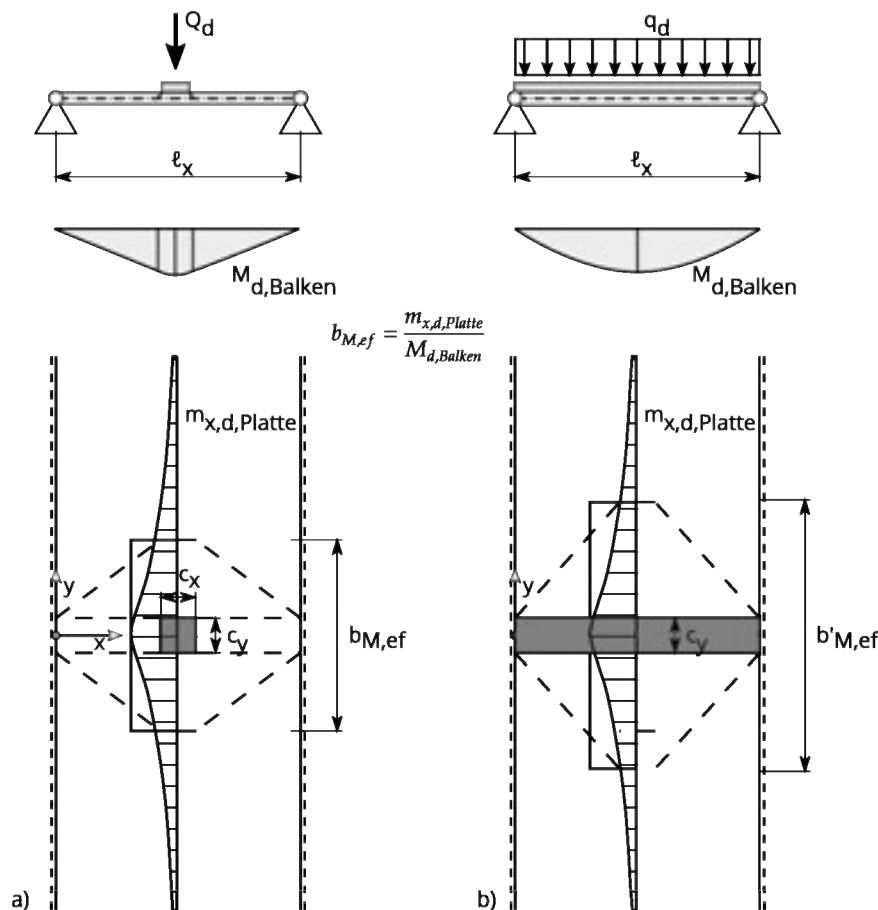


Figure 4.23 Distribution of the bending moments upon a) concentrated and b) linear load

The determination of the calculated load distribution width takes place on the basis of Booklet 240 (DAfStb, 1988) with the model of isotropic panels under additional consideration of the influence of orthotropy according to Girkmann, 1968 and an analytical solution for the infinitely long orthotropic panel strip. In order to cover all floor dimensions common in practical construction, the factors in the theoretically determined formulas were adjusted.

If a uniaxially stressed panel is limited by free edges at a distance ℓ_y , then numerical comparative calculations show, that the load distribution width is to be limited with $0.65 \cdot \ell_y$. For loads close to free edges, the calculated load distribution width has to be limited by the actually existing geometrical width, as shown in Figure 4.24.

The influence of butt joints, i.e. linear joints in parallel to the direction of span, was not analysed in detail. Therefore, conservatively – also with on the whole wider floors – not more than the width of one floor element b_y should be considered for the load propagation.

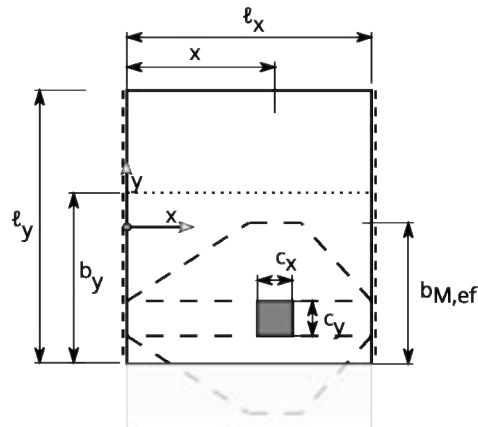


Figure 4.24 Reduced load distribution width for loads close to free edges

For the maximum bending moment from centred load ($x = l_x/2$)

$$b_{M,ef} = (c_y + 0.5 \cdot \ell_x) \cdot k_{ortho} \leq b_{M,max} \quad (4.28)$$

For a general layer x of the load application surface

$$b_{M,ef} = \left[c_y + 2.0 \cdot x \cdot \left(1 - \frac{x}{\ell_x} \right) \right] \cdot k_{ortho} \leq b_{M,max} \quad (4.29)$$

with the largest width to be applied

$$b_{M,max} = \min \left\{ \begin{array}{l} 0.65 \cdot \ell_y \\ b_y \end{array} \right. \quad (4.30)$$

The orthotropy factor is

$$k_{ortho} = \sqrt[4]{\frac{EI_{y,net}}{EI_{x,net}}} \quad (4.31)$$

with c_y the width of the contact area,

ℓ_x the span between the supports,

ℓ_y the width of the floor (transverse to the direction of span)

and b_y the width of a CLT panel.

The influence of the stiffness ratios on the load distribution is considered with the orthotropy factor k_{ortho} . It can be found analogously in the assumptions for the lateral distribution of concentrated loads in the verification of vibration according to ÖNORM B 1995-1-1:2015.

Effective width for bending stress

For linear loads, as they are applied by walls in parallel to the direction of span, the calculated load distribution width for bending is:

$$b'_{M,ef} = \ell_x \cdot k_{ortho} \leq \min \left\{ \begin{array}{l} 0.85 \cdot \ell_y \\ b_y \end{array} \right. \quad (4.32)$$

with

ℓ_y Width of the floor transverse to the main direction of load-bearing capacity

b_y Width of a CLT panel

The maximum bending moment with centred load application at the substitute beam then is:

$$M_{m,d} = Q_d \cdot \frac{2 \cdot \ell_x - c_x}{8} \approx \frac{Q_d \cdot \ell_x}{4} \quad (4.33)$$

The bending moment upon load application at position x is

$$M_{m,d} \approx Q_d \frac{(\ell_x - x)}{\ell_x} x \quad (4.34)$$

The bending moment of the panel is calculated as

$$m_{x,d} = \frac{M_{m,d}}{b_{M,ef}} \quad (4.35)$$

The bending stress is calculated from

$$\sigma_{m,d} = \frac{m_{x,d}}{W_{x,net}} = \frac{M_{m,d}}{b_{M,ef} \cdot W_{x,net}} \quad (4.36)$$

Effective width for shear stress

Lateral forces V_d are normally only decisive for loads close to the support. Thus, the shear stress as a consequence of a live load Q_d close to the support can be determined as follows.

With the effective width for the lateral force

$$b_{V,ef} \approx c_y \cdot 1.25 \quad (4.37)$$

the rolling shear stress is calculated as

$$\tau_{R,d} = Q_d \cdot \frac{S_{R,x}}{I_{x,net} \cdot b_{V,ef}} \quad (4.38)$$

For linear loads, as they are applied by walls in parallel to the direction of span, the calculated load distribution width is

$$b'_{V,ef} = 0.25 \cdot \ell \quad (4.39)$$

For the detailed verification of the shear capacity in the force application area, on the one hand, a determination of the internal forces can be undertaken using computer calculation (FEM), or on the other hand, the force can be assigned to the available interfaces in a circular section around the support. If the lateral forces are present from an exact determination of the internal forces, these can be directly used for the verification of the rolling shear or shear stresses, resp.

If the concentrated load is distributed onto sections in a critical circular section, then this circular section is determined with a load propagation angle of 35° from the edge of the load application area up to the central plane of the CLT panel.

First, the concentrated load action F_d is split into two portions of the two directions of load-bearing capacity of the panel¹: into one portion in sections transverse to the main

¹ According to Mestek, 2011, page 63, the number of layers is considered via the formula $0.67 \cdot n^{-0.1}$. Depending on the number of layers, this results in the following load portions in the main direction of load-bearing capacity (x-axis): 0.6 for 3 layers, 0.57 for 5 layers, 0.55 for 7 layers and 0.54 for 9 layers.

direction of load-bearing capacity (x-axis) $F_{x,d} = 0.6 \cdot F_d$ and one portion in sections transverse to the ancillary direction of load-bearing capacity (y-axis) $F_{y,d} = 0.4 \cdot F_d$. Subsequently, these two portions are divided to the number of available sections. This depends on the position of the concentrated load on the panel. In the internal area, two sections are available for both directions of load-bearing capacity, and the decisive lateral forces are $V_{x,d} = \frac{F_{x,d}}{2}$ and $V_{y,d} = \frac{F_{y,d}}{2}$. At the edge, only one section is available for one of the two directions, and the decisive lateral force then is, for example, $V_{x,d} = F_{x,d}$. The corner area has to be dealt with accordingly.

With these lateral forces and the previously determined width of the sections, the shear verifications can be undertaken.

Deflections

The calculated load distribution width for bending stress determined above can also be used for the conservative calculation of deflection.

Floor joints

As described above, the calculated load distribution width is limited with the element width b_y – i.e. the distance of the floor joints. With this assumption, it is guaranteed that the equilibrium is maintained by load distribution in the main direction of span alone. Lateral joint forces are then not required for maintenance of the equilibrium. The actually occurring lateral joint forces depend on the joint design and the joint stiffness resulting therefrom and can only be determined using suitable numerical models (FEM or grillage).

The higher the number of layers, the more uniformly the lateral forces are consequently distributed in the two directions of load-bearing capacity. Naturally, the actual distributions strongly depend on the static system.

Example 4.6 Panel strip with concentrated load

Determination of the design moment as a consequence of a concentrated load

Details:

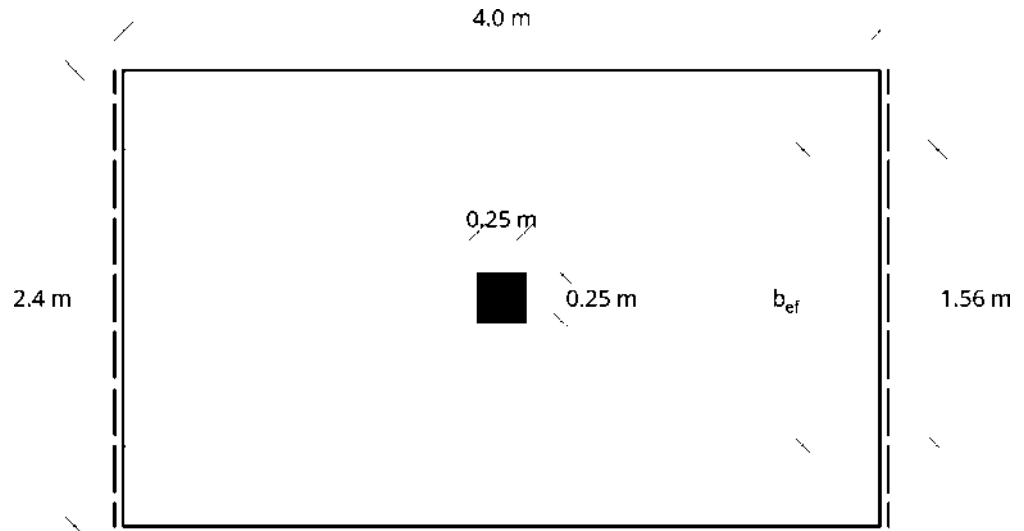
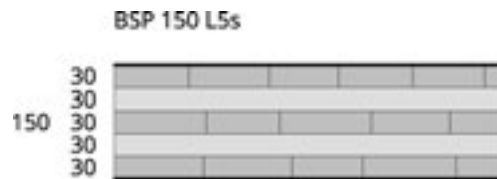


Figure 4.25 Floor with concentrated load

CLT floor panel 150-L5s (30l – 30w – 30l – 30w – 30l)



Bilaterally supported with a span of $\ell_x = 4.0$ m. The width of the floor is $\ell_y = 2.4$ m. A concentrated load $Q_k = 4$ kN acts as a load in the centre of the panel. The contact area is $c_x = c_y = 0.25$ m.

Sought:

Bending moment, bending stress in the main direction of load-bearing capacity, deflection

Cross-sectional values

$$I_{x,net} = I_{0,net} = I_{intrinsic} + I_{steiner} = 3 \cdot \frac{b \cdot d_1^3}{12} + 2 \cdot b \cdot d_1 \cdot z_1^2 = 3 \cdot \frac{100 \cdot 3^3}{12} + 2 \cdot 100 \cdot 3 \cdot 6^2 = 22,275 \text{ cm}^4$$

$$I_{y,net} = I_{90,net} = I_{intrinsic} + I_{steiner} = 2 \cdot \frac{b \cdot d_1^3}{12} + 2 \cdot b \cdot d_1 \cdot z_1^2 = 2 \cdot \frac{100 \cdot 3^3}{12} + 2 \cdot 100 \cdot 3 \cdot 3^2 = 5,850 \text{ cm}^4$$

$$k_{ortho} = \sqrt[4]{\frac{EI_{y,net}}{EI_{x,net}}} = \sqrt[4]{\frac{E \cdot 5,850}{E \cdot 22,275}} = 0.716$$

$$W_{x,net} = \frac{I_{x,net}}{z_{max}} = \frac{22,275}{7.5} = 2,970 \text{ cm}^3$$

Effective panel width

$$b_{M,ef} = (c_y + 0.5 \cdot \ell_x) \cdot k_{ortho} = (0.25 + 0.5 \cdot 4) \cdot 0.7159 = 1.61 \text{ m}$$

Maximum value:

$$b_{M,ef} = 1.61 \text{ m} \leq 0.65 \cdot \ell_y = 0.65 \cdot 2.4 = 1.56 \text{ m}$$

$$b_{M,ef} = 1.56 \text{ m}$$

Bending moment at the single-span beam

$$Q_d = \gamma_Q \cdot Q_k = 1.50 \cdot 4 = 6 \text{ kN}$$

$$M_{m,d} = Q_d \cdot \frac{2 \cdot \ell_x - c_x}{8} = 6 \cdot \frac{2 \cdot 4.0 - 0.25}{8} = 5.82 \text{ kNm}$$

Design moment as internal panel force

$$m_{x,d} = \frac{M_{m,d}}{b_{M,ef}} = \frac{5.82}{1.56} = 3.73 \text{ kNm/m}$$

Bending stress (here without verification of strength)

$$\sigma_{m,d} = \frac{m_{x,d}}{W_{x,net}} = \frac{3.73 \cdot 100}{2.970} \cdot 10 = 1.26 \text{ N/mm}^2$$

Deflection

$$w_{Q,inst} = \frac{1}{b_{M,ef}} \cdot \frac{Q_k \cdot \ell_x^3}{48 \cdot E \cdot I_{x,net}} = \frac{1}{1.56} \cdot \frac{4 \cdot 4^3}{48 \cdot \frac{11,550}{10} \cdot \frac{22,275}{100^2}} \cdot 1,000 = 0.641 \cdot 2.073 \text{ mm}$$

$$w_{Q,inst} = 1.33 \text{ mm}$$

A comparison with a FEM calculation as an orthotropic panel, as described in Chapter 1, results in the following

$$m_{x,d} = \gamma_Q \cdot m_{x,k} = 1.5 \cdot 2.2 = 3.3 \text{ kNm/m}$$

i.e. for the present example, a lower value from the FEM calculation with a deviation of 11 % compared to the manual calculation.

For deflection, the FEM calculation results in

$$w_{Q,inst} = 1.2 \text{ mm}$$

i.e. for this example, a lower value with a deviation of 9 % compared to the manual calculation.

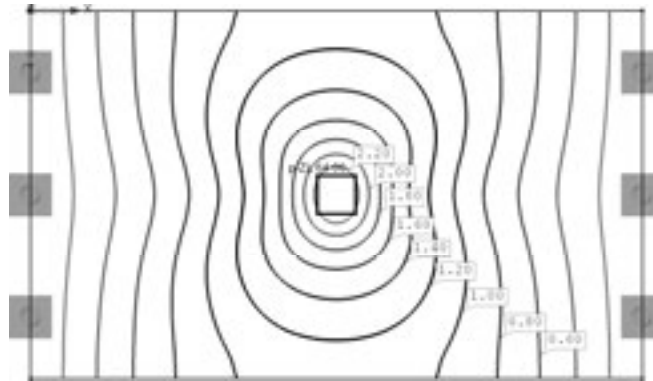


Figure 4.26 Isolines of the bending moments $m_{x,k}$ (characteristic level)

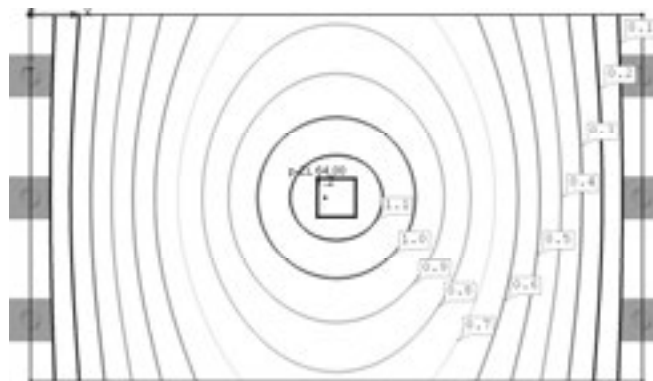


Figure 4.27 Isolines of deflection u_{inst}

4.5.3 Compression perpendicular to grain

Concentrated or linear loads transverse to the floor plane result in compression stresses perpendicular to grain. Upon stressing perpendicular to grain, timber shows an elasto-plastic load-deformation performance, since upon load increase above the elasticity limit, the cells of the timber structure are compressed and plastically deformed. The compression strength perpendicular to grain corresponds to that stress, which is measured in a compression test with a cuboid¹ and results after relief in a permanent deformation of 1 % of the height of the specimen and occurs at about 3 % to 4 % of the total deformation. Upon exceeding this strength value, failure does not yet occur in the compressed element, but the deformation increase progressively and the stiffness decreases. As long as the deformation do not result in design-relevant load redistributions in statically undetermined structures or even result in a loss of equilibrium, the verification of lateral pressure stresses shall be allocated to the verifications of serviceability². For rod-shaped elements, increase factors $k_{c,90}$ were derived therefrom and the respective actual contact length on each side increased by 3 cm into an effective contact length³.

For the dimensioning of the contact areas of load-applying structural elements on CLT floors an analogous approach is recommended. The ultimate limit state of compression perpendicular to grain without increase factors has to be analysed for those cases, where deformations can affect the load-bearing capacity of the structure. In the predominant other cases, the serviceability limit state has to be considered for compression perpendicular to grain. In that, the verification may be lowered to the characteristic load level, in order to keep the deformation at the level according to standard. If higher deformation is permitted upon dimensioning of the structural elements, then the structure shall be adjusted to these higher deformations (e.g. for multi-storey buildings).

In cross-laminated timber stressed by compression perpendicular to grain, the cross layers have a favourable effect due to limited horizontal deformations. The transverse strain of the timber is impeded by the higher extensional stiffness of the transverse layers. Thereby, the deformations as well as the tensile stresses perpendicular to grain are reduced, as shown, in principle, in Figure 4.28.

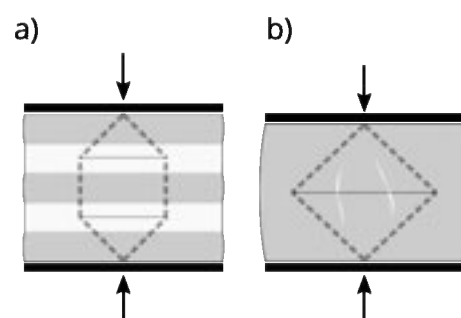


Figure 4.28 Interlocking effect a) cross layers (cross-laminated timber, plywood), b) unidirectional layout (solid wood, glued-laminated timber)

¹ Test description in EN 408. Also see Leijten et al., 2012

² See Blaß, 2004

³ EN 1995-1-1:2015, Section 6.1.5

With locally limited load introduction, the load propagates into a larger area. This likewise has a favourable effect on the compressive resistance perpendicular to grain of cross-laminated timber. Measurements of Halili, 2008 show, in principle, the improvements by the deformation limiting effect at a cube, on the one hand, and the load propagation in a panel of cross-laminated timber only centrally loaded, on the other hand, as shown in Figure 4.29. The increase values stated have to be considered as exemplary test results and do not apply in the general case.

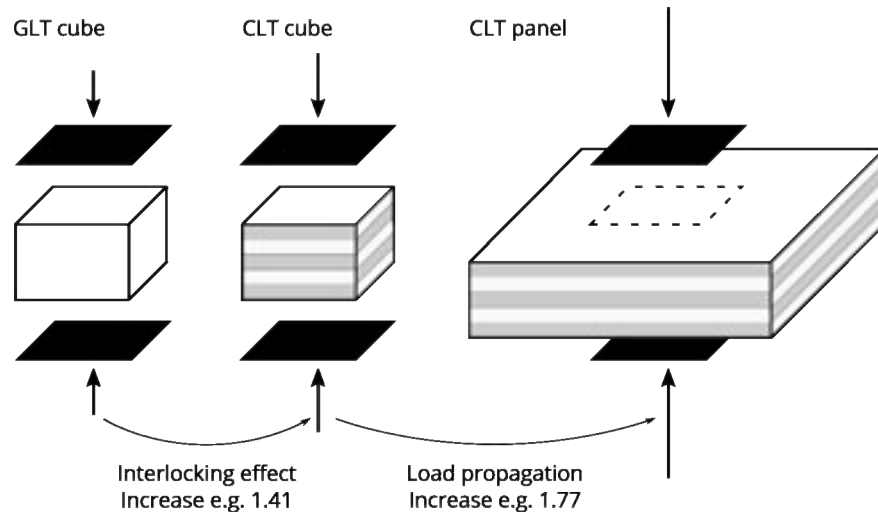


Figure 4.29 Lateral compressive strength of cross-laminated timber with examples for increase factors compared to GLT

The deformation limiting effect allows for an increase of the lateral compressive strength of $f_{c,90,k} = 2.5 \text{ N/mm}^2$ for glued-laminated timber to the 1.2-fold value $f_{c,90,k} = 3.0 \text{ N/mm}^2$ for cross-laminated timber¹.

Via the factor $k_{c,90}$, the real situation in the building is considered. Therefore, the verification of stress is as follows:

$$\sigma_{c,90,d} = \frac{F_d}{A_{90}} \leq k_{c,90} \cdot f_{c,0,d} \quad (4.40)$$

with

F_d Design compressive load perpendicular to the grain

A_{90} Contact area for supports and similar structural elements, and for walls the area including the outermost upright layers, as described in Section 6.3.

$k_{c,90}$ Factor taking into account the load configuration, the possibility of splitting and the degree of compressive deformation

$f_{c,0,d}$ design compressive strength perpendicular to the grain;

¹ ÖNORM B 1995-1-1:2015, Table NA.K.3

In the scientific evaluation of the subject of lateral pressure¹, models for the derivation of the increase factor $k_{c,90}$ on the basis of structural mechanics can be found, for rod-shaped as well as for two-dimensional structural elements. Since at the time of publication of the present volume, lively discussions about the models to be applied are still underway, the determinations from ÖNORM B 1995-1-1:2015, Section K.6.1.5 are taken over until detailed clarification.

For information purposes, formulas for the calculation of the elastic deformations are derived in Section 9.2 and summarised in this section, in order to be able to estimate their influence on the entire structure. With respect to the deformation behaviour, cross-laminated timber has a modulus of elasticity transverse to the fibre of $E_{90,mean} = 450 \text{ N/mm}^2$ – the 1.50-fold value of glued-laminated timber with $E_{90,mean} = 300 \text{ N/mm}^2$.

Table 4-2 Factor $k_{c,90}$ for load propagation in CLT floors

Walls		Supports		
Inside (centred)	Edge	Inside (centred)	Edge	Corner
1.80	1.50	1.80	1.50	1.30

Initial local deformations

The lateral pressure deformation of floors with concentrated or linear loads can be adjusted to the respective cases from the formulas 9.3 and 9.7 of Section 9.2 with the dimensions of Figure 4.30 and Figure 4.31. The deformation values are to be understood as benchmarks for the initial elastic deformation and can be considered as a decision-making aid for the execution of structural measures. As an example for such measures, exterior aperture plates for the transmission of tensile forces from an upper to a lower wall are to be stated.

Pischl, 2007 suggests considering displacements as a consequence of unavoidable inaccuracies in manufacture via a slack deformation $w_{slack} = 1.0 \text{ mm}$. Tests show that the final deformations as a consequence of lateral pressure depend more strongly on the wood moisture content than with other stresses. Therefore, higher k_{def} values than with other stresses shall be assumed. As an assumption in an approximate fashion, the values of the respectively higher utilisation class can be used (e.g. $k_{def} = 1.0$ for NKL 1 and $k_{def} = 2.0$ for NKL 2) until detailed clarification.

¹ Van der Put, 2008

Initial local deformations upon load passage of supports

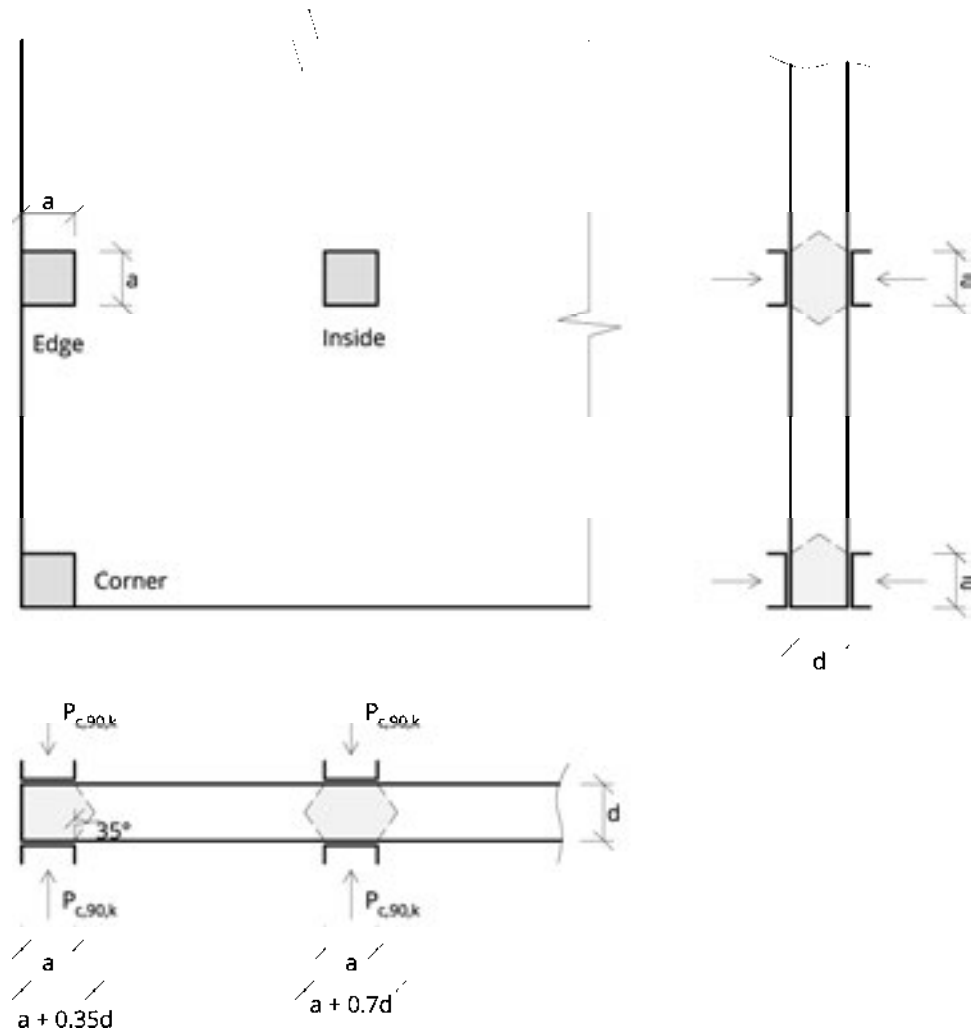


Figure 4.30 Assumed lateral pressure distribution for supports

Deformation with concentrated loads for load passages of supports in the interior (i.e. at least at the distance of the floor thickness away from the edge).

Assumption of even load propagation in both directions.

$$w_{inst} = w_{slack} + w_{el} = 1 \text{ mm} + \frac{P_{c,90,k} \cdot d}{E_{90,mean}} \cdot \frac{1}{a \cdot (a + 0.70 \cdot d)} \quad (4.41)$$

Deformation with concentrated loads for load passages of supports at the edge.

Assumption of uneven load propagation in both directions.

$$w_{inst} = w_{slack} + w_{el} = 1 \text{ mm} + \frac{P_{c,90,k} \cdot d}{E_{90,mean}} \cdot \frac{\ln\left(\frac{a + 0.70 \cdot d}{a + 0.35 \cdot d}\right)}{0.35 \cdot a \cdot d} \quad (4.42)$$

Deformation with concentrated loads for load passages of supports in the corner.

Assumption of even load propagation in both directions.

$$w_{inst} = w_{slack} + w_{el} = 1 \text{ mm} + \frac{P_{c,90,k} \cdot d}{E_{90,mean}} \cdot \frac{1}{a \cdot (a + 0.35 \cdot d)} \quad (4.43)$$

with

d Floor thickness

a Cross-sectional dimension of the square support

$P_{c,90,k}$ Characteristic value of the compressive load to be passed through

$E_{90,mean}$ Mean modulus of elasticity perpendicular to grain

The end deformation is respectively calculated as follows

$$w_{fin} = w_{inst} \cdot (1 + k_{def}) \quad (4.44)$$

Local deformations upon load passage of walls

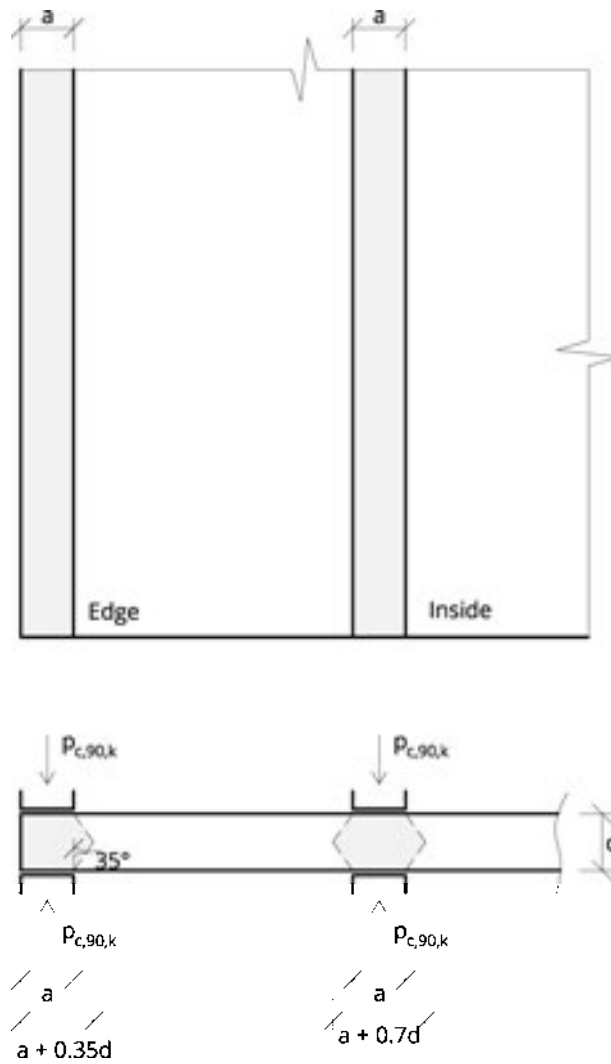


Figure 4.31 Assumed propagation of compression load for walls

Deformation with load passages of walls in the interior

$$w_{inst} = w_{slack} + w_{el} = 1 \text{ mm} + \frac{p_{c,90,k} \cdot t}{E_{90,mean}} \cdot \frac{\ln\left(\frac{a + 0.70 \cdot d}{a}\right)}{0.70 \cdot d} \quad (4.45)$$

Deformation with load passages of walls in the edge area

$$w_{inst} = w_{slack} + w_{el} = 1 \text{ mm} + \frac{p_{c,90,k} \cdot t}{E_{90,mean}} \cdot \frac{\ln\left(\frac{a + 0.35 \cdot d}{a}\right)}{0.35 \cdot d} \quad (4.46)$$

with

d Floor thickness

a Thickness of the wall

$q_{c,90,k}$ Characteristic value of compressive load per running metre of wall

$E_{90,mean}$ Mean modulus of elasticity perpendicular to grain

The end deformation is respectively calculated as follows

$$w_{fin} = w_{inst} \cdot (1 + k_{def}) \quad (4.47)$$

Example 4.7 Load passages of supports

Given:

Floor CLT 150 L5s (30l-30w-30l-30w-30l)

Sought:

Verification of the lateral compressive stresses for the passage of loads of supports with a cross-section of 14/14 cm and the characteristic value of axial force in the lower support $N_k = 35$ kN or the design value of $N_d = 49$ kN, resp., with $k_{mod} = 0.9$.

Estimation of deformation.

It is assumed in a simplified fashion, that at the top of the floor panel, the same force N acts as at the bottom. Naturally, the force acting from the top is lower by a portion from loads transmitted from the floor to the lower support. In good approximation, for the deformation calculation, the quantity of the lower force may also be applied for the upper load. With this assumption, no separation between portions from load passage from support to support and load application from floor to support is required.

Load passage from support to support

For the contact area of the support applies

$$a = 14 \text{ cm}$$

$$A = a^2 = 14^2 = 196 \text{ cm}^2$$

The characteristic compressive strength parallel to grain is

$$f_{c,0,k} = 3.0 \text{ N/mm}^2$$

$$f_{c,0,d} = k_{mod} \cdot \frac{f_{c,0,k}}{\gamma_M} = 0.9 \cdot \frac{3}{1.25} = 2.16 \text{ N/mm}^2$$

Verification

$$\sigma_{c,90,d} = \frac{N_d}{A_{90}} \leq k_{c,90} \cdot f_{c,0,d}$$

For **supports in the interior** applies $k_{c,90} = 1.80$

$$\sigma_{c,90,d} = \frac{49}{196} \cdot 10 \leq 1.80 \cdot 2.16$$

$$2.5 \text{ N/mm}^2 \leq 3.89 \text{ N/mm}^2$$

✓ Verification fulfilled ($\eta = 64$ %)

For **supports at the edge** applies $k_{c,90} = 1.50$

$$\sigma_{c,90,d} = 2.5 \text{ N/mm}^2 \leq 1.50 \cdot 2.16$$

$$2.5 \text{ N/mm}^2 \leq 3.24 \text{ N/mm}^2$$

✓ Verification fulfilled ($\eta = 77\%$)

For **supports in the corner** applies $k_{c,90} = 1.30$

$$\sigma_{c,90,d} = 2.5 \text{ N/mm}^2 \leq 1.30 \cdot 2.16$$

$$2.5 \text{ N/mm}^2 \leq 2.81 \text{ N/mm}^2$$

✓ Verification fulfilled ($\eta = 89\%$)

Initial deformations to be expected

$$E_{90,mean} = 450 \text{ N/mm}^2$$

Supports in the interior

$$w_{inst} = w_{slack} + w_{el} = 1 \text{ mm} + \frac{P_{c,90,k} \cdot d}{E_{90,mean}} \cdot \frac{1}{a \cdot (a + 0.70 \cdot d)}$$

$$w_{inst} = w_{slack} + w_{el} = 1 \text{ mm} + \frac{35 \cdot 1000 \cdot 150}{450} \cdot \frac{1}{140 \cdot (140 + 0.70 \cdot 150)}$$

$$w_{inst} = w_{slack} + w_{el} = 1 \text{ mm} + 0.34 \text{ mm} = 1.34 \text{ mm}$$

This corresponds to an elastic compression of

$$\varepsilon_{el} = \frac{1.34}{150} = 0.89\%$$

Supports at the edge

$$w_{inst} = w_{slack} + w_{el} = 1 \text{ mm} + \frac{P_{c,90,k} \cdot d}{E_{90,mean}} \cdot \frac{\ln\left(\frac{a + 0.70 \cdot d}{a + 0.35 \cdot d}\right)}{0.35 \cdot a \cdot d}$$

$$w_{inst} = w_{slack} + w_{el} = 1 \text{ mm} + \frac{35 \cdot 1000 \cdot 150}{450} \cdot \frac{\ln\left(\frac{140 + 0.70 \cdot 150}{140 + 0.35 \cdot 150}\right)}{0.35 \cdot 140 \cdot 150}$$

$$w_{inst} = w_{slack} + w_{el} = 1 \text{ mm} + \frac{35 \cdot 1000 \cdot 150}{450} \cdot \frac{0.241}{0.35 \cdot 140 \cdot 150}$$

$$w_{inst} = w_{slack} + w_{el} = 1 \text{ mm} + 0.38 \text{ mm} = 1.38 \text{ mm}$$

This corresponds to a compression of

$$\varepsilon_{el} = \frac{1.38}{150} = 0.92\%$$

Supports in the corner

$$w_{inst} = w_{slack} + w_{el} = 1 \text{ mm} + \frac{P_{c,90,k} \cdot d}{E_{90,mean}} \cdot \frac{1}{a \cdot (a + 0.35 \cdot d)}$$

$$w_{inst} = w_{slack} + w_{el} = 1 \text{ mm} + \frac{35 \cdot 1000 \cdot 150}{450} \cdot \frac{1}{140 \cdot (140 + 0.35 \cdot 150)}$$

$$w_{inst} = w_{slack} + w_{el} = 1 \text{ mm} + 0.43 \text{ mm} = 1.43 \text{ mm}$$

This corresponds to a compression of

$$\varepsilon_{el} = \frac{1.43}{150} = 0.95 \%$$

5 Ribbed plate

When using ribbed plates, an increase in stiffness of roofs and floors is possible with low material consumption and consequently an increase of the spans. The CLT panels are arranged with their outer layers in parallel to the direction of span. The ribs normally consist of glued-laminated timber and are rigidly connected with the CLT panel at the factory under controlled conditions in presses or by screw-press gluing. Thereby, from a static point of view, each of the ribs forms a T-cross-section with its associated effective part of the CLT panel. Upon standard application with ribs at the bottom of the CLT plate, compressive stresses become effective in the plate, while the ribs are predominantly subjected to tension and therefore expediently consist of glued-laminated timber with a combined layup.

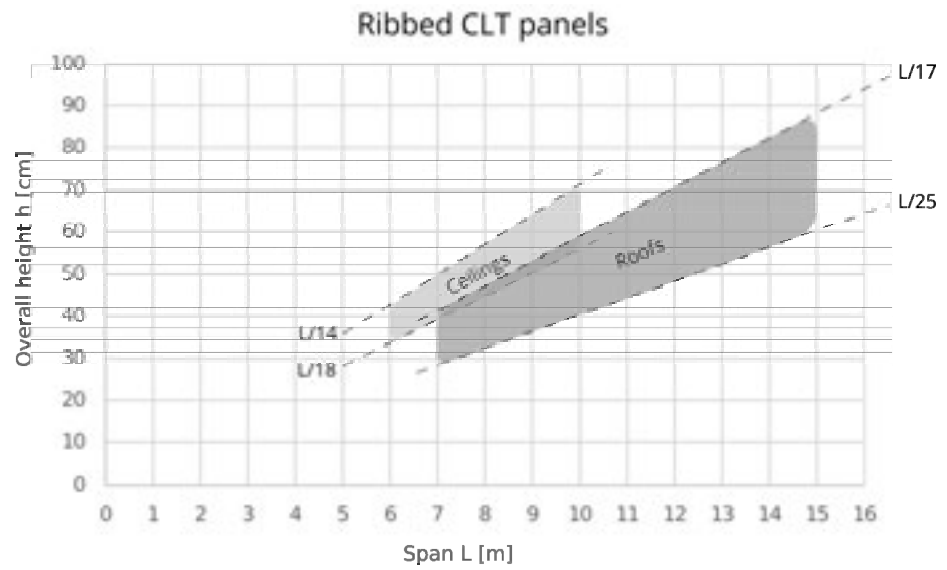
Between the ribs, installations can be inserted or acoustic panels arranged. Mounting of the ribbed plates is undertaken either by direct positioning of the ribs on a transverse beam or on a wall cut out in the form of the ribbed cross-section, by mounting on transverse end beams or by mounting of the sufficiently dimensioned plate with notched ribs. If the ribs are notched, then detachment of the ribs from the panel shall be avoided by mandatory reinforcement with vertically arranged screws as close to the rib end as possible. The screws shall be dimensioned for end reaction forces in an approximate fashion.

Failure of the pressure zone from cross-laminated timber is normally not decisive, since the panels are sufficiently compact.

The assumptions stated accordingly apply to box elements with upper and lower panels. In the hollow spaces of box elements, the spreading of fire shall be prevented and undesired amounts of water from emergency drainage shall be avoided. The disadvantages of hollow spaces, which cannot be inspected or only with increased effort, should be considered and, for example, inspection openings arranged.

5.1 Pre-design

With respect to the economic spans, there shall be a differentiation between roofs and floors, since normally higher loads act on floors and, in addition to the deflection requirements, vibration requirements shall also be fulfilled.



5.1.1 Recommendations for roofs

The element joint of ribbed plates for roofs is frequently executed between the ribs, as shown in Figure 5.1.

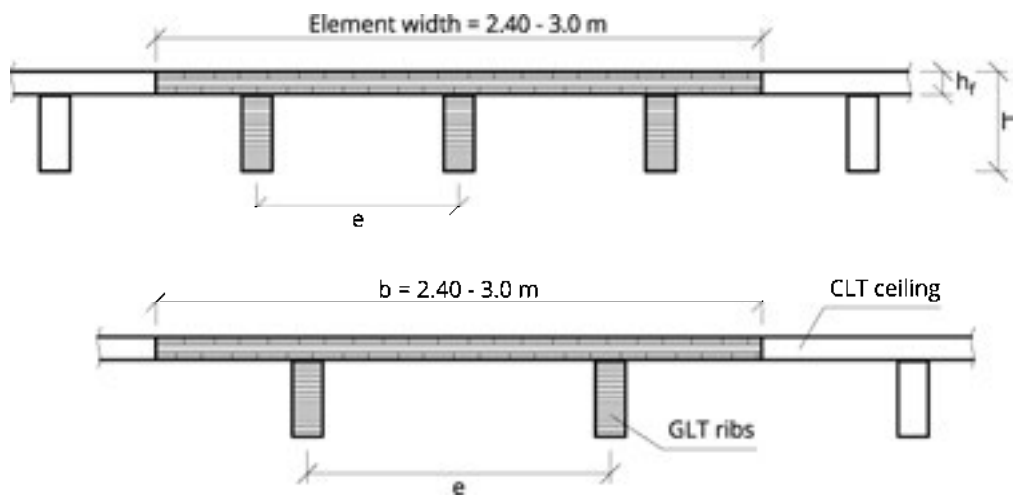


Figure 5.1 Ribbed plates with narrow and wide rib distances for roofs with joint of the CLT elements

Economic and structurally sensible areas for ribbed panels as roof elements are:

Economic spans: $L = 7.0$ to 15.0 m

Overall height: $h = \frac{L}{25}$ to $\frac{L}{17}$

Centre distance of the ribs: $e = 60$ to 120 cm

Panel thickness:
$$h_f = \max \begin{cases} \frac{e}{10} \text{ to } \frac{e}{5} \\ \frac{h}{4} \text{ to } \frac{h}{3} \\ \geq 9 \text{ cm} \end{cases}$$

The joint design is determined by profitability considerations with respect to assembly and structural requirements. In case of ribbed plates for roofs, joints can be executed as for plates without ribs and depending on the static structural requirements according to one of the variants in Figure 5.2.



Figure 5.2 Design proposals for the joint of the CLT elements

5.1.2 Recommendations for floors

Ribbed plates for floors are frequently executed with divided ribs, as shown in Figure 5.3.

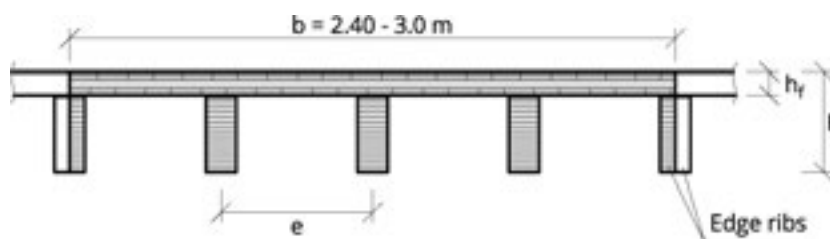


Figure 5.3 Ribbed plates for floors with joint in the edge ribs

Economic and structurally sensible areas for ribbed plates as floors are:

Economic spans: $L = 6.0$ to 9.0 m

Overall height: $h = \frac{L}{18}$ to $\frac{L}{14}$

Centre distance of the ribs: $e = 60$ to 80 cm

Plate thickness:
$$h_f = \max \begin{cases} \frac{e}{10} \text{ to } \frac{e}{5} \\ \frac{h}{4} \text{ to } \frac{h}{3} \\ \geq 9 \text{ cm} \end{cases}$$

Figure 5.4 shows possible designs for floors. For the connecting joints between the edge ribs, a design is recommended, which enables possible cupping of the plate in the construction phase without constraints.

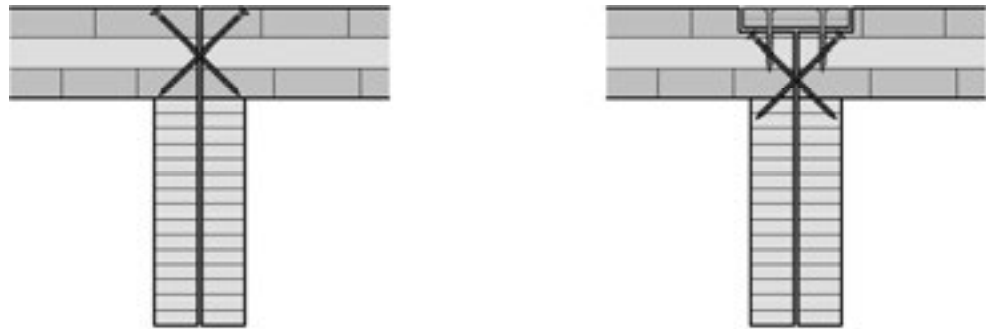


Figure 5.4 Design proposals for the design of the joint
a) for transmission of lateral joint forces
b) for transmission of tensile and lateral joint forces

5.2 Effective widths

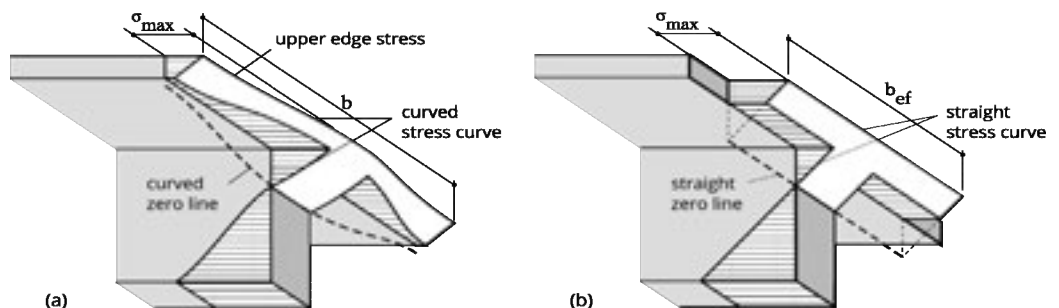


Figure 5.5 Effective width with (a) the actual stress distribution and (b) the linear stress distribution and effective width

Figure 5.5 shows the non-linear distribution of the bending stresses in a plate with a rib on the basis of Leonhardt, 1973. In order to attribute the problem to the beam theory with the assumption of a linear distribution of stresses, the effective width b_{ef} of the panel is determined such that the maximum edge stress in the panel σ_{max} is equal to the non-linear case.

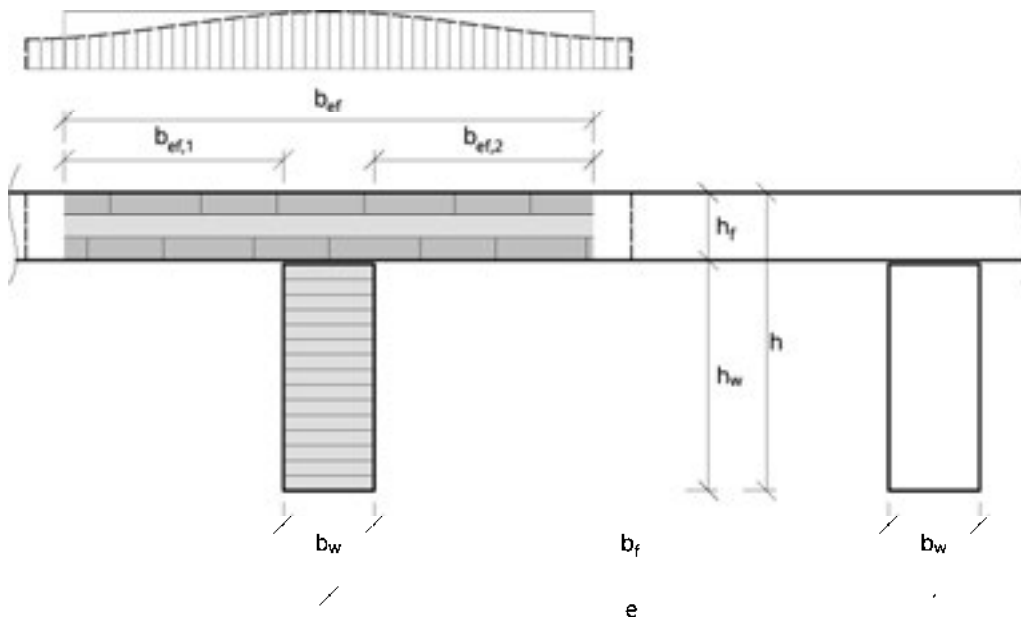


Figure 5.6 Distribution of compressive stresses in the pressure panel and effective width

In general, the effective width is calculated as the sum of the rib width and the plate portions to the left and right of the rib.

$$b_{ef} = \sum b_{ef,i} + b_w \quad (5.1)$$

5.2.1 Bending

Uniformly distributed loads:

The effective plate portions to the left and right of the rib considered can be determined for the verification of bending stresses in the span and the verification of serviceability of single-span beams and multi-span beams under predominantly uniform load according to Formula 5.2. On the basis of concrete construction, the formula was made dependent on the span and the clear rib distance. In order to take the orthotropy into consideration, the ratio of extensional stiffness and shear stiffness of the plate is furthermore included. The exponents result from the adjustment via variants of ribbed plates relevant in building practice. The background is summarised in Augustin et al., 3/2017.

$$b_{ef,i} = b_f \cdot \left\{ 0.5 - 0.35 \cdot \left(\frac{b_f}{\ell} \right)^{0.90} \cdot \left(\frac{EA_0}{S_{xy}^2} \right)^{0.45} \right\} \quad (5.2)$$

Depending on the ratios of geometry and stiffness, a fluctuation range results for the effective width with the effect of uniformly distributed loads

$$b_{ef,i} = b_f \cdot \{0.11 \text{ to } 0.45\} \quad (5.3)$$

Concentrated loads:

For the effective plate portions to the left and right of the rib considered, the following applies for the verification of bending stresses in the span and the verification of serviceability of single-span and multi-span beams and the verification of bending stress in the support area of multi-span beam under concentrated loads:

$$b_{ef,i} = \begin{cases} h_f \geq \frac{h_w}{2}: & b_f \cdot \left\{ 0.5 - 0.40 \cdot \left(\frac{b_f}{\ell}\right)^{0.15} \cdot \left(\frac{EA_0}{S_{xy}^*}\right)^{0.10} \right\} \\ h_f < \frac{h_w}{2}: & b_f \cdot \left\{ 0.5 - 0.275 \cdot \left(\frac{b_f}{\ell}\right)^{0.30} \cdot \left(\frac{EA_0}{S_{xy}^*}\right)^{0.30} \right\} \end{cases} \quad (5.4)$$

with

EA_0 Extensional stiffness of the CLT element in the longitudinal direction

S_{xy}^* Shear stiffness of the plate of the CLT element according to ÖNORM B 1995-1-1:2015, Formula (NA.K.1) or in Formula (7.3), resp.

ℓ Span of the single-span beam or reference length between the zero-crossings of moments, resp.

For verifications in the span of multi-span beams $\ell = 0.8 \cdot \ell_{span}$,

for verifications over central supports $\ell = 0.4 \cdot \ell_{span}$,

for cantilevers $\ell = 2 \cdot \ell_{cant}$.

b_f Clear distance between the ribs

h_w Height of the ribs

h_f Height of the CLT plate

5.2.2 Shear

Due to the local effect from the load application problem in the CLT panel, higher shearing stresses occur locally in the support area than those resulting according to the technical bending theory. Therefore, for the determination of the maximum rolling shear stress, a small effective width is applied for the panel.

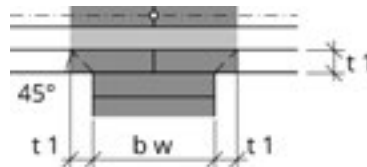


Figure 5.7 Effective width for the verification of shear over supports

For the effective width, as shown in Figure 5.7, the rib width plus the thickness of the outer layer of the CLT panel are assumed; the distribution angle for the bottommost

layer is approximately 45°. This assumption was verified using FE simulations and, compared to more exact models, results in acceptable deviations on the safe side.

$$b_{ef} = 2 t_1 + b_w \quad (5.5)$$

5.3 Modelling

Calculation of the ribbed plates is normally undertaken as a beam with T-cross-section, consisting of a rib and the panel in the effective panel width. As calculation models, the two methods described in the following are expedient. Alternative methods, as FEM models or the shear analogy method, may likewise be applied.

5.3.1 Rib cross-section as shear-flexible beam

Modelling as a shear-flexible beam is suitable for rib cross-sections with a rigid, i.e. glued joint. In the ultimate limit state (ULS), the cross-sectional values for the rigid compound are used. The stress verifications are undertaken with the net cross-sectional values. In the serviceability limit state of (SLS), the portion of shear deformation shall be considered via the shear stiffness and the shear correction factor.

The shear correction factor for ribbed plates can be generally calculated with the method described in Annex A.2 of Volume 1. As a good estimate, the formula for the shear correction factor resulting from comprehensive comparative calculations may be applied:

$$\alpha = \frac{1}{1.2} - 0.25 \cdot \frac{\left(\frac{b_{ef}}{b_w}\right)^{0.70}}{k_{rib}^{0.5}} \quad (5.6)$$

with

b_{ef} Effective width

b_w Width of the rib

k_{rib} Proportion factor

$$k_{rib} = \frac{h_w}{h_f}$$

5.3.2 Rib cross-section as flexibly connected beam

Modelling as flexibly connected cross-section elements can be used for rigid, i.e. glued joints and for flexibly designed joints with mechanical fasteners.

The calculation is undertaken with the general gamma method according to Schelling, as described in Annex A.1 of Volume 1.

The verifications in the ultimate limit states (ULS) as well as the verifications in the serviceability limit states (SLS) are undertaken with the effective cross-sectional values. Upon execution with mechanical fasteners, their arrangement shall be according to ÖNORM EN 1995-1-1:2015, Annex B for flexibly connected flexural beam.

5.4 Screw-press gluing

In gluing, the biaxial panel stiffness of cross-laminated timber has a favourable effect on the load distribution from the screw head into the glue line. Screw-press gluing can

be undertaken on the basis of ÖNORM B 1995-1-1:2015, Annex H. Deviating from the standard specification, panels with a larger thickness can be used, since the distribution of pressing becomes more favourable with increasing thickness or stiffness, resp., if parallel and planar contact surfaces can be assured.

With admissible glue line thicknesses of no more than 0.3 mm, use of an adhesive according to ÖNORM EN 15425, ÖNORM EN 301 or ÖNORM EN 302, Type I is possible.

The surfaces to be glued shall be sanded or planed and free from dust and other contaminations. The requirements of the adhesive manufacturer shall be observed. The difference in moisture content of the parts to be glued together shall be max. 5 % and the wood moisture content of the parts to be glued together shall be coordinated with the adhesive used. The screw-press gluing shall be performed by qualified personnel and requires, as any bonding operation, particular diligence and documentation.

The screw connection should be undertaken with partially threaded screws TGS with a minimum diameter $d = 6$ mm and an embedded depth of the screw tip of at least $7d$ or at least the thickness of the part to be glued on, resp. As screws, washer head screws or screws with respective washers shall be used. The head diameter should have the following proportion to the outer thread diameter: $d_{head} \geq 2.4 \cdot d$.

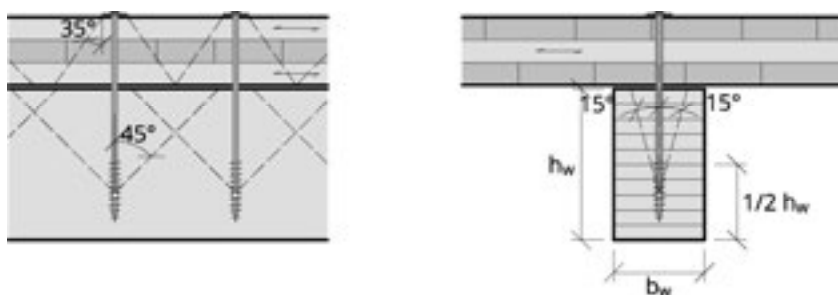


Figure 5.8 Screw-press gluing

The length of the screws shall be determined considering the force propagation angles from the screw head or from the centre of the thread, resp. As propagation angle of the screw's tensile forces from the head and the centre of gravity of the thread in the glue line, an angle of 35° can be assumed for CLT. In glued-laminated timber, 45° in the direction of fibre and 15° transverse to the fibre is assumed, as shown in Figure 5.8.

Ongoing tests show that the load distribution of the relatively stiff CLT panels is favourable. Pending reliable research results, according to the standard, at least one screw per 150 cm² of glued surface shall be arranged at a distance of max. 15 cm to the next screw. According to the standard, the edge distance of the screws to the unloaded end shall be limited with $a \leq 10 \cdot d$.

Element tolerances may result in the fact that the element surfaces to be bonded are not located in one plane, as indicated in Figure 5.9. Comparative calculations resulted in the fact that element curvatures of the adherends with common dimensions tolerated by standards (see e.g. EN 14081) can be compensated by partially threaded screws (TGS $d=8$ mm) according to the specification above.

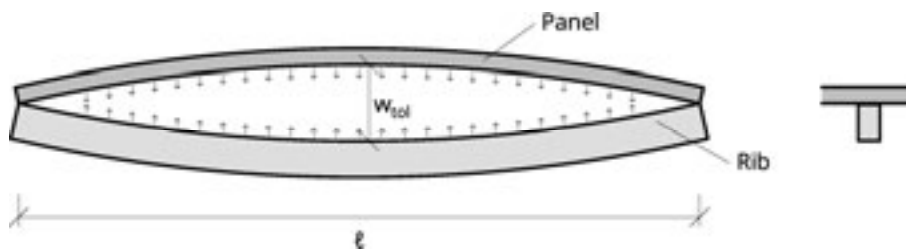


Figure 5.9 Compensation of tolerances by the screws

5.5 Local loads

Transverse to the direction of span of the ribbed plates, it's the task of the CLT plate, among other things, to distribute concentrated live loads onto the ribs. The static system is a plate strip with orthotropic properties. Upon compliance with the rib distances according to Section 5.1, the load-bearing capacity as well as sufficient stiffness of the plate are normally given for these concentrated loads.

More exact calculations of such panel strips under concentrated loads may be undertaken according to Section 9.2.

Example 5.1 Ribbed plate

The ribbed plate of the following calculation example consists of a GLT beam with the dimensions 160×320 mm and a 5-layer CLT panel with a constant layer thickness of 30 mm ($t_{\text{CLT}} = 150$ mm; 30-30-30-30-30 mm). The centre distance of the GLT ribs is $s = 0.660$ m. The static system is a single-span beam with the length $L = 8.10$ m. As construction materials, GL32c according to EN 14080:2013 is used for the GLT beam, and the characteristic material values according to Section 3.1 for the CLT plate. The ribbed plate is loaded by the dead weight $g_{1,k}$, the permanent load $g_{2,k} = 4.58$ kN/m² and a live load of Category C with $q_k = 5.00$ kN/m².

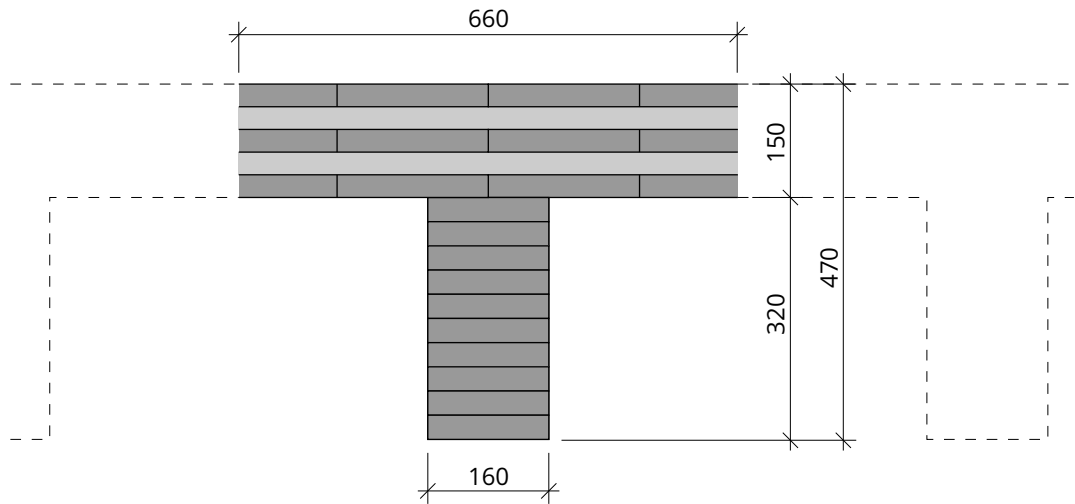


Figure 5.10 Cross-section of the ribbed plate (dimensions in mm)

Characteristic plate values

Material parameters for the CLT plate:

$$E_{0,\text{lay,mean}} = 11,550 \text{ N/mm}^2$$

$$E_{90,\text{lay,mean}} = 0$$

$$G_{0,\text{lay,mean}} = 690 \text{ N/mm}^2$$

$$G_{r,\text{lay,mean}} = 65 \text{ N/mm}^2$$

Extensional stiffness in longitudinal direction:

$$D_x = 3 \cdot 0.03 \cdot 11,550 \cdot 10^3 = 1.04 \cdot 10^6 \text{ kN/m}$$

Extensional stiffness in transverse direction:

$$D_y = 2 \cdot 0.03 \cdot 11,550 \cdot 10^3 = 6.93 \cdot 10^5 \text{ kN/m}$$

Shear stiffness of the plate according to ÖNORM B 1995-1-1:2015:

$$S_{xy}^* = \frac{690 \cdot 10^3 \cdot 0.15}{1 + 6 \cdot 0.43 \cdot \left(\frac{0.03}{0.15}\right)^{1.21}} = 7.57 \cdot 10^4 \text{ kN/m}$$

Effective width

Ratio of span to rib distance:

$$\frac{L}{s} = \frac{8.10}{0.660} = 12.3$$

Ratio of span to overall height:

$$\frac{L}{h} = \frac{8.10}{0.470} = 17.2$$

Clear rib distance:

$$b_f = 0.660 - 0.160 = 0.500 \text{ m}$$

Ratio of rib height to panel thickness:

$$\frac{h_w}{h_f} = \frac{0.32}{0.15} = 2.13$$

For the uniformly distributed load or the span area, resp.:

$$b_{\text{ef},F} = 0.160 + 2 \cdot 0.25 \cdot \left\{ 1.0 - 0.70 \cdot \left(\frac{0.500}{8.10} \right)^{0.90} \cdot \left(\frac{1.04 \cdot 10^6}{7.57 \cdot 10^4} \right)^{0.45} \right\} = 0.567 \text{ m}$$

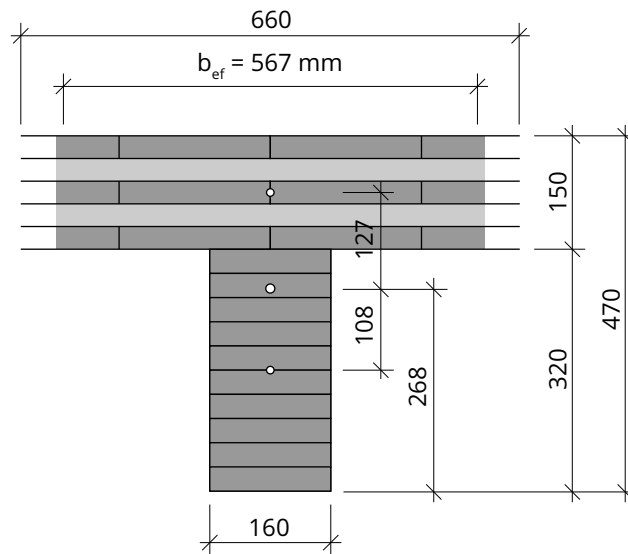
For the concentrated load or the support area, resp.:

$$b_{\text{ef},S,2} = 0.160 + 2 \cdot 0.25 \cdot \left\{ 1.0 - 0.80 \cdot \left(\frac{0.500}{8.10} \right)^{0.15} \cdot \left(\frac{1.04 \cdot 10^6}{7.57 \cdot 10^4} \right)^{0.10} \right\} = 0.318 \text{ m}$$

$$b_{\text{ef},S,3-5} = 0.160 + 2 \cdot 0.25 \cdot \left\{ 1.0 - 0.55 \cdot \left(\frac{0.500}{8.10} \right)^{0.30} \cdot \left(\frac{1.04 \cdot 10^6}{7.57 \cdot 10^4} \right)^{0.30} \right\} = 0.398 \text{ m}$$

Linear interpolation for $\frac{h_w}{h_f}$ between 2 and 3:

$$b_{\text{ef},S} = 0.318 + \frac{0.398 - 0.318}{3.00 - 2.00} \cdot (2.13 - 2.00) = 0.328 \text{ m}$$

Cross-sectional values in the span area

Figure 5.11 Cross-section of a rib in the span area (dimensions in mm)

Calculation of the position of the centre of gravity:

$$z_s = \frac{160 \cdot 320 \cdot 160 \cdot 13,500 + 567 \cdot 3 \cdot 30 \cdot (320 + 75) \cdot 11,550}{160 \cdot 320 \cdot 13,500 + 567 \cdot 3 \cdot 30 \cdot 11,550} = 268 \text{ mm}$$

$$e = \frac{320}{2} + \frac{150}{2} = 235 \text{ mm}$$

$$e_w = 268 - \frac{320}{2} = 108 \text{ mm}$$

$$e_f = 320 + \frac{150}{2} - 268 = 127 \text{ mm}$$

Bending stiffness:

$$\begin{aligned} (EI)_{ef} &= 13,500 \cdot \left[\frac{160 \cdot 320^3}{12} + 160 \cdot 320 \cdot 108^2 \right] + \\ &+ 11,550 \cdot \left[\frac{3 \cdot 567 \cdot 30^3}{12} + 567 \cdot 30 \cdot \left(150 - \frac{30}{2} + 320 - 268 \right)^2 \right] + \\ &+ 567 \cdot 30 \cdot \left(150 - \frac{30}{2} - 60 + 320 - 268 \right)^2 + 567 \cdot 30 \cdot \left(\frac{30}{2} + 320 - 268 \right)^2 \Big] = \\ &= 13,500 \cdot 1.03 \cdot 10^9 + 11,550 \cdot 9.49 \cdot 10^8 = 2.49 \cdot 10^{13} \text{ Nmm}^2 \end{aligned}$$

Shear correction factor (approximation formula):

$$\kappa = \frac{1}{1.2} - 0.25 \cdot \frac{\left(\frac{567}{160} \right)^{0.7}}{2.13^{0.5}} = 0.418$$

Shear stiffness:

$$(GA)_{ef} = 0.418 \cdot (3 \cdot 690 \cdot 567 \cdot 30 + 2 \cdot 65 \cdot 567 \cdot 30 + 650 \cdot 160 \cdot 320) = 2.96 \cdot 10^7 \text{ N} \\ = 2.958 \cdot 10^4 \text{ kN}$$

Cross-sectional values in the support area

The transition from the GLT rib to the CLT plate is a local load application problem. Here, higher shearing stresses occur locally in the CLT plate than would result according to the technical bending theory. Therefore, for the determination of the maximum rolling shear stress, it is suggested to use an effective width in the size of the GLT beam width plus a distribution width of the bottommost outer layer of the CLT panel oriented in parallel to the GLT axis. In that, the load distribution angle is assumed with 45° . The suggested method of calculation is verified using a FE calculation and resulted in acceptable deviations.

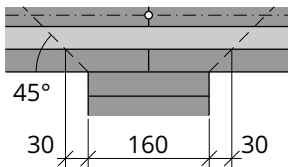


Figure 5.12 Effective width for the determination of the shear or rolling shear stresses, resp. (dimensions in mm)

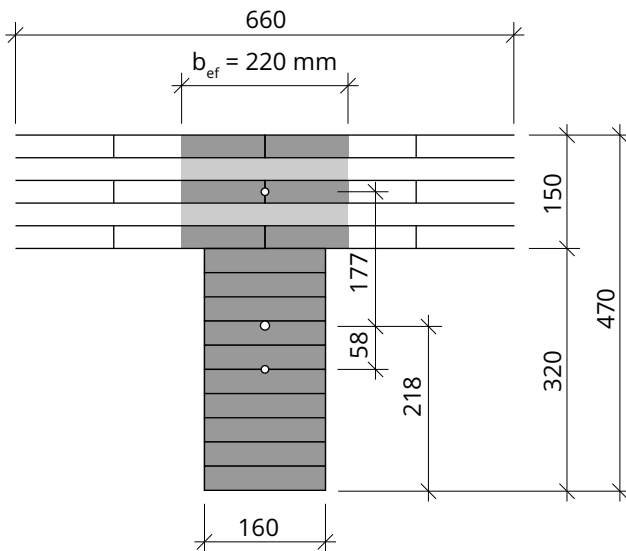


Figure 5.13 Cross-section of a rib in the support area

Calculation of the position of the centre of gravity:

$$z_s = \frac{160 \cdot 320 \cdot 160 \cdot 13,500 + 220 \cdot 3 \cdot 30 \cdot (320 + 75) \cdot 11,550}{160 \cdot 320 \cdot 13,500 + 220 \cdot 3 \cdot 30 \cdot 11,550} = 218 \text{ mm}$$

$$e = \frac{320}{2} + \frac{150}{2} = 235 \text{ mm}$$

$$e_w = 218 - \frac{320}{2} = 58 \text{ mm}$$

$$e_f = 320 + \frac{150}{2} - 218 = 177 \text{ mm}$$

Bending stiffness:

$$\begin{aligned} (EI)_{ef} &= 13,500 \cdot \left[\frac{160 \cdot 320^3}{12} + 160 \cdot 320 \cdot 58^2 \right] + \\ &+ 11,550 \cdot \left[\frac{3 \cdot 220 \cdot 30^3}{12} + 220 \cdot 30 \cdot \left(150 - \frac{30}{2} + 320 - 218 \right)^2 \right] + \\ &+ 220 \cdot 30 \cdot \left(150 - \frac{30}{2} - 60 + 320 - 218 \right)^2 + 220 \cdot 30 \cdot \left(\frac{30}{2} + 320 - 218 \right)^2 \Big] = \\ &= 13,500 \cdot 6.09 \cdot 10^8 + 11,550 \cdot 6.69 \cdot 10^8 = 1.59 \cdot 10^{13} \text{ Nmm}^2 \end{aligned}$$

Load

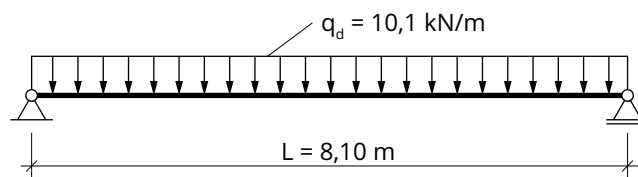


Figure 5.14 System and loads

The dead weight of the ribbed plate is $g_{1,k} = (0.660 \cdot 0.150 + 0.160 \cdot 0.320) \cdot 5.50 = 0.826 \text{ kN/m}$. The characteristic value of the permanent load results in $g_{2,k} = 4.58 \text{ kN/m}^2$ (build-up). This and the live load $q_k = 5.00 \text{ kN/m}^2$ have an impact over the entire width s . Thus, $g_{2,k} \cdot s = 3.02 \text{ kN/m}$ and $q_k \cdot s = 3.30 \text{ kN/m}$ results as the line load of the ribbed plate.

Thus, the load of the ribbed plate is $q_d = 1.35 \cdot (0.826 + 3.02) + 1.50 \cdot 3.30 = 10.1 \text{ kN/m}$.

Verifications in the ultimate limit state (ULS)

Bending stress verification

Maximum bending moment in the centre of span:

$$M_{y,\max} = \frac{10.1 \cdot 8 \cdot 10^2}{8} = 82.8 \text{ kNm}$$

Bending edge stresses:

$$\sigma_{o,\max} = \frac{82.8 \cdot 10^6}{2.49 \cdot 10^{13}} \cdot (268 - 470) \cdot 11,550 = -7.76 \text{ N/mm}^2$$

$$\sigma_{u,\max} = \frac{82.8 \cdot 10^6}{2.49 \cdot 10^{13}} \cdot 268 \cdot 13,500 = 12.0 \text{ N/mm}^2$$

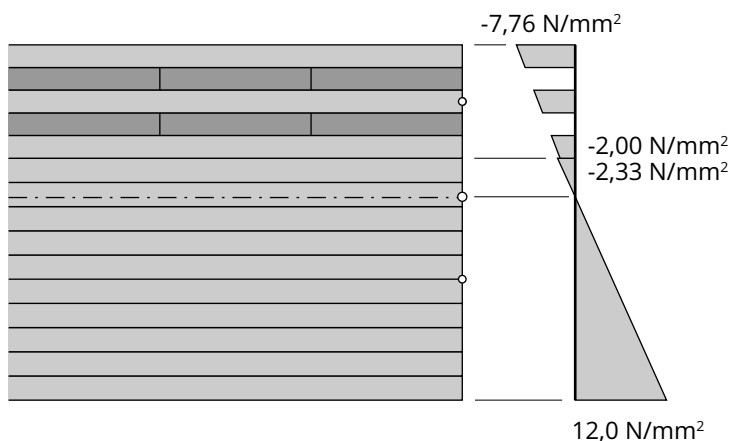


Figure 5.15 Progression of the normal stresses

Verification of normal bending stresses in the GLT beam:

$$12.0 \text{ N/mm}^2 \leq \frac{0.9 \cdot 32.0}{1.25} = 23.0 \text{ N/mm}^2 \quad (\eta = 52.2 \%)$$

Verification of normal bending stresses in the CLT plate:

$$7.76 \text{ N/mm}^2 \leq 1.09 \cdot \frac{0.9 \cdot 24.0}{1.25} = 18.8 \text{ N/mm}^2 \quad (\eta = 41.3 \%)$$

Shear stress verification

Maximum lateral force at the support:

$$V_{z,\max} = \frac{10.1 \cdot 8.10}{2} = 40.9 \text{ kN}$$

Shear stresses τ_{xz} :

Static moment at the level of the centre of gravity:

$$S_y(z_S) = 160 \cdot 218 \cdot \frac{218}{2} = 3.80 \cdot 10^6 \text{ mm}^3$$

Static moment at the level of the bond line GLT/CLT:

$$S_y(z = -102) = 160 \cdot 320 \cdot 58 = 2.97 \cdot 10^6 \text{ mm}^3$$

Static moment at the level of the decisive transverse layer in the CLT plate:

$$S_y(z = -132) = 220 \cdot 60 \cdot (470 - 218 - 30 - 15) = 2.73 \cdot 10^6 \text{ mm}^3$$

Maximum shear stress ($z = 0$):

$$\tau_{\max} = \frac{40.9 \cdot 10^3 \cdot 3.80 \cdot 10^6 \cdot 13,500}{1.59 \cdot 10^{13} \cdot 160} = 0.825 \text{ N/mm}^2$$

Shear stress in the bondline of GLT/CLT:

$$\tau(z = -102) = \frac{40.9 \cdot 10^3 \cdot 2.97 \cdot 10^6 \cdot 13,500}{1.59 \cdot 10^{13} \cdot 160} = 0.645 \text{ N/mm}^2$$

Maximum rolling shear stress ($z = -132 \text{ mm}$):

$$\tau_{r,\max} = \frac{40.9 \cdot 10^3 \cdot 2.73 \cdot 10^6 \cdot 11,550}{1.59 \cdot 10^{13} \cdot (160 + 2 \cdot 30)} = 0.369 \text{ N/mm}^2$$

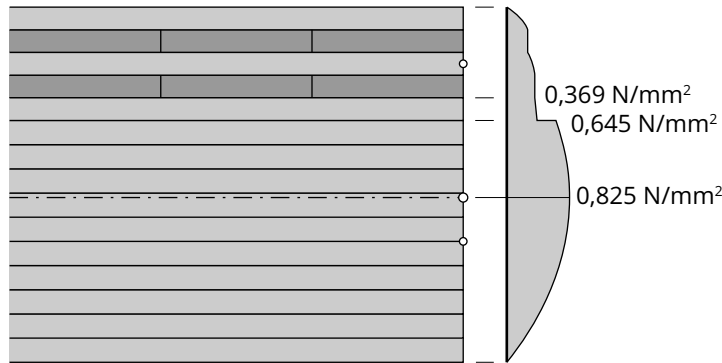


Figure 5.16 Progression of the shear stress

Verification of the maximum shear stress in the GLT beam:

$$0.825 \text{ N/mm}^2 \leq \frac{0.9 \cdot 3.5}{1.25} = 2.52 \text{ N/mm}^2 \quad (\eta = 32.7 \%)$$

Verification of the rolling shear stress in the CLT plate (assumption $b/t > 4$):

$$0.369 \text{ N/mm}^2 \leq \frac{0.9 \cdot 1.10}{1.25} = 0.792 \text{ N/mm}^2 \quad (\eta = 46.6 \%)$$

Verifications in the serviceability limit state

For the verifications in the serviceability limit state, the calculation is undertaken with the effective width for the uniformly distributed load in an approximate fashion.

Verification of deflection

Deflection due to a “uniformly distributed unit load”

$$w_{“1.0 \text{ kN/m}”} = \frac{5 \cdot 1.0 \cdot 8100^4}{384 \cdot 2.49 \cdot 10^{13}} + \frac{1.0 \cdot 8100^2}{8 \cdot 2.96 \cdot 10^7} = 2.25 + 0.277 = 2.53 \text{ mm/(kN/m)}$$

Note:

The consideration of the deflection portion due to the shear flexibility of the CLT plate is around 11 % and should therefore also be considered.

Deflection due to the characteristic combination of loads

$$w_{1.0 \text{ kN/m}''} \cdot (g_{2,k} \cdot s + q_k \cdot s) = 2.53 \cdot (3.02 + 3.30) = 16.0 \text{ mm} \leq \frac{L}{300}$$

$$\frac{L}{300} = \frac{8,100}{300} = 27.0 \text{ mm}$$

$$16.0 \text{ mm} < 27.0 \text{ mm} (\eta = 59.3 \%)$$

Deflection due to the quasi-permanent combination of loads

$$w_{1.0 \text{ kN/m}''} \cdot (g_{1,k} + g_{2,k} \cdot s + \psi_2 \cdot q_k \cdot s) \cdot (1 + k_{\text{def}}) - w_c =$$

$$2.53 \cdot (0.826 + 3.02 + 0.6 \cdot 3.30) \cdot (1 + 0.69) - 0 = 24.9 \text{ mm} \leq \frac{L}{250}$$

$$\frac{L}{250} = \frac{8,100}{250} = 32.4 \text{ mm}$$

$$24.9 \text{ mm} \leq 32.4 \text{ mm} (\eta = 76.9 \%)$$

Note:

According to EN 1995-1-1:2009, Section 2.3.2.2, the coefficient of deformation $k_{\text{def}} = 0.69$ results from the geometric mean of the values for CLT with $k_{\text{def,CLT}} = 0.80$ and for GLT with $k_{\text{def,GLT}} = 0.60$.

Verification of vibration

Assumptions:

- Floor class II according to ÖNORM B 1995-1-1:2015-06
- Width of the floor span: $b_D = 12.0 \text{ m}$
- Concrete screed ($E = 25,000 \text{ N/mm}^2$); thickness: $d = 65 \text{ mm}$

Natural frequency

Effective bending stiffness (incl. bending stiffness of the screed) in longitudinal direction in relation to a rib of the ribbed plate:

$$(EI)_{\text{1,ef}} = 2.49 \cdot 10^7 + 2.50 \cdot 10^{10} \cdot \frac{0.660 \cdot 0.065^3}{12} = 2.49 \cdot 10^7 + 3.78 \cdot 10^5 = 2.53 \cdot 10^7 \text{ Nm}^2$$

Blurred bending stiffness in longitudinal direction in relation to 1 m:

$$(EI)_{\text{1,ef,1m}} = \frac{2.53 \cdot 10^7}{0.660} = 3.83 \cdot 10^7 \text{ Nm}^2/\text{m}$$

Effective bending stiffness (incl. bending stiffness of the screed) in transverse direction in relation to 1 m:

$$(EI)_{b,ef,1m} = 1.155 \cdot 10^{10} \cdot \left(2 \cdot \frac{1.00 \cdot 0.03^3}{12} + 2 \cdot 1.00 \cdot 0.03 \cdot 0.03^2 \right) + 2.50 \cdot 10^{10} \\ \cdot \frac{1.00 \cdot 0.065^3}{12} = 6.76 \cdot 10^5 + 5.72 \cdot 10^5 = 1.25 \cdot 10^6 \text{ Nm}^2/\text{m}$$

$$f_1 = \frac{\pi}{2 \cdot 8 \cdot 10^2} \cdot \sqrt{\frac{2.53 \cdot 10^7}{(83 + 302)}} \cdot \sqrt{1 + \left(\frac{8.10}{12.0}\right)^4 \cdot \frac{1.25 \cdot 10^6}{3.83 \cdot 10^7}} = 6.14 \cdot 1.003 = 6.16 \text{ Hz}$$

$$f_1 = 6.16 \text{ Hz} > f_{II,limit} = 6.00 \text{ Hz}$$

Stiffness criterion

$$b_F = \frac{8.10}{1.1} \cdot \sqrt[4]{\frac{1.25 \cdot 10^6}{3.83 \cdot 10^7}} = 3.13 \text{ m}$$

$$w(1\text{kN}) = \frac{1.0 \cdot 10^3 \cdot 8 \cdot 10^3}{48 \cdot 3.83 \cdot 10^7 \cdot 3.13} + \frac{1.0 \cdot 10^3 \cdot 8.10}{4 \cdot 2.96 \cdot 10^7 \cdot 3.13} = \\ = 9.20 \cdot 10^{-5} + 2.20 \cdot 10^{-5} = 1.141 \cdot 10^{-4} \text{ m} = 0.11 \text{ mm} \leq w_{II,limit} = 0.50 \text{ mm}$$

6 Walls

Walls of cross-laminated timber serve as a spatial enclosure with requirements to noise, humidity, thermal and fire protection and as structural walls as part of the load bearing structure. Load-bearing walls serve the absorption of vertical loads (from dead weight, live loads on the floors and snow load of the roof), horizontal loads transverse to the wall plane (from wind or for fall protection) and horizontal loads in the wall plane (for bracing of the building). Due to their relatively large statically usable height, load-bearing shear walls can be effectively used to suspend floor loads higher up or to realise building cantilevers.

The load-bearing capacity of walls is mostly determined by the risk of buckling, the fire performance and the load transfer at the base of the wall. The application of local loads may normally take place by compression on end grain sections. The propagation of vertical local loads in the wall plane becomes even more favourable with a higher portion of horizontal board layers.

6.1 Buckling of walls

The buckling behaviour of walls of cross-laminated timber depends, among other things, on the distribution of the compressive forces in the wall considered. For verification of the load-bearing capacity, it is normally assumed that the entire wall deforms in a cylindrical shape. This shape occurs, if walls are only held at the top and at the bottom and are uniformly stressed by a vertical superimposed load and/or a horizontal load. The verification may then be undertaken as a buckling member.

If vertical edges are supported or if there are local load effects from zones of high compressive stress adjacent to zones of low compressive stress, then this has a beneficial effect on the load-bearing performance. The increase of the load-bearing capacity in these situations is associated with a more exact analysis of the spatial bulging behaviour, which is why this is analysed in special cases only, especially as fire resistance and sill compression likewise shall be verified.

6.1.1 Cross-laminated timber as shear-flexible buckling beam

Beside the buckling length, the buckling behaviour of members is determined by the ratio of cross-sectional area to stiffness against deformation of the member. The stiffness against deformation is composed of a portion of bending stiffness and a portion of shear stiffness, which for cross-laminated timber cannot always be neglected. With the portion of shear stiffness, the critical buckling load is reduced¹.

In the buckling analysis, the influence of the shear flexibility can be considered via a factor k_{cs} , using which the slenderness of the buckling member is increased. This enables a direct comparison of the two models – the extended gamma method from Volume 1 and the shear-flexible beam according to Timoshenko presented here.

¹For calculation of the critical buckling load for general shear-flexible beams, see Petersen, 1992, Section 1.2.12.1

Gamma method

$$k_{cs} = \sqrt{\frac{I_{0,net}}{I_{0,ef}}} \quad (6.1)$$

Shear-flexible beam

$$k_{cs} = \sqrt{1 + \frac{\pi^2 EI_{0,net}}{GA_s \cdot \ell_k^2}} \quad (6.2)$$

with

- k_{cs} Factor for consideration of shear flexibility for buckling
- $EI_{0,net}$ Bending stiffness (net cross-section)
- GA_s Effective shear stiffness $GA_s = \neq GA$
- ℓ_k Buckling length

The slenderness of the shear-flexible beam then results in

$$\lambda = \frac{\ell_k}{i_{0,net}} \cdot k_{cs} \quad (6.3)$$

The straightness factor for cross-laminated timber as a shear-flexible beam member is determined as follows:¹

$$\beta_c = 0.1 \quad (6.4)$$

The further calculation and the verification against bending buckling may be undertaken according to EN 1995-1-1:2015.

$$\lambda_{rel} = \frac{\lambda}{\pi} \sqrt{\frac{f_{c,0,k}}{E_{0.05}}} \quad (6.5)$$

$$k = 0.5 [1 + \beta_c (\lambda_{rel} - 0.3) + \lambda_{rel}^2] \quad (6.6)$$

$$k_c = \frac{1}{k + \sqrt{k^2 - \lambda_{rel}^2}} \quad (6.7)$$

Verification of buckling stress

$$\frac{\sigma_{c,0,d}}{k_c f_{c,0,d}} + \frac{\sigma_{m,d}}{f_{m,d}} \leq 1 \quad (6.8)$$

¹ Deviating from the suggestion in ÖNORM B 1995-1-1:2015, Annex K, K.6.3, the following determinations are made: The coefficient of imperfection for cross-laminated timber is – due to the production conditions comparable to glued-laminated timber – assumed with $\beta_c = 0.1$. For that, the buckling analysis is undertaken under consideration of shear flexibility. This results in verifications at approximately the same safety level.

Example 6.1 Wall as shear-flexible beam

For a wall of CLT 90-3s (30l-30w-30l), the verification against buckling shall be undertaken.

The buckling length is $\ell_k = 2.95$ m

From the wind load, the design values of internal forces are given:

$$N_d = 57 \text{ kN}$$

$$M_d = 1.31 \text{ kNm}$$

Characteristic building material values

$$E_{0,mean} = 11\,550 \text{ N/mm}^2; \quad E_{0,05} = \frac{5}{6} E_{0,mean} = 9\,625 \text{ N/mm}^2$$

$$G_{0,mean} = 690 \text{ N/mm}^2; \quad G_{0,05} = \frac{5}{6} G_{0,mean} = 575 \text{ N/mm}^2$$

$$G_{R,mean} = 65 \text{ N/mm}^2; \quad G_{R,05} = \frac{5}{6} G_{R,mean} = 54 \text{ N/mm}^2$$

Strength values

Characteristic values

$$f_{c,0,k} = 21.00 \text{ N/mm}^2$$

$$f_{m,k} = 24.00 \text{ N/mm}^2$$

$k_{mod} = 1.0$ (short-term/instantaneous, with wind as lateral load)

$$\gamma_M = 1.25$$

Design values

$$f_{c,0,d} = k_{mod} \cdot \frac{f_{c,0,k}}{\gamma_M} = 1.0 \cdot \frac{21.00}{1.25} = 16.80 \text{ N/mm}^2$$

$$f_{m,d} = k_{mod} \cdot \frac{f_{m,k}}{\gamma_M} = 1.0 \cdot \frac{24.00}{1.25} = 19.20 \text{ N/mm}^2$$

Cross-sectional values

Shear stiffness

$$GA = \sum G_{mean} \cdot b_i \cdot d_i = 2 \left(\frac{690}{10} \cdot 100 \cdot 3 \right) + \frac{65}{10} \cdot 100 \cdot 3 = 43\,350 \text{ kN}$$

$$GA_{05} = \frac{5}{6} \cdot GA = \frac{5}{6} \cdot 43\,350 = 36\,125 \text{ kN}$$

with the shear correction factor

$$\varkappa = 0.196$$

$$GA_{0,05,s} = \varkappa \cdot GA_{05} = 0.196 \cdot 36\,125 = 7\,081 \text{ kN}$$

Strength values according to Section 3.1

The shear correction factor according to Table 9-1 is used in an approximate fashion.

Extensional and bending stiffness

$$A_{0,net} = 2 \cdot 100 \cdot 3 = 600 \text{ cm}^2$$

$$EI_{net} = \sum E_{i,mean} \left(\frac{b_i \cdot d_i^3}{12} + b_i \cdot d_i \cdot a_i^2 \right) = 11\,550 \cdot 2 \left(\frac{100 \cdot 3^3}{12} + 100 \cdot 3 \cdot 3^2 \right) \cdot 10^{-5} = 676 \text{ kNm}^2$$

$$EI_{0,05,net} = \frac{5}{6} \cdot EI_{net} = \frac{5}{6} \cdot 676 = 563 \text{ kNm}^2$$

Section modulus

$$I_{0,net} = 5\,850 \text{ cm}^4$$

$$W_{0,net} = \frac{I_{0,net}}{z_{max}} = \frac{5\,850}{4.5} = 1\,300 \text{ cm}^3$$

Buckling analysis

Slenderness

$$k_{cs} = \sqrt{1 + \frac{\pi^2 EI_{0,05,net}}{GA_{0,05,s} \cdot \ell_k^2}} = \sqrt{1 + \frac{\pi^2 \cdot 563}{7\,081 \cdot 2.95^2}} = 1.044$$

$$i_{y,net} = \sqrt{\frac{I_{0,net}}{A_{0,net}}} = \sqrt{\frac{5\,850}{600}} = 3.122 \text{ cm}$$

$$\lambda = \frac{\ell_k}{i_{0,net}} \cdot k_{cs} = \frac{2.95 \cdot 100}{3.122} \cdot 1.044 = 94.5 \cdot 1.044 = 98.65$$

Relative slenderness ratio

$$\lambda_{rel} = \frac{\lambda}{\pi} \sqrt{\frac{f_{c,0,k}}{E_{0,05}}} = \frac{98.66}{\pi} \sqrt{\frac{21}{9\,625}} = 1.467$$

$$k = 0.5 \left[1 + \beta_c (\lambda_{rel} - 0.3) + \lambda_{rel}^2 \right] = 0.5 \left[1 + 0.1 (1.467 - 0.3) + 1.467^2 \right] = 1.634$$

$$k_c = \frac{1}{k + \sqrt{k^2 - \lambda_{rel}^2}} = \frac{1}{1.634 + \sqrt{1.634^2 - 1.467^2}} = 0.425$$

Verification of buckling stress

$$\begin{aligned} \frac{\sigma_{c,0,d}}{k_c f_{c,0,d}} + \frac{\sigma_{m,d}}{f_{m,d}} &= \frac{N_d}{A_{0,net}} + \frac{M_d}{W_{0,net}} \leq 1 \\ &= \frac{57}{600} \cdot 10 + \frac{1.31 \cdot 100}{1\,300} \cdot 10 = 0.133 + 0.053 = 0.186 \leq 1 \end{aligned}$$

✓ Fulfilled (19 %)

Note: The effect of shear flexibility on the relative slenderness ratio is higher with compact members than with slender members. In the range of slenderness relevant in building practice between 60 and 150, the load of the shear-flexible member is about 3 % to 10 % lower than that of the shear-rigid member.

6.1.2 Influence of openings

The previous example refers to Example 11.5.1 in Volume 1. In that, the distribution of the axial forces in shear walls with an opening was very roughly assumed as constant in the net cross-section of the remaining wall segment.

In view of the utilisation of the load-bearing capacity of the wall below 20 %, this is acceptable. More exact results are obtained from calculations using the finite element method or framework models. A good estimate is obtained by considering the wall area located above the openings as a beam with a constant cross-section. For lintels over cut-outs as part of a monolithic wall, the beam is modelled with constrained ends.. For inserted lintels interrupted by joints a simple supported beam is appropriate. The support of the beam is undertaken with translation springs, which are respectively located at the centre of strips, which result by segmenting the load bearing wall in wall pillars. For the width of the wall pillars, a dimension of $b = 30$ cm is recommended. Wall pillars with less than 60 cm in width shall be divided into two strips by cutting them in half.

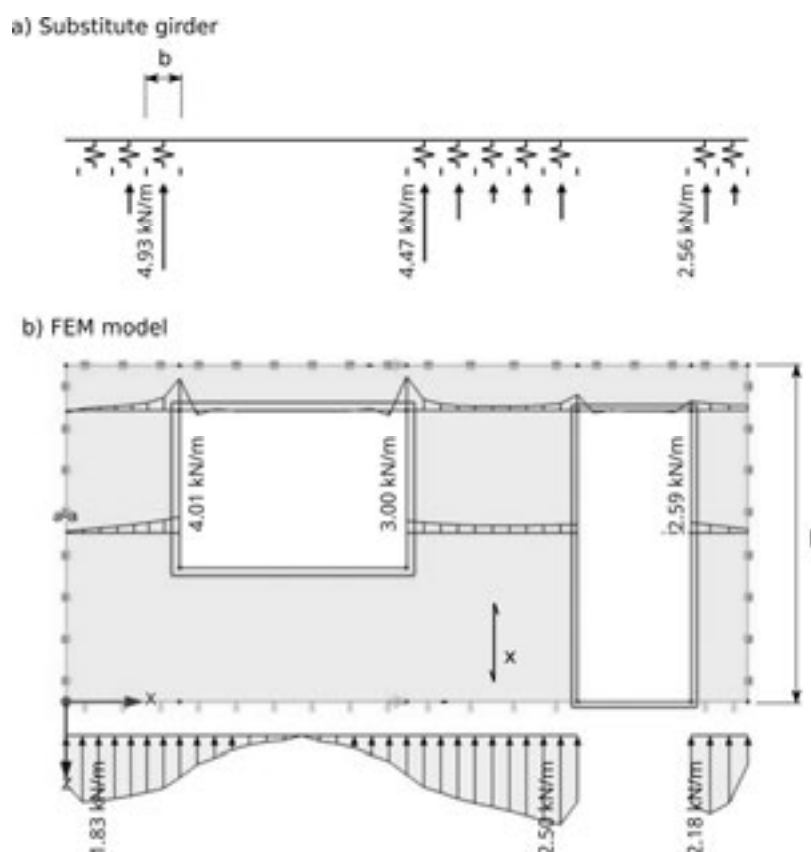


Figure 6.1 Exemplary comparison of the distributions of normal forces as a consequence of a vertical unit load at the top of the wall
a) Model as substitute beam on individual translation springs and
b) FEM model

For the substitute beam, its cross-section height h_T can be assumed from the wall dimension in the lintel area. The width b_T results from the sum of the layer thicknesses located in the y-direction.

$$b_T = b \cdot \sum d_y \quad (6.9)$$

The spring rigidity of the respective wall column can be determined from

$$c = \frac{EA}{h} = \frac{E \cdot b \cdot \sum d_x}{h} \quad (6.10)$$

For a 3 m high wall of CLT 120 3s (40l-40w-40l), for a strip with a width of $b = 30$ cm, a spring rigidity c results in:

$$c = \frac{E \cdot b \cdot \sum d_x}{h} = \frac{1\,155 \text{ kN/cm}^2 \cdot 30 \text{ cm} \cdot 8 \text{ cm}}{300 \text{ cm}} = 924 \text{ kN/cm} = 92\,400 \text{ kN/cm} \quad (6.11)$$

Alternatively to the support by springs, the calculation may also be undertaken with rigid supports. In that, all supports subjected to tension shall be removed after the first calculation step.

6.2 Application of local loads

In Volume 1, it was suggested to distribute concentrated loads with a load propagation angle of 30° to the vertical up to a quarter, at most, of the wall height to an effective pillar width $w_{i,ef}$ and to undertake the buckling analysis with this wall pillar.

The load distributions in general orthotropic plates were derived and analysed by Bogensperger et al., 2014. In that, the roughly estimated assumption of Volume 1 could be confirmed by and large. The analyses, however, show that neither the influence of the wall's cross-sectional layout nor the width of the loaded area should be neglected.

With a three-layer wall of equally thick layers with two vertical and one horizontal layer results a propagation angle of about $\alpha_i = 25^\circ$. For an ever increasing portion of the vertical layers, the angle tends towards $\alpha_i = 15^\circ$ and for an ever increasing portion of horizontal layers towards $\alpha_i = 45^\circ$.

With larger load application lengths, as they commonly occur by partial line loads, the load propagation angle decreases and with ever increasing load application lengths tends towards $\alpha_i = 0^\circ$. This means, that with a wall uniformly loaded over its entire length, no load propagation occurs anymore.

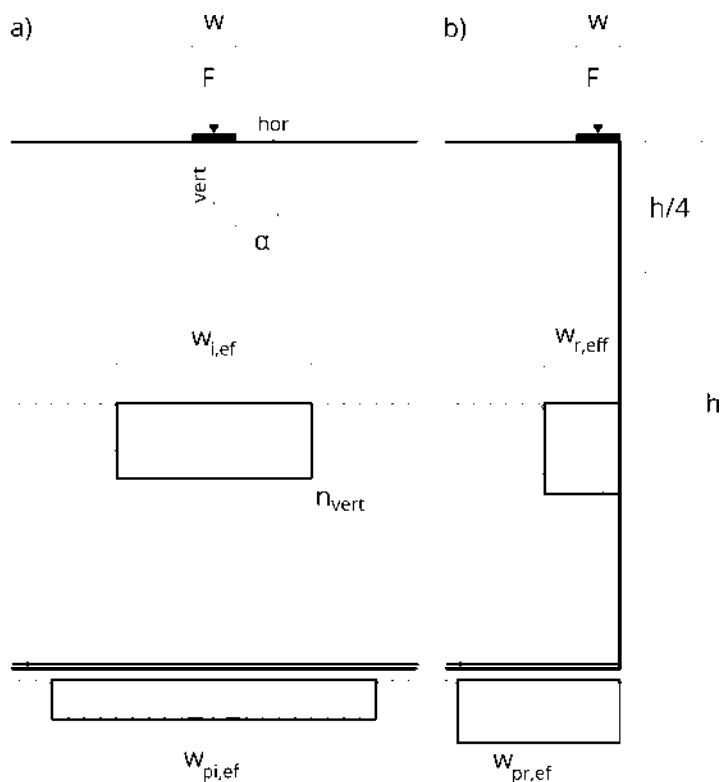


Figure 6.2 Effective column width for a) interior load application and b) load application at the edge

With low wall heights, the calculated load propagation angle α_i decreases, since the load propagation actually is non-linear and initially runs in a slightly more acute angle.

An elastic support of the wall by sills or on CLT floor elements results in an increase in the load propagation angle. This effect, however, is neglected in most cases.

The effect from local loads normally has to be superimposed with that from uniform loads.

The verification of the wall against buckling with the stated effective pillar width has to be considered as conservative. Beneficial effects, like retentions by transverse walls or adjacent areas with lower compressive stresses, are not considered as a conservative assumption. More exact results can be achieved with numerical models applying the 2nd order theory and the verification against panel bulging.

6.2.1 Practical estimate for concentrated loads

For wall layups frequently used in building practice under concentrated loads, the propagation angle α_i can be estimated with good approximation as a mixed value of 45° for the portion of horizontal layers d_{hor} and 15° for the portion of vertical layers d_{vert} . From the load application length w , the load is distributed to an effective pillar width $w_{i,ef}$ up to a quarter of the wall height. The buckling analysis then shall be undertaken with the wall pillar of width $w_{i,ef}$.

Boundary conditions

The assumptions apply to wall layups with thickness ratios in the range of:

$$\frac{1}{5} \leq \frac{d_{hor}}{d_{vert}} \leq \frac{3}{1}$$

The calculated load application length is limited with $w \leq 20$ cm (e.g. load application by a joist with $b = 20$ cm) and the wall height should be at least $h \geq 2.75$ m.

Load application in the wall's interior

For the load propagation angle of concentrated loads inside the wall

$$\alpha_i = \frac{d_{hor} \cdot 45^\circ + d_{vert} \cdot 15^\circ}{d_{hor} + d_{vert}} \quad (6.12)$$

Thus, according to Figure 6.2, the following results for the effective pillar width of the wall

$$w_{i,ef} = w + 2 \cdot \frac{h}{4} \cdot \tan(\alpha_i) \quad (6.13)$$

Pressing at the base of the wall can be estimated with the effective pressing width $w_{pi,ef}$:

$$w_{pi,ef} = 1.2 \cdot w_{i,ef} \quad (6.14)$$

Load application at the edge

For concentrated loads applied at the edge of the wall, the effective pillar width shall be reduced compared to that from the undisturbed interior of the wall:

$$w_{r,ef} = 0.45 \cdot w_{i,ef} \quad (6.15)$$

Pressing at the base of the wall with concentrated loads at the edge of the wall can be estimated with the effective pressing width $w_{pr,ef}$:

$$w_{pr,ef} = 1.2 \cdot w_{r,ef} \quad (6.16)$$

with

d_{vert}	Sum of the thicknesses of vertical layers
d_{hor}	Sum of the thicknesses of horizontal layers
w	Load application width
h	Wall height

6.2.2 Practical estimate for partial line loads and low wall heights

If the force is applied on larger support width $w > 20$ cm (e.g. steel beam with a width $b = 30$ cm) or if the wall height is lower than $h < 2.75$ m, then load propagation angles deviating from Section 6.2.1 result. In this case, the layup of the wall's cross-section and the ratio from load application width w and wall height h are considered more generally than in Section 6.2.1 by the coefficients k_{ortho} and k_w . The coefficients are obtained by simplifications of the theoretical derivation.

Load application in the wall's interior

The load propagation angle for loads in the interior – i.e. at a distance of at least $2 \cdot w_{i,ef}$ from the end of the wall – applies to the propagation angle:

$$\alpha_i = k_{ortho} \cdot k_w \cdot 30^\circ \quad (6.17)$$

with the coefficient for consideration of the element layup

$$k_{ortho} = 1.1 \cdot \sqrt[4]{\frac{EA_{hor}}{EA_{vert}}} = 1.1 \cdot \sqrt[4]{\frac{d_{hor}}{d_{vert}}} \quad (6.18)$$

and the coefficient for consideration of the load application width w

$$k_w = 1 - 1.5 \cdot \frac{w}{h} \geq 0 \quad (6.19)$$

Thus, according to Figure 6.2, the following results for the effective pillar width

$$w_{i,ef} = w + 2 \cdot \frac{h}{4} \cdot \tan(\alpha_i) \quad (6.20)$$

Pressing at the base of the wall can be estimated with the effective pressing width $w_{pi,ef}$:

$$w_{pi,ef} = \left(1.3 - 0.9 \frac{w}{h} + 0.5 \left(\frac{w}{h} \right)^2 \right) \cdot w_{i,ef} \geq w_{i,ef} \quad (6.21)$$

Load application at the edge

For cases with load application at the end of the wall (case b in Figure 6.2), the following value shall be used for the effective wall width:

$$w_{r,ef} = 0.9 \cdot \sqrt[4]{\frac{w}{h}} \cdot w_{i,ef} \quad (6.22)$$

For pressing at the base of the wall as a consequence of load application at the edge results:

$$w_{pr,ef} = \left(0.5 + 0.85 \frac{w}{h} - 0.45 \left(\frac{w}{h} \right)^2 \right) \cdot w_{i,ef} \geq w_{r,ef} \quad (6.23)$$

with

d_{vert} Sum of the thicknesses of vertical layers

d_{hor} Sum of the thicknesses of horizontal layers

w Load application width

h Wall height

Example 6.2 Application of local loads into a wall

Given: CLT 90 Q3s (30I-30w-30I)

Sought: Verification for the wall with local loads at the centre of the wall, on the one hand, and at the end of the wall, on the other hand.

Wall height $h = 3$ m, load application width $w = 20$ cm. Action: $F_d = 100$ kN, $k_{mod} = 0.8$

Load propagation angle

Thickness ratios, wall height and load application width correspond to the boundary conditions for concentrated loads of Section 6.2.1.

The load propagation angle accordingly results in

$$\alpha_i = \frac{d_{hor} \cdot 45^\circ + d_{vert} \cdot 15^\circ}{d_{hor} + d_{vert}} = \frac{30 \cdot 45^\circ + 60 \cdot 15^\circ}{90} = 25^\circ$$

Load application in the wall's interior

Effective pillar width

$$w_{i,ef} = w + 2 \cdot \frac{h}{4} \cdot \tan \alpha = 20 + 2 \cdot \frac{300}{4} \cdot \tan 25^\circ = 89.86 \text{ cm} = 0.899 \text{ m}$$

Axial force per 1 m strip of the wall for buckling analysis at the 1 m strip

$$n_d = \frac{F_d}{b_{ef}} = \frac{100}{0.899} = 112 \text{ kN/m}$$

Load application at the wall end (edge)

$$w_{r,ef} = 0.45 \cdot w_{i,ef} = 0.45 \cdot 89.86 = 40.47 \text{ cm} = 0.405 \text{ m}$$

Axial force per 1 m strip of the wall for buckling analysis at the 1 m strip

$$n_d = \frac{F_d}{b_{ef}} = \frac{100}{0.405} = 247 \text{ kN/m}$$

The buckling analysis shall be undertaken with the axial force of the edge load.

Buckling analysis

The characteristic strength values and the buckling coefficient are taken over from Example 6.1 and adjusted to the given modification factor $k_{mod} = 0.8$.

$$\frac{\sigma_{c,0,d}}{k_c f_{c,0,d}} = \frac{\frac{N_d}{A_{0,net}}}{k_c f_{c,0,d}} \leq 1$$

$$k_c = 0.425$$

$$f_{c,0,d} = 0.8 \cdot \frac{21}{1.25} = 13.44 \text{ N/mm}^2$$

$$\frac{\frac{N_d}{A_{0,net}}}{k_c f_{c,0,d}} = \frac{\frac{247}{600} \cdot 10}{0.425 \cdot 13.44} = 0.72 \leq 1$$

✓ Verification fulfilled ($\eta = 72\%$)

For the verification of sill pressing, for the case of load application at the edge, an effective pressing length of

$$w_{pr,ef} = 1.2 \cdot w_{r,ef} = 1.2 \cdot 40.47 = 48.56 \text{ cm}$$

$$w_{pr,ef} = 0.486 \text{ m}$$

can be assumed.

6.3 Sill pressing

On the basis of tests on sill pressing, an effective width is expediently applied for sill pressing due to the transverse expansion restraint of the sill. This approach has not been anchored in standards and cannot be found in all technical approvals yet.

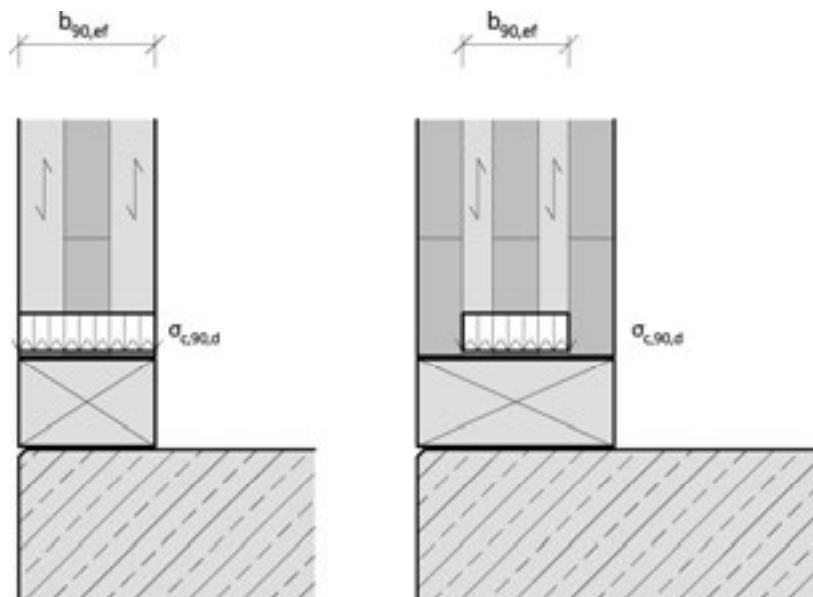


Figure 6.3 Effective widths for sill compressing

According to Figure 6.3, for the effective width for determination of the pressing area for the verification of compression perpendicular to grain of the embedded sills under CLT walls, the entire element width, including the outermost upright layers $b_{90,ef}$, is applied. Therefore, for compression perpendicular to grain, the entire gross width is considered, only exterior transverse layers are not considered in that.

The application of this effective width for sill compression perpendicular to grain shall be justified by the responsible engineer of the static verification and discussed, if necessary, with the test authorities.

Example 6.3 Sill pressing

The wall is supported on a sill C24. The axial force from Example 6.1 shall be applied to this sill. The associated value for the modification factor is determined with $k_{mod} = 0.8$.

$$\sigma_{c,90,d} = \frac{N_d}{A_{90,ef}} \leq f_{c,90,d} = k_{mod} \cdot \frac{f_{c,90,k}}{\gamma_M}$$

$$\sigma_{c,90,d} = \frac{57}{900} \cdot 10 \leq f_{c,90,d} = 0.8 \cdot \frac{2.5}{1.3} = 1.53 \text{ N/mm}^2$$

$$\sigma_{c,90,d} = 0.63 \leq 1.53 \text{ N/mm}^2$$

✓ Verification fulfilled ($\eta = 41\%$)

7 Finite element modelling

For static calculations, the two-dimensional cross-laminated timber elements are normally theoretically cut into “strips” and considered as uniaxially stressed members. With this conservative assumption, floors can be calculated as simple supported beams and walls as columns.

In some cases, however, the load-bearing behaviour has to be considered as a two-dimensional element and the load distribution to be analysed as a diaphragm or as a plate, in order to use the full potential of the two-dimensional structural elements. Associated models are grillages, i.e. planar grids of members in both lamella directions, or finite element models, i.e. faces combined from discrete elements.

This chapter describes the basic principles for modelling as a two-dimensional structure using the finite element method and shows their applications. The calculation as grillage has been described in Volume 1.

7.1 Calculation sequence

Calculation and verification of cross-laminated timber members using the finite element method follow the scheme in Figure 7.1. For calculation, as described in the following section, suitable finite elements shall be used. In some software solutions, pre-processors are available: programme parts automatically calculating the model behaviour from the layout and the characteristic building material properties of the layers. For static calculations, however, the use of pre-processors is not required. The individual stiffness values for the static model may also be determined “by hand” and directly entered as characteristic values of the stiffness matrix. The stiffness matrix is identical in both cases. Manual calculation is generally required for the correct determination of torsional stiffness.

The geometry of the static system is described by the central plane of the cross-laminated timber members. According to that, the support conditions are determined with point and linear supports and the mostly articulated coupling of the elements with linear joints. After definition of the actions and their combinations, as a result of the static calculation, the deformations can be determined, and therefrom the internal forces.

The structural element verifications may ultimately be performed in an automated fashion via a post-processor at the level of the stresses in the layers or determined by direct comparison of the internal forces with the respectively associated cross-sectional load-bearing capacity by manual calculation, as described in Volume 1, Sections 4.3.3 and 4.4.3.

In the following examples, the calculation of stiffnesses and cross-sectional load-bearing capacities is performed by hand, in order to be able to perform a calculation according to the finite element method without pre- and post-processors.

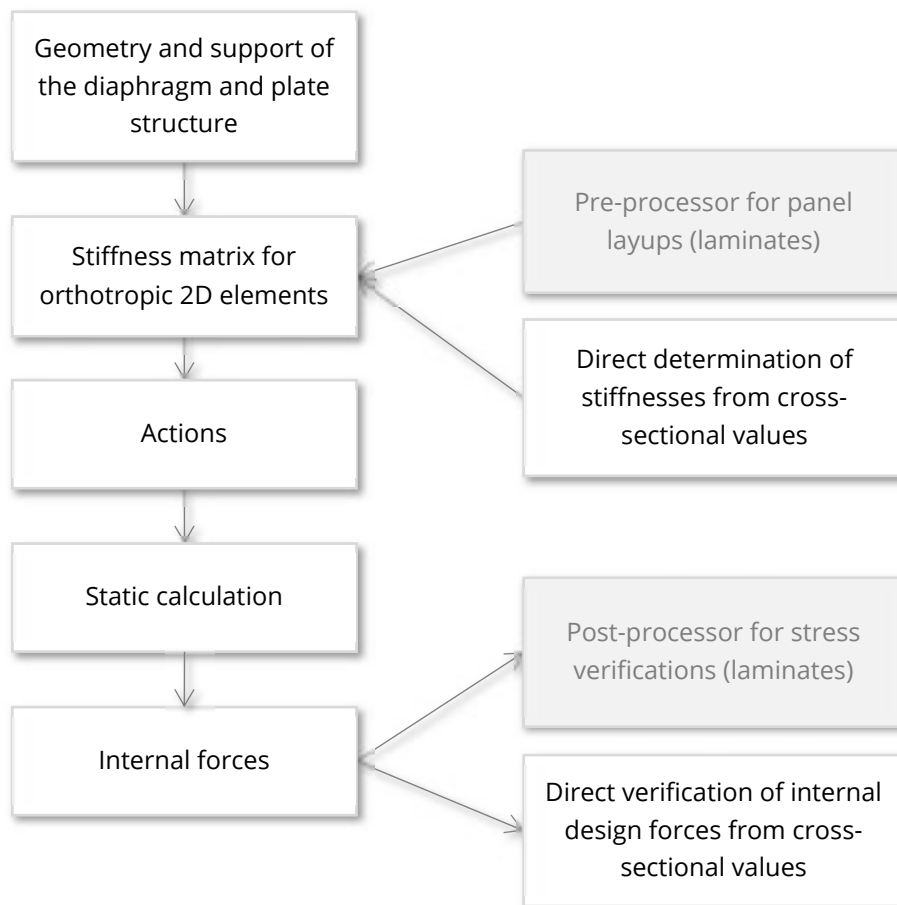


Figure 7.1: Flowchart of the static calculation of cross-laminated timber elements

7.2 Finite element models

7.2.1 Shell elements for diaphragm and plate effect

Due to its composition of layers arranged at right angles to one another, the material behaviour of cross-laminated timber is orthotropic. That means, that the force-deformation behaviour along the two main directions of load-bearing capacity is different. Mutual influencing of longitudinal and transverse stressing does not have to be applied for cross-laminated timber. The influence of shear deformations in the panel, however, shall be considered.

Therefore, orthotropic Mindlin-Reissner elements are best suited as finite elements for cross-laminated timber. Mindlin-Reissner elements can be considered a two-dimensional equivalent of the Timoshenko beam, while finite elements according to the Kirchhoff theory shall be considered analogous to the classic Bernoulli beam, i.e. do not map shear deformations of the panel. Mindlin-Reissner elements are also designated as *thick plates* and Kirchhoff elements as *thin plates*.

The deformations of the Kirchhoff elements without shear portions are, depending on slenderness and panel layup, by about 20 to 30 % above those of the Mindlin-Reissner elements. The stress results, too, can deviate in this order of magnitude.

In the general case, via the finite shell elements, the load-bearing effect as a diaphragm as well as that as a plate is mapped.

Via the stiffnesses of the shell elements, the relation between the strains of the element and the internal forces is established. These are stated for a Mindlin-Reissner element for cross-laminated timber in Figure 7.2 in the form of a matrix. From the stiffness matrix results, that there is no relation between normal stresses in the one direction and normal expansions in the other direction, i.e. that the transverse expansion for cross-laminated timber is generally neglected. This can be justified by the relatively low coefficient of transverse expansion of timber, the panel layup of individual lamellas and the formation of butt joints transverse to the main direction of load-bearing capacity. The behaviour of cross-laminated timber upon torsional stresses is complex. The torsional stiffness is low and results in internal forces, which normally are not relevant for dimensioning. The assumption of complete torsional flexibility results in slightly higher deflections and bending moments in the panel and is conservative. The load-bearing performance of panels without torsional stiffness largely corresponds to that of a grillage of shear-flexible Timoshenko beams. Due to the missing transverse strain impediment and the high directional dependence of CLT panels, the use of the tables for panels (e.g. Czerny tables) known from concrete construction is not possible.

Orthotropic Mindlin-Reissner elements as shear-flexible, 'thick' panels. No influence of transverse expansion.

$$\begin{matrix} \left\{ \begin{matrix} m_x \\ m_y \\ m_{xy} \\ v_{x,z} \\ v_{y,z} \\ n_x \\ n_y \\ n_{xy} \end{matrix} \right\} \end{matrix} = \begin{bmatrix} \begin{matrix} EI_x & 0 & 0 \\ 0 & EI_y & 0 \\ 0 & 0 & k_D GI_T \end{matrix} & \begin{matrix} 0 & 0 \\ 0 & 0 \\ 0 & 0 \end{matrix} & \begin{matrix} 0 & 0 & 0 \\ \kappa_x GA_x & 0 & 0 \\ 0 & \kappa_y GA_y & 0 \end{matrix} \\ \begin{matrix} EA_x & 0 & 0 \\ 0 & EA_y & 0 \\ 0 & 0 & k_S GA_{gross} \end{matrix} \end{bmatrix} \cdot \begin{matrix} \left\{ \begin{matrix} \kappa_y \\ \kappa_x \\ \kappa_{xy} \\ \gamma_{xz} \\ \gamma_{yz} \\ \varepsilon_x \\ \varepsilon_y \\ \gamma_{xy} \end{matrix} \right\} \end{matrix}$$

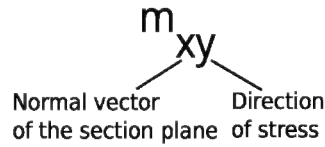
Figure 7.2 Stiffness matrix of a cross-laminated timber element as an orthotropic diaphragm and plate element

7.2.2 Internal forces

For diaphragms and plates, the internal forces convention originating from concrete construction is normally used, as can be retrieved from Figure 7.3. The internal forces are related to a panel strip with one metre in width and therefore designated with the lowercase letters *m* for moments, *v* for lateral forces and *n* for diaphragm or normal forces, resp. In the first index, the internal forces are designated with the axis, which is normal to the sectional plane. The second index stands for the direction, in which the stresses act as a consequence of the internal force. If first and second index match one another, then the second index is omitted. For cross-laminated timber, this means that,

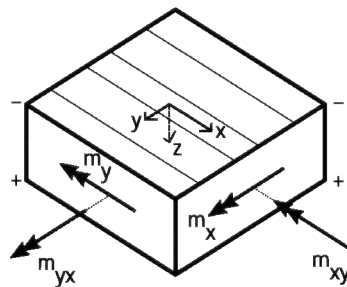
for example, those lamellas are stressed by m_x , which run in the x-direction of the panel element. It is urgently recommended to determine the x-direction as the direction of the outer layers for all elements.

a) Convention for internal forces of shell elements



Internal forces are positive, when they generate tensile stresses at the area's bottom side (z positive)

b) Internal moments (pos. section)

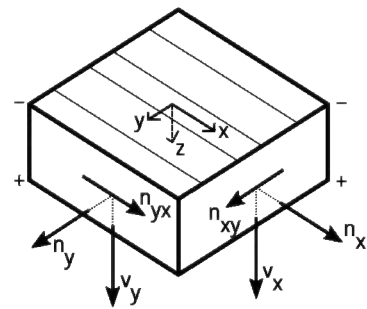


$$m_{yx} = m_{xy}$$

$$m_{xx} = m_x$$

$$m_{yy} = m_y$$

c) Internal forces (pos. section)



$$n_{xy} = n_{yx}$$

$$n_{xx} = n_x$$

$$n_{yy} = n_y$$

Figure 7.3 Internal forces in two-dimensional structural elements according to the conventions of common FEM programmes

With respect to the signs it is determined, that bending moments are positive, if they result in tensile stresses at the positive surface side, i.e. that side with the larger z-coordinate. All other internal forces are positive, if at the positive (right-hand side) section, the stresses resulting from them point in the positive axis direction. The positive directions at the negative (left-hand side) sections are reversed, for reasons of equilibrium.

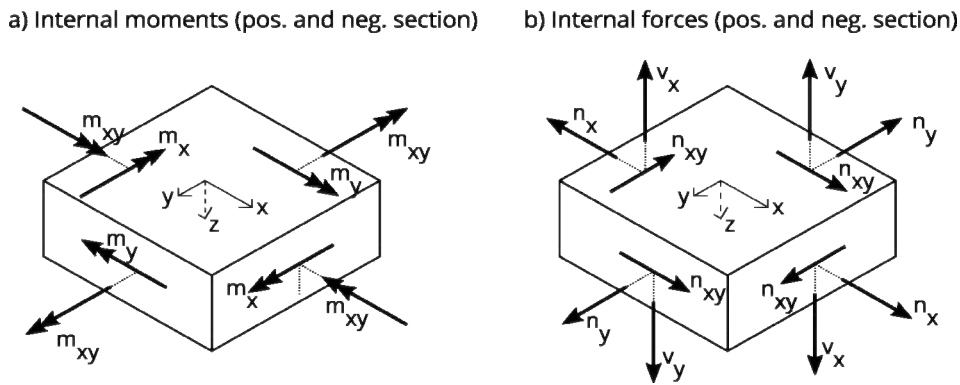


Figure 7.4 Internal forces of the opposite sections

7.2.3 Stiffnesses

The individual stiffness portions can be calculated from the net cross-sectional values in the two main directions of the cross-laminated timber panel.

The stiffnesses for bending EI_x and EI_y as well as strain EA_x and EA_y shall be calculated for the rigid composite cross-section. The stiffnesses for torsion $k_D GI_T$ and shear in the panel plane $k_S GA_{gross}$ can be determined from the gross cross-section with respectively associated reduction factors. For determination of the shear stiffnesses $\kappa_x GA_x$ and $\kappa_y GA_{s,y}$, the shear correction factors according to Timoshenko κ_x and κ_y shall be calculated for the two main directions of load-bearing capacity.

The reduction factors for the determination of torsional stiffness and shear stiffness in the panel plane were suggested in Volume 1 as a respectively simple factor independent of the element layout. ÖNORM B 1995-1-1:2015 includes a more exact suggestion, which considers the influence of longitudinal joints or longitudinal cracks of the lamellas. Both are based on the work of Silly, 2010.

For torsional stiffness applies

$$K_{xy} = k_D GI_T = k_D \cdot G_{0,mean} \cdot \frac{b \cdot d^3}{12} \quad (7.1)$$

$$k_D = \frac{1}{1 + 6 p_D \left(\frac{d_{max}}{a} \right)^{q_D}} \quad (7.2)$$

with

b Unit width of the CLT element ($b = 1$ m)

d Overall thickness of the cross-laminated timber panel

d_{max} Thickness of the thickest individual layer

a Mean board width; recommended is the determination with $a = 150$ mm.

p_D, q_D Parameters for torsional stiffness according to Table NA.K.4 of ÖNORM B 1995-1-1:2015

Parameters of torsional stiffness

Parameters for torsional stiffness	Number of layers		
	3	5	7 and more
p_D	0.89	0.67	0.55
q_D	1.33	1.26	1.23

For the shear stiffness in the panel plane applies

$$S_{xy}^* = k_S GA = k_D \cdot G_{0,mean} \cdot b \cdot d \tag{7.3}$$

$$k_S = \frac{1}{1 + 6 p_S \left(\frac{d_{max}}{a}\right)^{q_S}} \tag{7.4}$$

with

- b Unit width of the CLT element ($b = 1$ m)
- d Overall thickness of the cross-laminated timber element
- d_{max} Thickness of the thickest individual layer
- a Mean board width. Recommended is the determination with $a = 150$ mm.
- p_S, q_S Parameters for shear stiffness according to Table NA.K.4 of ÖNORM B 1995-1-1:2015

Parameters of shear stiffness

Parameters for shear stiffness	Number of layers	
	3	5, 7 and more
p_S	0.53	0.43
q_S	1.21	

7.2.4 Cross-sectional load-bearing capacity

The cross-sectional load-bearing capacities for bending, axial force and shear can be determined by rearranging the associated stress verifications to the level of internal forces. For determination and verification of the torsional shearing stresses, additional considerations are required:



Figure 7.5 Assumed distribution of shearing stresses as a consequence of torsion

Compared to a member with rectangular cross-section, the curve of the shear stresses from torsion is largely linear for panels across the cross-sectional height, as shown in

Figure 7.5. Therefrom, the torsional load-bearing capacity $m_{R,T,d}$ can be determined from the bending section modulus of the gross cross-section W .

$$W_T = \frac{b \cdot d^2}{6}$$

$$m_{R,T,d} = W_T \cdot f_{v,d}$$

with

b 100 cm (1 m panel strip)

d Overall thickness of the element

$f_{v,d}$ Design value of shear strength

7.2.5 Load application problems

For the analysis of load application problems, in some cases, models are required, which map the cross-laminated timber panels also in the thickness direction.

Upon predominantly uniaxial load distribution with planar stress states, as for example with notches, a planar model of homogeneous panel elements can be used. For that, the individual layers are defined as panels with a constant thickness d and provided with the characteristic building material values $E_{0,mean}$ and $G_{0,mean}$ for longitudinal layers as well as $E_{90,mean}$ and $G_{R,mean}$ for transverse layers.

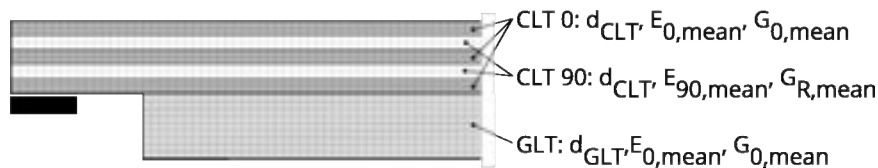


Figure 7.6 Plate model for a notch

Spatial modelling using volume elements normally is too elaborate for practical construction purposes.

7.2.6 Singularities

Due to the assumptions for the calculation model, singularities of deformations and stresses may occur for diaphragms as well as for plates (Rombach, 2015).

Examples for this are

- Openings and re-entrant corners in diaphragms and plates
- Concentrated loads or point supports in diaphragms and plates
- Blunt corners of plates

Here, result values are called singularities, which in one point are directed towards infinity. Numerical calculation methods, like the finite element method, provide only finite values in these areas, too, wherein the stress peaks increase with refinement of the grid division.

Since this is a model problem only, an "exact" calculation of the maximum values is generally not required. A real structure has no singularities. The stress concentrations are reduced by rearrangements.

Recommended grid division
15 cm to 30 cm

Normally, the grid division for structural element analyses, i.e. diaphragms or plates of cross-laminated timber with an element size of a mean board width of 15 cm up to about twice that, i.e. 30 cm, is sensible. At least the edges of each element should be divided into 6 elements. The coarser the finite element grid, the less the influence of singularities occurs.

Since for cross-laminated timber a linear elastic material behaviour is applied, without the possibility to plastically rearrange stresses, the influences of singularities with a purely numerical cause compared to actually occurring areas susceptible to cracks, as they occur, for example, by round openings in plates, cannot always be clearly defined. The definition of elastic supports and the enlargement of the grid width to about 30 cm, however, proved to be practical.

The most sensible handling of singularities is the integration of the result values via an area close to the singularity. By adding up the theoretically infinite sizes over relatively short lengths, the results remain in balance with the actions and assume sizes sensible for dimensioning.

7.3 CLT as an orthotropic finite element

The individual stiffness portions for the stiffness matrix of the orthotropic Mindlin-Reissner shell element are calculated for the plate according to Section 4.3.2 of Volume 1. The diaphragm portions are determined according to Section 4.4.2 of Volume 1.

Example 7.1 Characteristic values for the FEM calculation

Details

For an panel of cross-laminated timber, the required stiffness quantities for the static calculation and the subsequent verification of the load-bearing capacity shall be determined at the internal forces level. In that, a general load-bearing effect as a shell element is assumed, i.e. with a possible combination of diaphragm and plate stresses.



CLT 150 L5s

Characteristic building material properties and dimensions

$$E_{0,mean} = 11,550 \text{ N/mm}^2 \text{ [7.1]}$$

$$G_{0,mean} = 690 \text{ N/mm}^2$$

$$G_{R,mean} = 65 \text{ N/mm}^2 \text{ [7.1]}$$

The thickness of the individual layers is constant

$$d_1 = d_i = 3 \text{ cm}$$

The overall thickness of the panel is

$$d = 15 \text{ cm}$$

[7.1] Acc. to
ÖNORM B 1995-1-1:2015
Table NA.K.3

Determination of the panel stiffnesses**Bending stiffness EI_x**

$$K_x = EI_0 = E_{0,mean} \cdot I_{0,net}$$

$$I_{0,net} = I_{intrinsic} + I_{steiner} = 3 \cdot \frac{b \cdot d_1^3}{12} + 2 \cdot b \cdot d_1 \cdot z_1^2 = 3 \cdot \frac{100 \cdot 3^3}{12} + 2 \cdot 100 \cdot 3 \cdot 6^2 = 22,275 \text{ cm}^4$$

$$K_x = EI_0 = \frac{11,550}{10} \cdot \frac{22,275}{100^2} = 2,573 \text{ kNm}^2/\text{m}$$

Bending stiffness in EI_y

$$K_y = EI_{90} = E_{0,mean} \cdot I_{90,net}$$

$$I_{90,net} = I_{intrinsic} + I_{steiner} = 2 \cdot \frac{b \cdot d_1^3}{12} + 2 \cdot b \cdot d_1 \cdot z_1^2 = 2 \cdot \frac{100 \cdot 3^3}{12} + 2 \cdot 100 \cdot 3 \cdot 3^2 = 5,850 \text{ cm}^4$$

$$K_y = EI_{90} = \frac{11,550}{10} \cdot \frac{5,850}{100^2} = 676 \text{ kNm}^2/\text{m}$$

Torsional stiffness^[7.2]

$$K_{xy} = k_D GI_T = \frac{1}{1 + 6 \cdot p_D \left(\frac{d_{max}}{a}\right)^{q_D}} \cdot G_{0,mean} \cdot b \cdot \frac{d^3}{12}$$

$$p_D = 0.67$$

$$q_D = 1.26$$

$$K_{xy} = k_D GI_T = \frac{1}{1 + 6 \cdot 0.67 \left(\frac{3}{15}\right)^{1.26}} \cdot G_{0,mean} \cdot b \cdot \frac{d^3}{12}$$

$$K_{xy} = 0.654 \cdot \frac{690}{10} \cdot 100 \cdot \frac{15^3}{12} \cdot 100^{-2} = 127 \text{ kNm}^2/\text{m}$$

[7.2] Acc. to
ÖNORM B 1995-1-1:2015
(NA.K.2)

The panel layup consequently results in a reduction of the torsional stiffness of the cross-laminated timber element by the factor $k_T = 0.654$. In most software solutions for general, layered cross-sections, this factor is not automatically considered and shall be manually included via a respective setting.

Shear stiffness upon stressing by $v_{x,z}$

Shear correction factor according to Timoshenko

^[7.3] Shear correction factor for $G_{90}/G_0=65/690$

$$\kappa_0 = 0.231 \quad [7.3]$$

Shear stiffness

$$S_x = GA_s = \kappa_0 \cdot \sum G_i \cdot A_i = \kappa_0 \cdot (3 \cdot G_{0,mean} \cdot b \cdot d + 2 \cdot G_{R,mean} \cdot b \cdot d)$$

$$S_x = GA_s = 0.231 \cdot \left(3 \cdot \frac{690}{10} \cdot 100 \cdot 3 + 2 \cdot \frac{65}{10} \cdot 100 \cdot 3 \right) = 15.246 \text{ kN/m}$$

Shear stiffness upon stressing by $v_{y,z}$

Shear correction factor

^[7.4] Shear correction factor for $G_{90}/G_0=65/690$

$$\kappa_{90} = 0.179 \quad [7.4]$$

Shear stiffness

$$S_y = GA_s = \kappa_{90} \cdot \sum G_i \cdot A_i = (3 \cdot G_{R,mean} \cdot b \cdot d + 2 \cdot G_{0,mean} \cdot b \cdot d)$$

$$S_y = GA_s = 0.179 \cdot \left(3 \cdot \frac{65}{10} \cdot 100 \cdot 3 + 2 \cdot \frac{690}{10} \cdot 100 \cdot 3 \right) = 8,458 \text{ kN/m}$$

Stiffness matrix for the plate

$$C_{plate} = \begin{bmatrix} K_x & 0 & 0 & 0 & 0 \\ 0 & K_y & 0 & 0 & 0 \\ 0 & 0 & K_{xy} & 0 & 0 \\ 0 & 0 & 0 & S_x & 0 \\ 0 & 0 & 0 & 0 & S_y \end{bmatrix} = \begin{bmatrix} 2,573 & 0 & 0 & 0 & 0 \\ 0 & 676 & 0 & 0 & 0 \\ 0 & 0 & 8,951 & 0 & 0 \\ 0 & 0 & 0 & 15,246 & 0 \\ 0 & 0 & 0 & 0 & 8,458 \end{bmatrix}$$

K_x, K_y, K_{xy} in kNm^2/m ; S_x, S_y in kN/m

Determination of the plate stiffnesses

Extensional stiffness in the x-direction (main direction of load-bearing capacity)

$$D_x = EA_0 = E_{0,mean} \cdot A_{0,net}$$

$$A_{0,net} = 3 \cdot b \cdot d = 3 \cdot 100 \cdot 3 = 900 \text{ cm}^2$$

$$D_x = EA_0 = \frac{11,550}{10} \cdot 900 = 1,039,500 \text{ kN/m}$$

Extensional stiffness in the y-direction (transverse to the main direction of load-bearing capacity)

$$D_y = EA_{90} = E_{0,mean} \cdot A_{90,net}$$

$$A_{90,net} = 2 \cdot b \cdot d = 2 \cdot 100 \cdot 3 = 600 \text{ cm}^2$$

$$D_y = EA_{90} = \frac{11,550}{10} \cdot 600 = 693,000 \text{ kN/m}$$

Shear stiffness in the plate plane

$$D_{xy} = \frac{1}{1 + 6 \cdot p_s \left(\frac{d_{max}}{a}\right)^{q_s}} \cdot G_{0,mean} \cdot b \cdot d$$

For five-layer elements applies:

$$p_s = 0.43$$

$$q_s = 1.21$$

$$D_{x,y} = \frac{1}{1 + 6 \cdot 0.43 \left(\frac{3}{15}\right)^{1.21}} \cdot G_{0,mean} \cdot b \cdot d = 0.731 \cdot \frac{690}{10} \cdot 100 \cdot 15 = 75,659 \text{ kN/m}$$

Stiffness matrix for the diaphragm

$$C_{diaphragm} = \begin{bmatrix} D_x & 0 & 0 \\ 0 & D_y & 0 \\ 0 & 0 & D_{xy} \end{bmatrix} = \begin{bmatrix} 1,039,500 & 0 & 0 \\ 0 & 693,000 & 0 \\ 0 & 0 & 75,659 \end{bmatrix}$$

D_x, D_y, D_{xy} in kN/m

Determination of the load-bearing resistances**Characteristic value of the load-bearing moment in the x-direction**

$$m_{R,x,k} = W_{0,net} \cdot k_{sys} \cdot f_{m,k}$$

$$W_{0,net} = \frac{I_{0,net}}{z_{1,o}} = \frac{22,275}{7.5} = 2,970 \text{ cm}^3$$

$$m_{R,x,k} = \frac{2,970 \cdot 1.1 \cdot \frac{24}{10}}{100} = 78.4 \text{ kNm/m}$$

Characteristic value of the load-bearing moment in the y-direction

$$m_{R,y,k} = W_{90,net} \cdot k_{sys} \cdot f_{m,k}$$

$$W_{90,net} = \frac{I_{90,net}}{z_{2,o}} = \frac{5,850}{4.5} = 1,300 \text{ cm}^3$$

$$m_{R,y,k} = \frac{1,300 \cdot 1.1 \cdot \frac{24}{10}}{100} = 34.3 \text{ kNm/m}$$

Characteristic value of the torsional load-bearing moment

For cross-laminated timber as a panel-shaped element, it is assumed that torsional moments result in shearing stresses with a linear curve across the panel thickness. According to this assumption, torsion does not result in circumferential torsional shearing stresses like in rectangular cross-sections, but is exclusively distributed via shearing stresses in parallel to the panel plane with an approximately linear curve across the height.

The torsional resistance then corresponds to the section modulus of the gross cross-section and results in

$$W_T = \frac{b \cdot d^2}{6} = \frac{100 \cdot 15^2}{6} = 3,750 \text{ cm}^3$$

$$m_{R,T,k} = W_T \cdot f_T = \frac{3,750}{100} \cdot \frac{2.5}{10} = 9.38 \text{ kNm/m}$$

Characteristic value of the resistance to lateral force $v_{x,z}$

Static moment for the maximum rolling shear stress

$$S_{R,0} = \sum b \cdot d_i \cdot z_i = b \cdot d_1 \cdot 2d_1 = 100 \cdot 3 \cdot 6 = 1,800 \text{ cm}^3$$

$$v_{R,x,k} = \frac{f_{V,R,k} \cdot I_0 \cdot b}{S_{R,0}} = \frac{\frac{1.1}{10} \cdot 22,275 \cdot 100}{1,800} = 136.1 \text{ kN/m}$$

Characteristic value of the resistance to lateral force $v_{y,z}$

Static moment for the maximum rolling shear stress

$$S_{R,90} = \sum b \cdot d_i \cdot z_i = b \cdot d_1 \cdot d_1 = 100 \cdot 3 \cdot 3 = 900 \text{ cm}^3$$

$$v_{R,y,k} = \frac{I_0 \cdot b}{S_{R,0}} \cdot f_{V,R,k} = \frac{5,850 \cdot 100}{900} \cdot \frac{1.1}{10} = 71.5 \text{ kN/m}$$

Characteristic value of the axial resistance in the x-direction

Tension

$$n_{R,x,t,k} = A_{0,net} \cdot f_{t,0,k} = 900 \cdot \frac{14}{10} = 1,260 \text{ kN/m}$$

Pressure

$$n_{R,x,c,k} = A_{0,net} \cdot f_{c,0,k} = 900 \cdot \frac{21}{10} = 1,890 \text{ kN/m}$$

Characteristic value of the axial resistance in the y-direction**Tension**

$$n_{R,y,c,k} = A_{90,net} \cdot f_{t,0,k} = 600 \cdot \frac{14}{10} = 840 \text{ kN/m}$$

Pressure

$$n_{R,y,c,k} = A_{90,net} \cdot f_{c,0,k} = 600 \cdot \frac{21}{10} = 1,260 \text{ kN/m}$$

Characteristic value of the shear resistance in the panel plane

$$n_{R,xy,k} = \min \begin{cases} f_{V,S,k} \cdot \min(A_{0,net}, A_{90,net}) & (a) \\ f_{V,T,k} \cdot \frac{\min(A_{0,net}, A_{90,net}) \cdot a}{3 \cdot d_{i,max}} & (b) \\ f_{V,k} \cdot A_{Gross} & (c) \end{cases}$$

(a) Shearing-off of the individual lamellas

(b) Torsion in the glued joints

(c) Shearing-off of the entire cross-section

with

a ... Mean board width (recommended $a = 150$ mm)

$$n_{R,xy,k} = \min \begin{cases} \frac{5,0}{10} \cdot \min(100 \cdot 9; 100 \cdot 6) = 300 \text{ kN/m} & (a) \\ \frac{2,5}{10} \cdot \frac{\min(100 \cdot 9; 100 \cdot 6) \cdot 15}{3 \cdot 3} = 250 \text{ kN/m} & (b) \\ \frac{2,5}{10} \cdot 100 \cdot 15 = 375 \text{ kN/m} & (c) \end{cases}$$

$$n_{R,xy,k} = 250 \text{ kN/m}$$

Verifications**Normal stresses in the main direction of load-bearing capacity (x)**

$$\frac{m_{x,d}}{m_{R,x,d}} + \frac{n_{x,d}}{n_{R,x,d}} \leq 1$$

Normal stresses in the ancillary direction of load-bearing capacity (y)

$$\frac{m_{y,d}}{m_{R,y,d}} + \frac{n_{y,d}}{n_{R,y,d}} \leq 1$$

Shearing stresses

The superimposition of the internal forces generating shearing stresses follows general considerations of construction mechanics and analogously corresponds to the superimposition according to ÖNORM B 1995-1-1:2015, Equation NA.6.15-E1.

$$\sqrt{\left(\frac{v_{x,d}}{v_{R,x,d}}\right)^2 + \left(\frac{v_{y,d}}{v_{R,y,d}}\right)^2} + \frac{m_{xy,d}}{m_{R,xy,d}} + \frac{n_{xy,d}}{n_{R,xy,d}} \leq 1$$

Example 7.2 Linearly supported roofing panel with bilateral overhang

Details

Dimensions of the roofing slab according to Figure 7.7. The outer layers of the floor panel CLT 150 L5s (30l-30w-30l-30w-30l) run in the direction of the main directions of load-bearing capacity applied. The projection of the roof is 1.25 m in the main direction of load-bearing capacity and 1.0 m normal to that. The linear support is formed by a 3 m high wall of CLT 90 Q3s (30l-30w-30l).

Service class: NKL 1

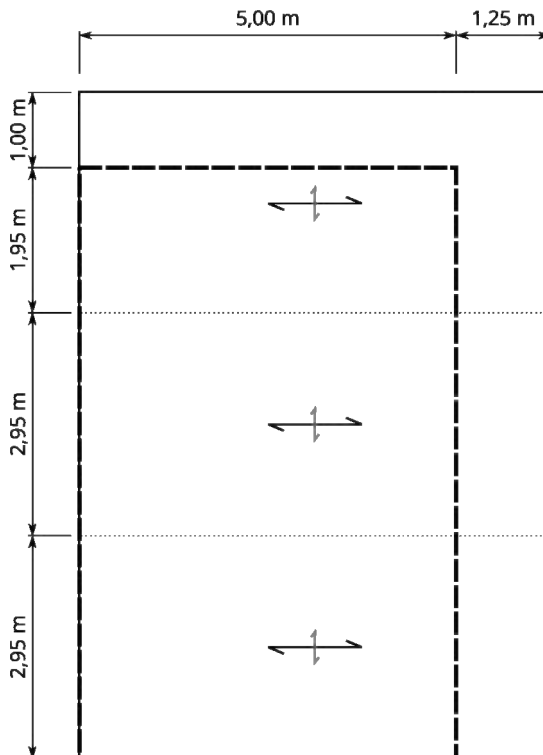


Figure 7.7: Dimensions of the floor panel

Actions

$g_k = 1.60 \text{ kN/m}^2$ (Permanent loads)

$s_k = 1.35 \text{ kN/m}^2$ (Snow load at the roof from the tabulated value for Graz.)

$$s_{\text{Ground},k} = 1.65 \text{ kN/m}^2, s_k = \mu_1 \cdot s_{\text{Ground},k} = 0.8 \cdot 1.65 \approx 1.35 \text{ kN/m}^2$$

Load category: snow below 1000 m of sea level)

$n_k = 1.0 \text{ kN/m}^2$ (Live loads at the roof, Category H)

Static calculation

Load coefficients

The coefficient of deformation for cross-laminated timber in the service class NKL 1 is

$$k_{\text{def}} = 0.8.$$

[AT]
ÖNORM B 1995-1-1:2015,
Table NA.K.2

The load coefficients for the two load portions are:

For permanent loads g_k : $k_{mod} = 0.6$ and for snow loads s_k below 1000 m above sea level:
Load duration short-term: $k_{mod} = 0.9$, $\psi_2 = 0.0$

[AT]
ÖNORM B 1995-1-1:2015,
Table NA.K.1

Definition of the static model

For calculation as a plate, the vertical deflection u_z , the torsion about the x-axis φ_x and the torsion about the y-axis φ_y are selected as the system's degrees of freedom. The remaining three degrees of freedom are not of interest for the calculation of panels.

The roofing panel is defined as an overall system, i.e. with cantilevers in two directions and its adjacent panels. Thus, the influence of the joint design is considered in the static construction model. The grain of the outer layers is parallel to the local x-direction. The butt joints are defined as ideal linear joints. The support by the walls is modelled by linear supports in the wall's central axis with vertical translation springs-. Within the scope of the FEM calculation, the stiffness of the wall can be determined from $c = \frac{EA}{h}$.

With the flexible support, the influence of the singularity and thus the local increase of the support pressures in the corner of the two exterior walls is reduced. For the wall CLT 90-Q3s (30l-30w-30l) with a height $h = 3$ m, the stiffness per running metre of wall results in:

$$c = \frac{E \cdot b \cdot \sum d_x}{h} = \frac{11,550/10 \cdot 100 \cdot 6}{3} = 231,000 \text{ kN/m}^2$$

For the finite element model of the panels, orthotropic Mindlin-Reissner elements are used. The behaviour of the panels is determined by the individual terms of the stiffness matrix from Section 7.2.3. The division of the FE grid was determined with an edge length of 15 cm per FEM element.

The actions g_k and s_k are defined as separate load cases and respectively applied as full load across the entire surface. Live loads of Category H at the roof n_k shall not be applied simultaneously with the snow load. A comparison of the envelopes from the unfavourable superposition of the live loads acting span-wise shows, that here the snow load is decisive as full load.

Results of the static calculation

For the serviceability limit state SLS, the initial deflection is limited with

$$u_{inst} = u_{g,k} + u_{s,k} \leq \frac{l}{300}$$

[AT]
ÖNORM B 1995-1-1:2015,,
Table NA.7.2

wherein here, too, the dead weight g_1 is fully considered as part of the permanent loads. The verification of end deflection follows with:

$$u_{net,fin} = (u_{g,k} + \psi_2 \cdot u_{s,k}) (1 + k_{def}) \leq \frac{l}{250}$$

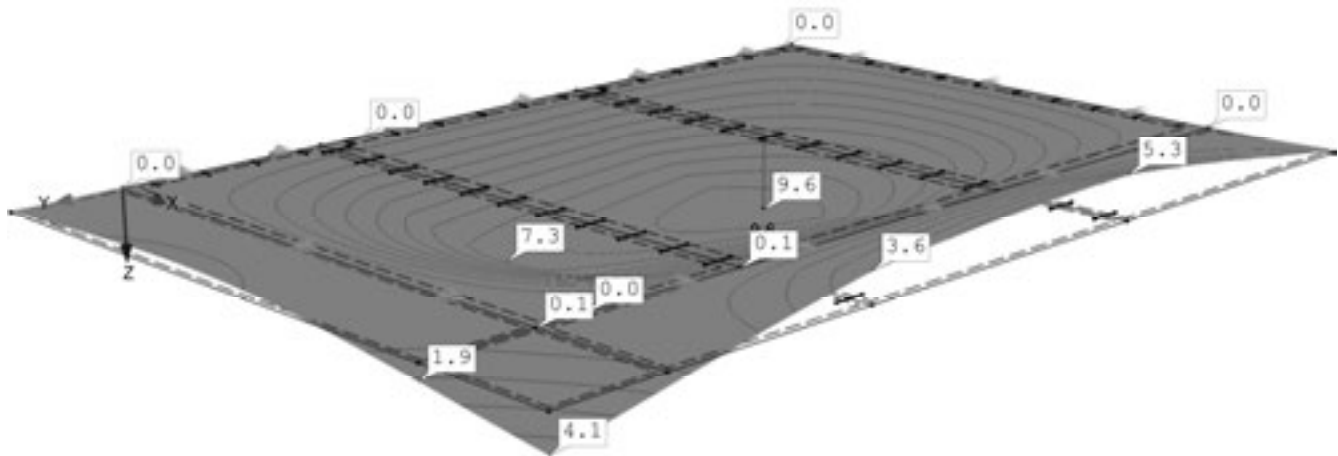
[AT]
ÖNORM B 1995-1-1:2015,
Table NA.7.2

In the ultimate limit state ULS, the results of the load cases are combined to

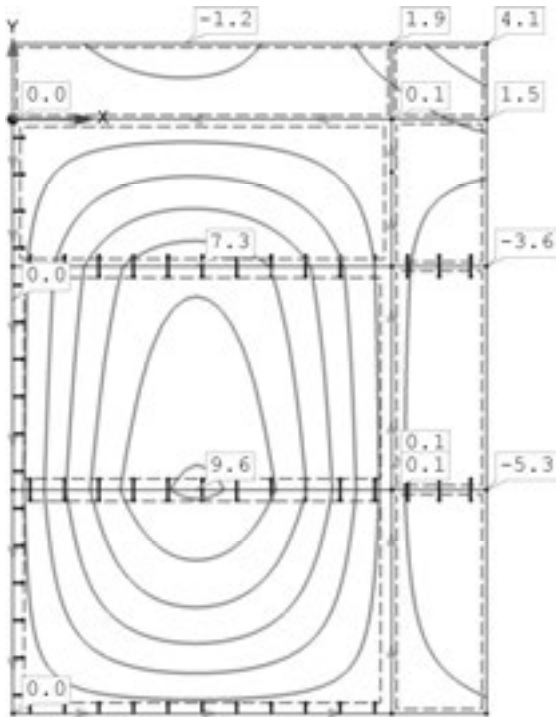
$$E_d = \gamma_G \cdot E_{g,k} + \gamma_Q \cdot E_{s,k}$$

The results of the static calculation using the finite element method are graphically depicted on the following pages using isolines or in sections, resp.

a) Deformed shape – Perspective u_{inst} [mm]

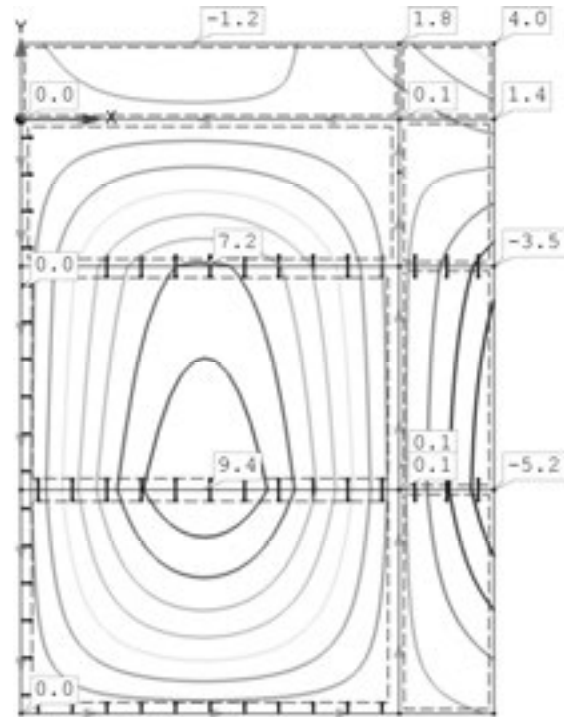


b) Instantaneous deflections u_{inst} [mm]



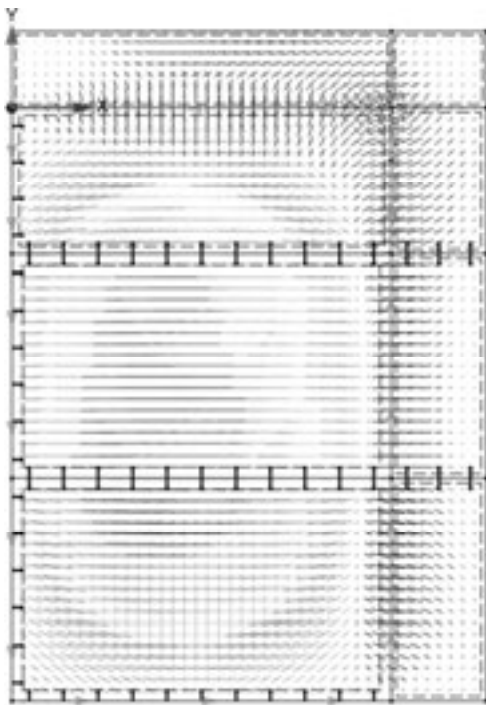
max $u_{inst} = 4.1$ mm

c) Final deflections $u_{net,fin}$ [mm]

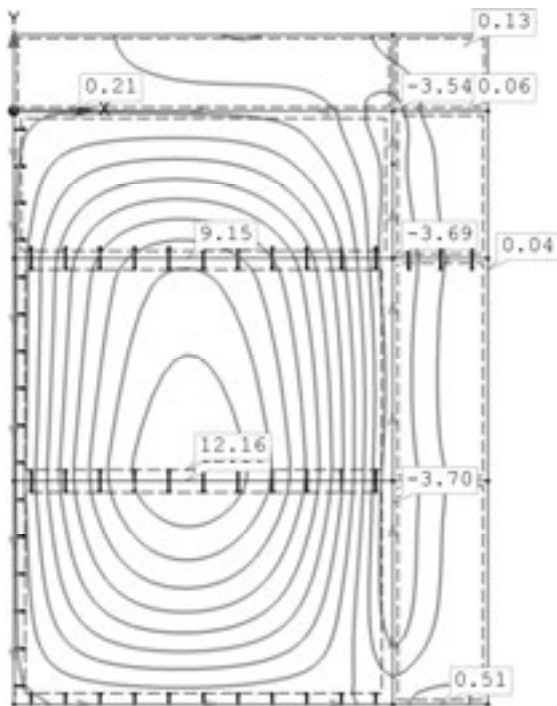


max $u_{net,fin} = 4.0$ mm

d) Trajectories of the main moments

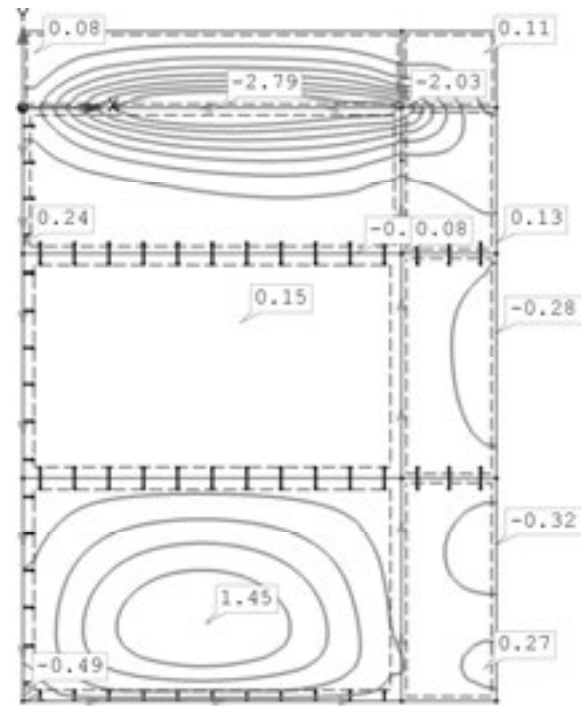


e) Bending moments m_x [kNm/m]



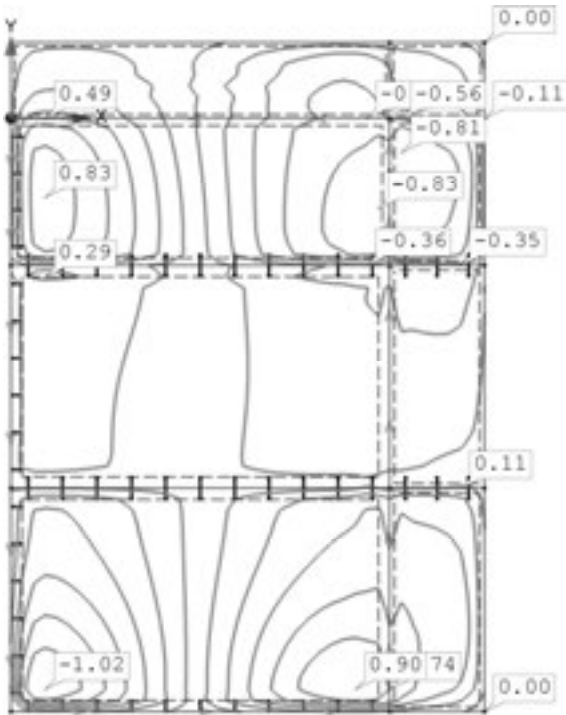
$\min m_{x,d} = -3.70$ kNm
 $\max m_{x,d} = 12.16$ kNm

f) Bending moments m_y [kNm/m]



$\min m_{y,d} = -2.79$ kNm
 $\max m_{y,d} = 1.45$ kNm

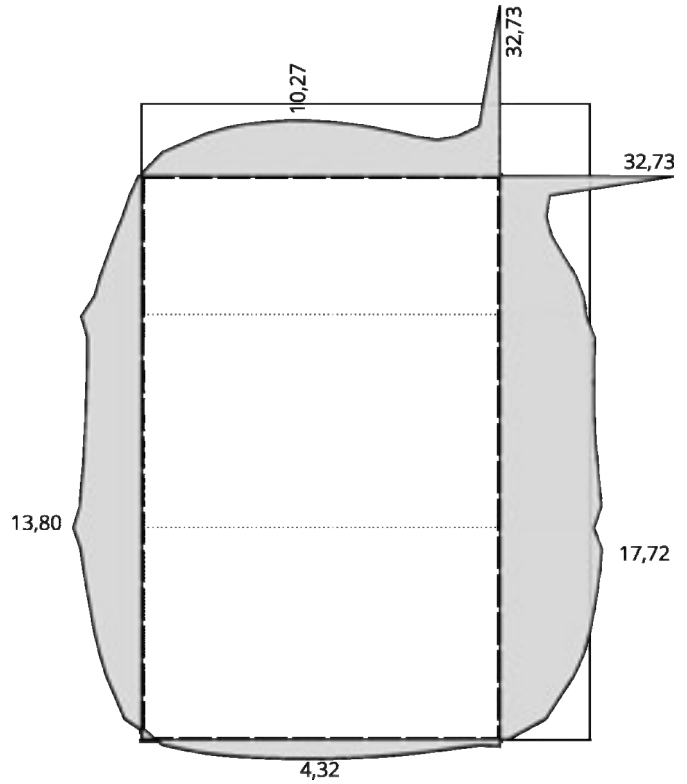
g) Torsional moments m_{xy} [kNm/m]



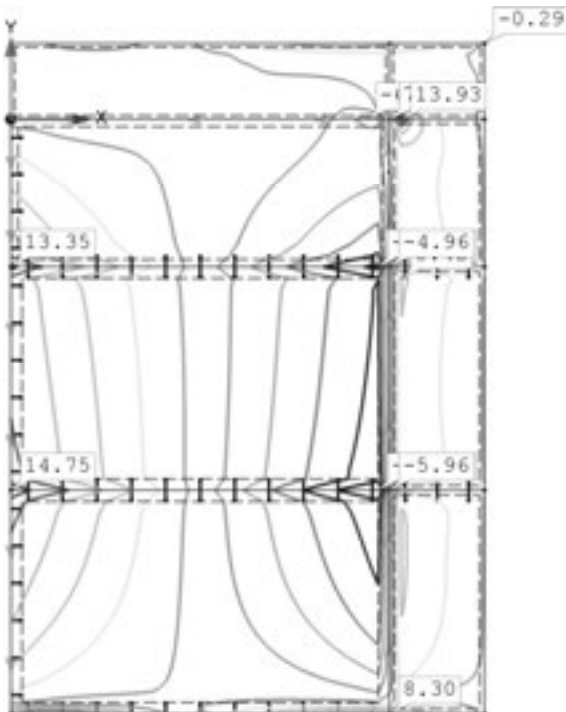
$\min m_{xy,d} = -1.02$ kNm

$\max m_{xy,d} = 0.90$ kNm

h) Reaction forces [kN/m]



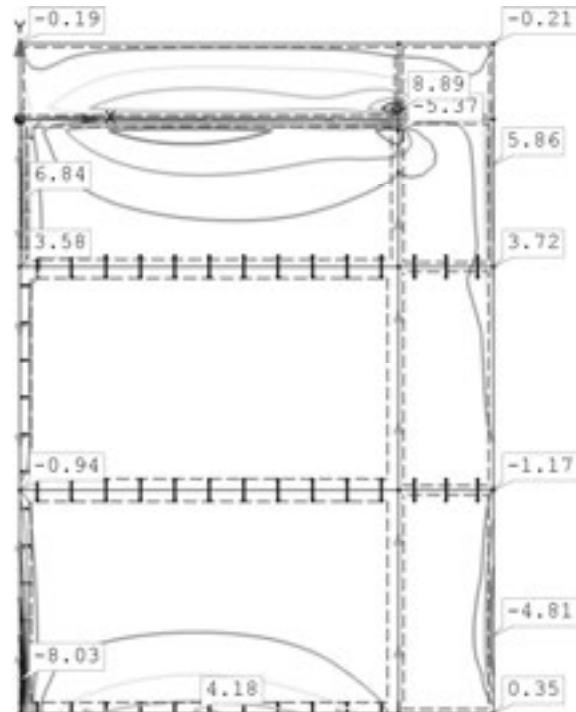
i) Lateral force v_x [kN/m]



$\min v_{x,d} = -14.47$ kN/m

$\max v_{x,d} = 14.75$ kN/m

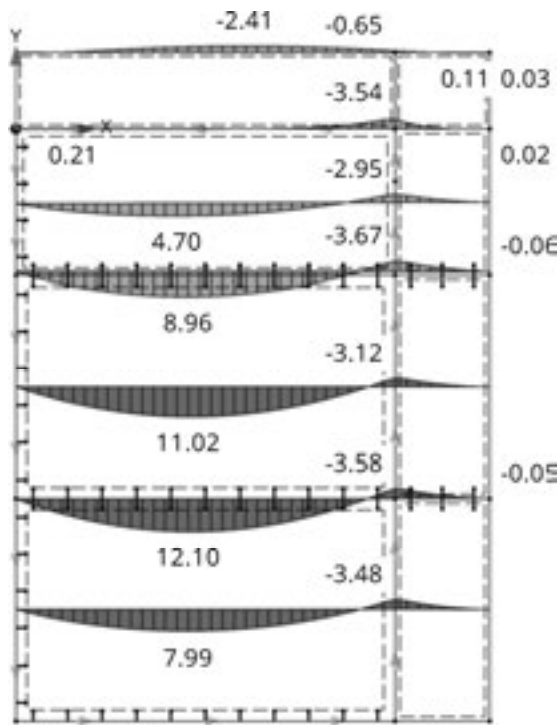
j) Lateral force v_y [kN/m]



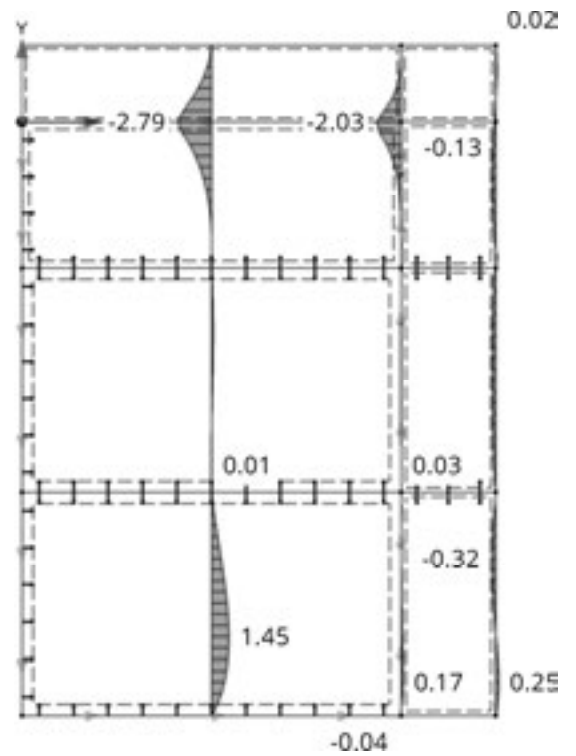
$\min v_{y,d} = -8.03$ kN/m

$\max v_{y,d} = 8.89$ kN/m

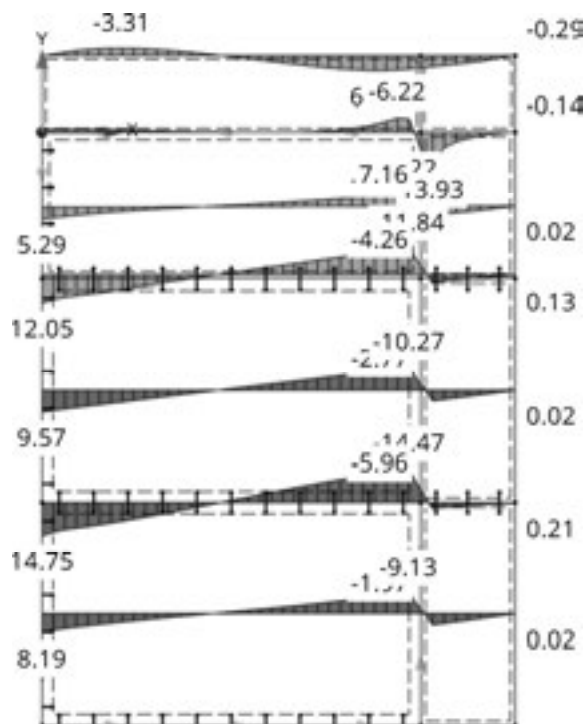
k) Bending moment m_x in sections



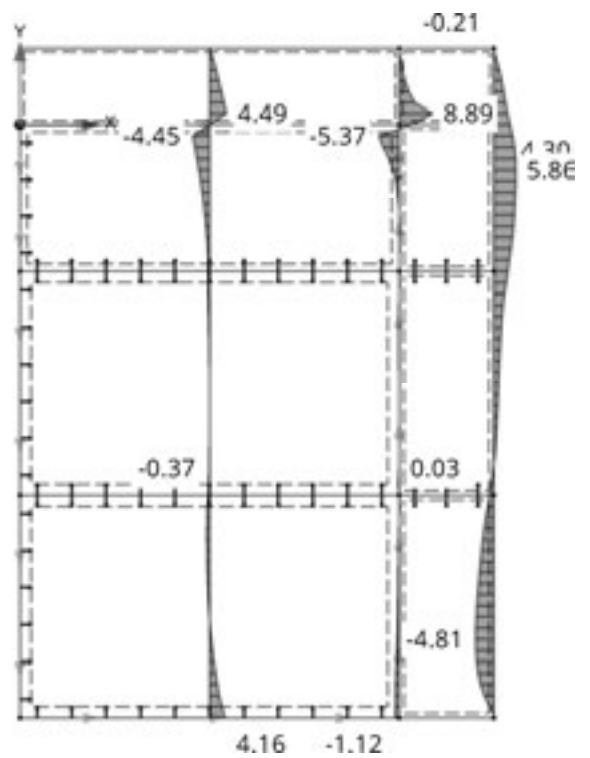
l) Bending moment m_y in sections



m) Lateral force v_x in sections



n) Lateral force v_y in sections



Verifications

Serviceability limit states SLS

Deflection at the projecting corner

As reference length for the deflection limitation, the length along the diagonal is used

- **Verification of instantaneous deflection**

$$\max u_{inst} \leq w_{inst,adm}$$

$$w_{inst,adm} = \frac{l}{300} = \frac{\sqrt{c_x^2 + c_y^2}}{300} = \frac{\sqrt{1,250^2 + 1,000^2}}{300} = \frac{1600}{300} = 5.3 \text{ mm}$$

$$4.1 \text{ mm} \leq 5.3 \text{ mm}$$

✓ Verification fulfilled ($\eta = 78 \%$)

- **Verification of final deflection**

$$w_{net,fin,adm} = \frac{l}{250} = \frac{1600}{250} = 6.4 \text{ mm}$$

$$\max u_{net,fin} \leq w_{net,fin,adm}$$

$$4.0 \leq 6.4 \text{ mm}$$

✓ Verification fulfilled ($\eta = 63 \%$)

Ultimate limit states ULS

The decisive combination of actions in the present example is for all internal design forces $g + s$ with $k_{mod} = 0.9$.

The characteristic values of the cross-sectional resistances were determined in Section 7.3.

The partial safety factor for cross-laminated timber is $\gamma_M = 1.25$.

- **Verification of bending moments m_x**

For this bending stress about the strong axis, the projection is not relevant for dimensioning. The decisive span moment is $\max m_{x,d} = 12.16 \text{ kNm/m}$.

$$m_{x,d} \leq m_{R,x,d} = k_{mod} \cdot \frac{m_{R,x,k}}{\gamma_M} = 0.9 \cdot \frac{78.4}{1.25} = 56.45 \text{ kNm/m}$$

$$12.16 \leq 56.45 \text{ kNm/m}$$

✓ Verification fulfilled ($\eta = 22 \%$)

- **Verification of bending moments m_y**

$$\min m_{y,d} = -2.79 \text{ kNm/m}$$

$$m_{y,d} \leq m_{R,y,d} = k_{mod} \cdot \frac{m_{R,y,k}}{\gamma_M} = 0.9 \cdot \frac{34.3}{1.25} = 24.7 \text{ kNm/m}$$

$$2.79 \leq 24.70 \text{ kNm/m}$$

✓ Verification fulfilled ($\eta = 12 \%$)

- **Verification of shear stresses**

- Torsional moments m_{xy}

The largest torsional moment, in respect of its amount, results in $\min m_{xy,d} = -1.02 \text{ kNm}$ in the area of the panel supported on three sides at the end without projection.

- Lateral forces v_x

$$v_{x,d} = 13.93 \text{ kN/m in the area of the projection}$$

$$v_{x,d} = 14.75 \text{ kN/m in the area of the support in the span}$$

- Lateral forces v_y

$$v_{y,d} = 8.89 \text{ kN/m in the area of the projection}$$

$$v_{y,d} = 8.03 \text{ kN/m in the area of the support in the span}$$

- Interaction of the internal forces

For the interaction, here, the maximum internal forces are superimposed without consideration of their location.

$$v_{R,x,k} = 136.1 \text{ kN/m}$$

$$v_{R,y,k} = 71.5 \text{ kN/m}$$

$$\sqrt{\left(\frac{v_{x,d}}{v_{R,x,d}}\right)^2 + \left(\frac{v_{y,d}}{v_{R,y,d}}\right)^2} + \left(\frac{m_{xy,d}}{m_{R,xy,d}}\right) \leq 1$$

$$\sqrt{\left(\frac{v_{x,d}}{k_{mod} \cdot \frac{v_{R,x,k}}{\gamma_M}}\right)^2 + \left(\frac{v_{y,d}}{k_{mod} \cdot \frac{v_{R,y,k}}{\gamma_M}}\right)^2} + \left(\frac{m_{xy,d}}{k_{mod} \cdot \frac{m_{R,xy,k}}{\gamma_M}}\right) \leq 1$$

$$\sqrt{\left(\frac{14.75}{0.9 \cdot \frac{136.1}{1.25}}\right)^2 + \left(\frac{8.89}{0.9 \cdot \frac{71.5}{1.25}}\right)^2} + \left(\frac{1.02}{0.9 \cdot \frac{9.38}{1.25}}\right) \leq 1$$

$$\sqrt{0.0227 + 0.0298} + 0.15 \leq 1$$

$$0.229 + 0.15 \leq 1$$

$$0.38 \leq 1$$

✓ Verification fulfilled ($\eta = 38 \%$)

- **Verification of support pressure**

A singularity is present in the exterior corner. In calculations, the reaction forces at the corner point tend towards infinity. The selection of the element size of 15 cm gives practical results. Since the load-bearing capacity with support pressure is sufficiently high, balancing of the reaction forces by averaging across an area of about 30 cm in both directions is omitted.

If in the model, instead of an elastic linear support, a rigid support is applied, then this increases the peak value of the reaction force by about 38 %. If averaging is undertaken across a length of 30 cm, then the average value with rigid support is only about 6 % higher.

$$\max a_d = 32.73 \text{ kN/m}$$

$$b_{ef} = 9 \text{ cm}$$

$$f_{c,90,k} = 3.0 \text{ N/mm}^2$$

The design value of the support's load-bearing capacity is

$$a_{R,d} = b_{ef} \cdot k_{c,90} \cdot f_{c,90,d} = b_{ef} \cdot k_{c,90} \cdot k_{mod} \cdot \frac{f_{c,90,k}}{\gamma_M}$$

Coefficient of lateral pressure $k_{c,90}$

The load-bearing wall is located inside the floor.

The width of the pressing area is determined according to Section 6.3:

$$b_{90,ef} = 9 \text{ cm}$$

Coefficient of lateral pressure according to Table 4-2:

$$k_{c,90} = 1.8$$

The design value of resistance of the support pressure is:

$$a_{R,d} = A_{90,ef} \cdot k_{c,90} \cdot k_{mod} \cdot \frac{f_{c,90,k}}{\gamma_M} = 100 \cdot 9 \cdot 0.9 \cdot \frac{3.0}{10 \cdot 1.25} = 202 \text{ kN/m}$$

The verification at the level of the support load per running metre is:

$$a_d \leq a_{R,d}$$

$$32.73 \text{ kN/m} \leq 202 \text{ kN/m}$$

✓ Verification fulfilled ($\eta = 16 \%$)

Example 7.3 Canopy with point support

Given:

Roofing panel with unilateral linear support and point supports on the opposite side according to Figure 7.8.

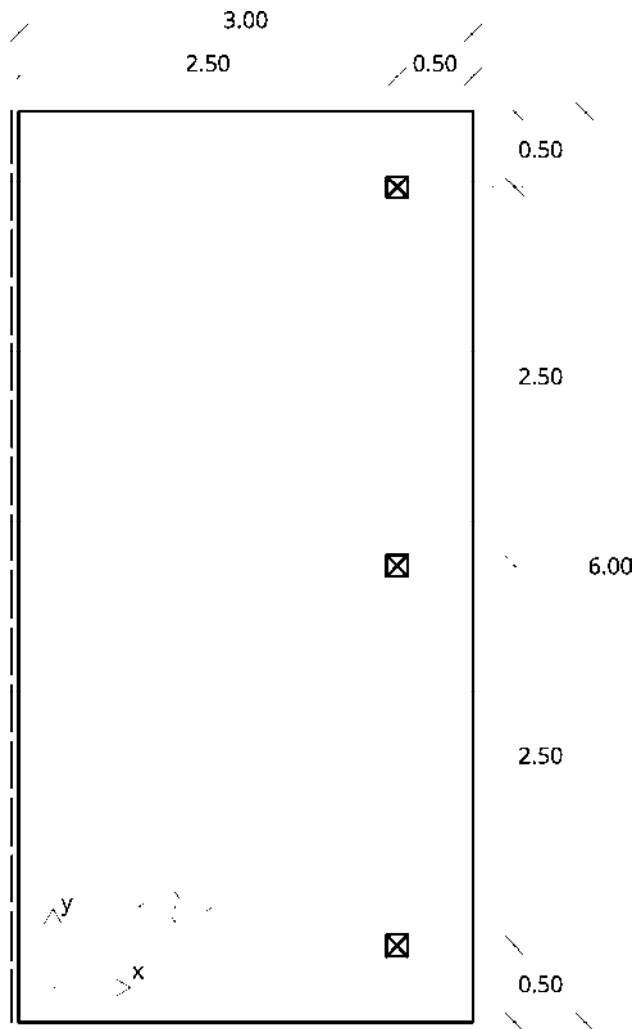


Figure 7.8 Point-supported roofing panel

Element: CLT 150 L5s (30l-30w-30l-30w-30l); $k_{mod} = 0.9$

Material system according to Section 3.1

Sought:

Determination of the internal forces using the FEM method

Internal forces for verification of the central support

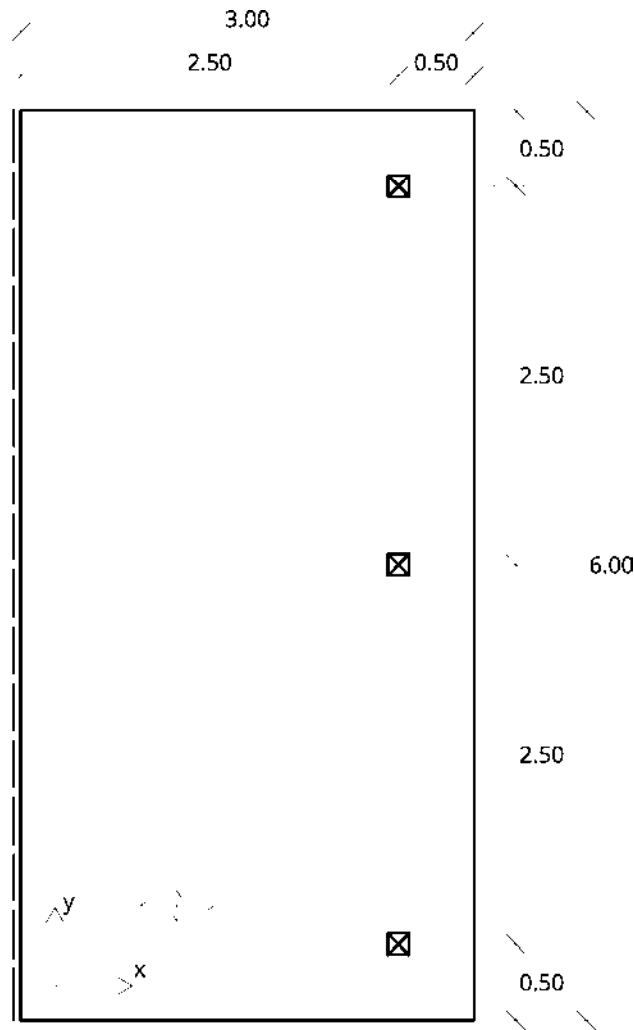


Figure 7.9 System

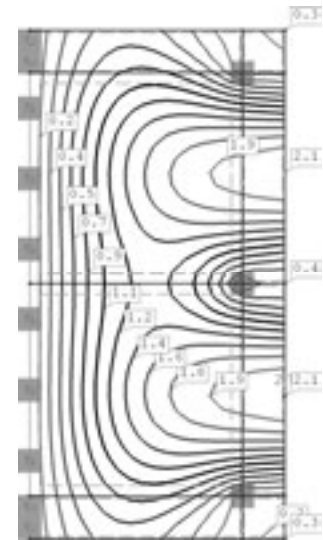


Figure 7.10 Instantaneous deformations u_{inst}

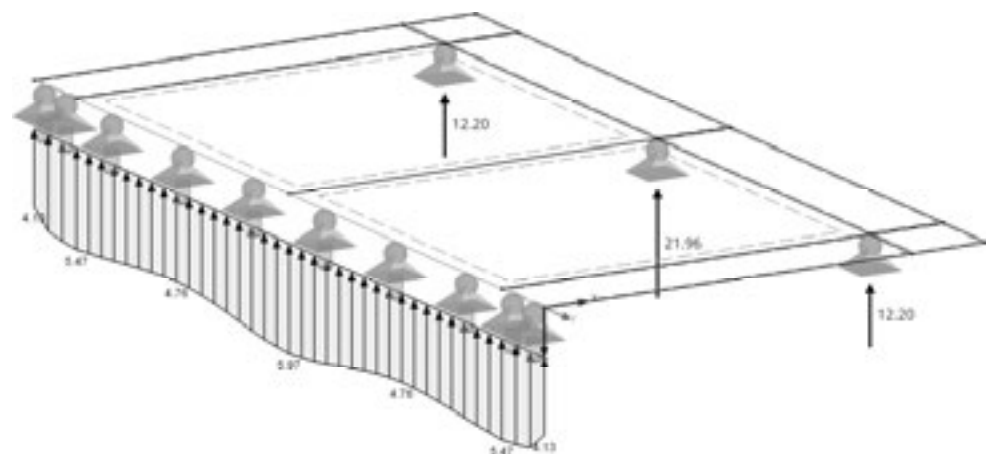


Figure 7.11 Support reactions

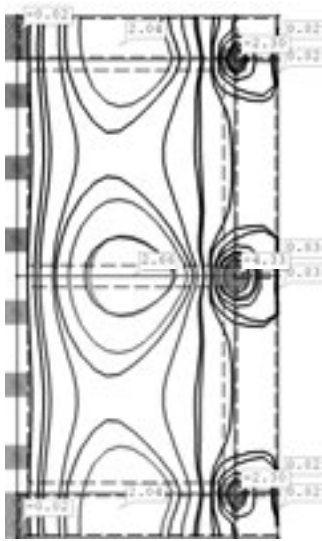


Figure 7.12 min m_x and max m_x

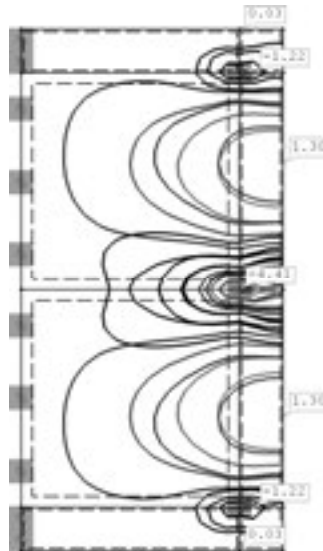


Figure 7.13 min m_y and max m_y

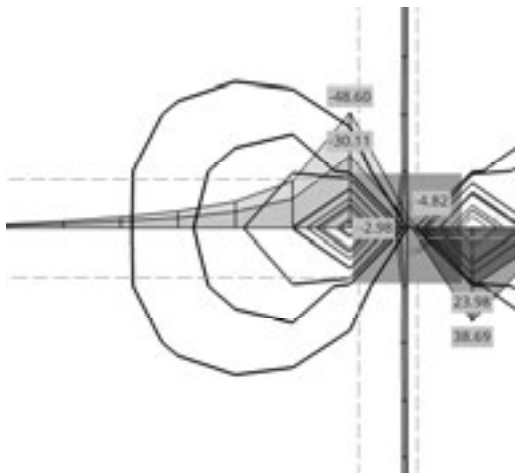


Figure 7.14 min v_x and max v_x in the area of the central support (isolines and sections)

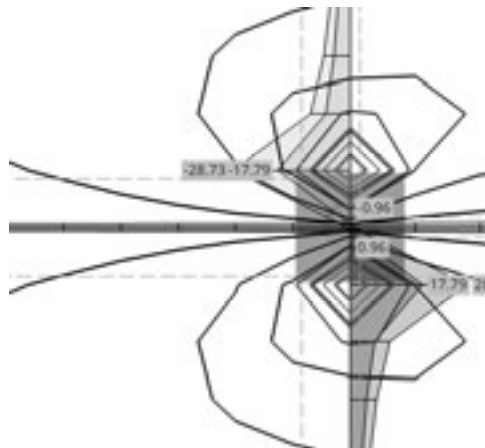


Figure 7.15 min v_y and max v_y in the area of the central support (isolines and sections)

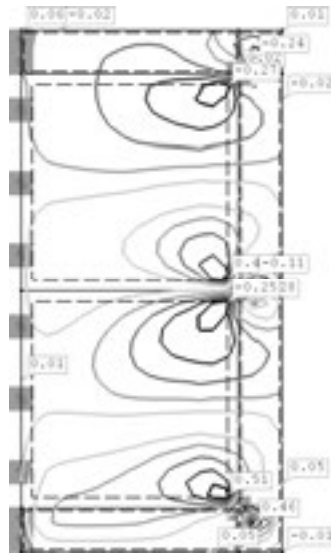


Figure 7.16 max m_{xy}

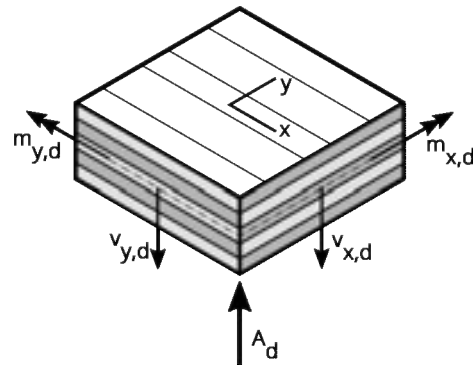


Figure 7.17 Internal forces at the floor panel over the central support

The design values of the internal forces at the central support in the ultimate limit state are designated in Figure 7.17 and summarised in the following.

$$A_d = 21.96 \text{ kN}$$

$$m_{x,d} = -4.33 \text{ kNm/m}$$

$$m_{y,d} = -4.41 \text{ kNm/m}$$

$$m_{xy,d} = 0.06 \text{ kNm/m}$$

$$v_{x,d} = \begin{bmatrix} -48.60 \text{ kN/m} \\ 38.69 \text{ kN/m} \end{bmatrix}$$

$$v_{y,d} = \begin{bmatrix} 28.73 \text{ kN/m} \\ -28.73 \text{ kN/m} \end{bmatrix}$$

$$k_{mod} = 0.9$$

Verifications**Verification of compression perpendicular to grain at support**

$$k_{c,90} = 1.80$$

$$A_{R,d} = 1.80 \cdot 14 \cdot 14 \cdot 0.9 \cdot \frac{3.0}{10 \cdot 1.25} = 76.2 \text{ kN}$$

$$A_d \leq A_{R,d}$$

$$21.96 \text{ kN} \leq 76.2 \text{ kN}$$

✓ Verification fulfilled ($\eta = 28 \%$)

Verification of shear stresses v_x

$$\tau_{r,x,d} = \frac{v_{x,d} \cdot S_y(z = 45 \text{ mm})}{I_{0,net}} = \frac{-48.60 \cdot 1,000 \cdot 30 \cdot 60}{22,275 \cdot 10^4} = -0.39 \text{ N/mm}^2$$

$$\tau_{r,x,d} \leq f_{V,R,d} = 0.9 \cdot \frac{1.1}{1.25} = 0.79 \text{ N/mm}^2$$

$$0.39 \text{ N/mm}^2 \leq 0.79 \text{ N/mm}^2$$

✓ Verification fulfilled ($\eta = 49 \%$)

Verification of shear stresses v_y

$$\tau_{r,y,d} = \frac{v_{y,d} \cdot S_y(z = 15 \text{ mm})}{I_{90,net}} = \frac{-28.73 \cdot 1,000 \cdot 30 \cdot 30}{5,850 \cdot 10^4} = -0.44 \text{ N/mm}^2$$

$$\tau_{r,y,d} \leq f_{V,R,d} = 0.9 \cdot \frac{1.1}{1.25} = 0.79 \text{ N/mm}^2$$

$$0.44 \text{ N/mm}^2 \leq 0.79 \text{ N/mm}^2$$

✓ Verification fulfilled ($\eta = 56 \%$)

Verification of bending moments m_x

$$\sigma_{x,d} = \frac{m_{x,d} \cdot t_{CLT}/2}{I_{0,net}} = \frac{-4.33 \cdot 1,000 \cdot 1,000 \cdot 75}{22,275 \cdot 10^4} = -1.46 \text{ N/mm}^2$$

$$\sigma_{x,d} \leq f_{m,d} = 0.9 \cdot \frac{24.0}{1.25} = 17.28 \text{ N/mm}^2$$

$$1.46 \text{ N/mm}^2 \leq 17.28 \text{ N/mm}^2$$

✓ Verification fulfilled ($\eta = 8 \%$)

Verification of bending moments m_y

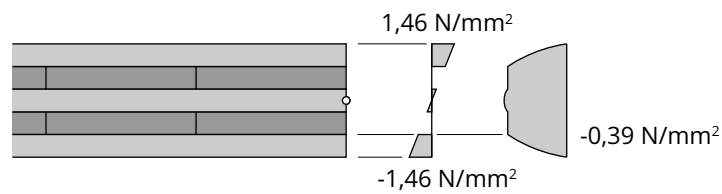
$$\sigma_{y,d} = \frac{m_{y,d} \cdot \left(\frac{t_{CLT}}{2} - t_1 \right)}{I_{90,net}} = \frac{-4.41 \cdot 1,000 \cdot 1,000 \cdot (75 - 30)}{5,850 \cdot 10^4} = -3.39 \text{ N/mm}^2$$

$$\sigma_{y,d} \leq f_{m,d} = 0.9 \cdot \frac{24.0}{1.25} = 17.28 \text{ N/mm}^2$$

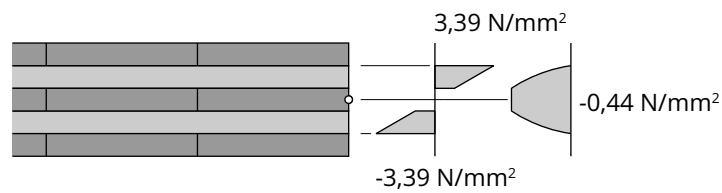
$$3.39 \text{ N/mm}^2 \leq 17.28 \text{ N/mm}^2$$

✓ Verification fulfilled ($\eta = 20\%$)

Bending and shearing stresses in the x-direction



Bending and shearing stresses in the y-direction



8 Erratum and amendments to Volume 1

8.1 Erratum

8.1.1 Design value of action (load-bearing capacity)

Formula (3.1)* is correctly

$$E_d = \sum \gamma_G \cdot E_{G,i,k} + \gamma_Q \cdot E_{Q,1,k} + \sum \psi_0 \cdot \gamma_Q \cdot E_{Q,i,k} \quad (3.1)^*$$

8.1.2 Withdrawal of screws

The screw pairs in Figures 9-13* and 9-14* should have a distance from one another of $2.5 \cdot d$.

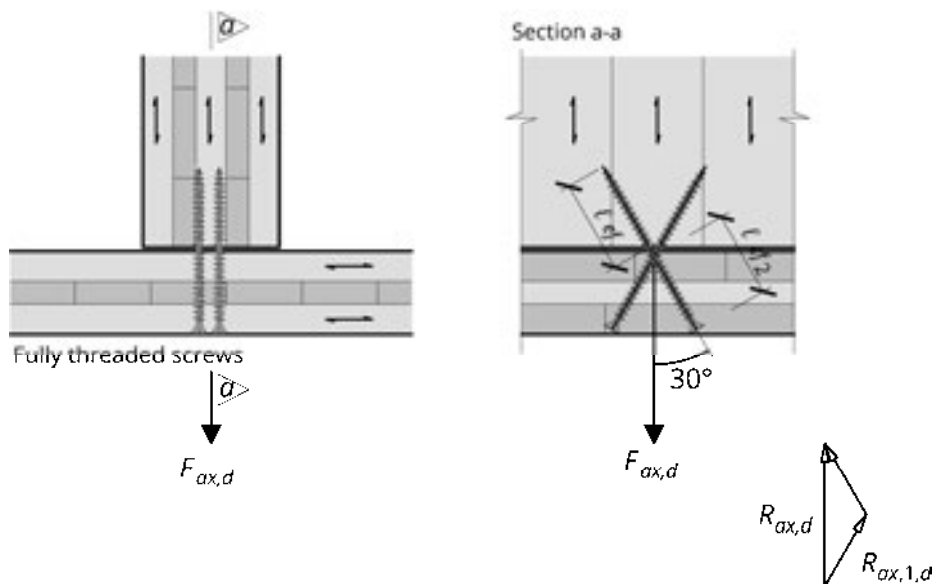


Figure 9-13* Suspension using fully threaded screws inclined in the wall plane

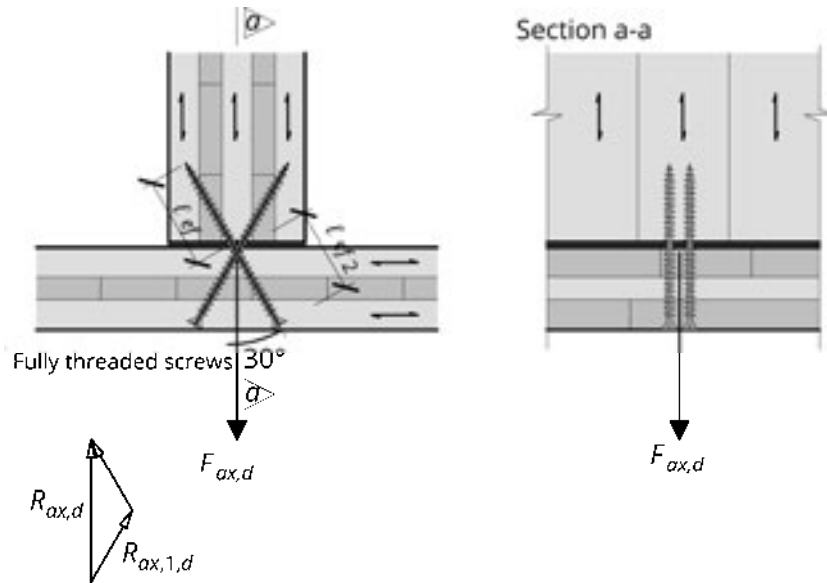


Figure 9-14* Suspension using fully threaded screws inclined out of the wall plane

8.1.3 Horizontal acceleration earthquake

The formulas (10.4)* and (10.5)* are correctly

$$a_{hor} = \frac{S_e(T)}{q} \quad (10.4)^*$$

$$a_{hor} = 2.5 \cdot a_g \cdot \frac{S}{q} \quad (10.5)^*$$

8.1.4 General gamma method according to Schelling

The coefficient matrix on page 153 is correctly

Coefficient matrix
[V]

	1	2	3	4
1	$\left[C_{1,2} + \frac{\pi^2 EA_1}{\ell^2} \right] \cdot a_1$	$- C_{1,2} \cdot a_2$	0	0
2	$- C_{1,2} \cdot a_1$	$\left[C_{1,2} + C_{2,3} + \frac{\pi^2 EA_2}{\ell^2} \right] \cdot a_2$	$- C_{2,3} \cdot a_3$	0
3	0	$- C_{2,3} \cdot a_2$	$\left[C_{2,3} + C_{3,4} + \frac{\pi^2 EA_3}{\ell^2} \right] \cdot a_3$	$- C_{3,4} \cdot a_4$
4	0	0	$- C_{3,4} \cdot a_3$	$\left[C_{3,4} + \frac{\pi^2 EA_4}{\ell^2} \right] \cdot a_4$

8.2 Standard adjustments and new findings

8.2.1 Minimum distances of self-tapping woodscrews

Table 9-8* shall be adapted to the determinations in ÖNORM B 1995-1-1:2015.

Table 9-8*

		Load in the	Load at angle α to the	Load transverse to the
		direction of fibre of the top layer		
Distance	in the direction of fibre of the top layer	a_1		$4 d$
	at right angles to the direction of fibre of the top layer	a_2		$2.5 d$
Edge distance	stressed edge of the top layer	$a_{3,t}$		$6 d$
	unstressed edge of the top layer	$a_{3,c}$		$6 d$
	stressed edge of the transverse layer	$a_{4,t}$		$6 d$
	unstressed edge of the transverse layer	$a_{4,c}$		$2.5 d$

Tests show that the reduction of several consecutive fasteners in the direction of fibre to a number effective in calculations n_{ef} in cross-laminated timber is not required due to the crack-limiting effect of the cross layers.

8.2.2 Verification of vibration

In the latest version of ÖNORM B 1995-1-1:2015, the verification of vibration was adjusted to a lesser extent following publication of Volume 1. The changes are documented in this volume (see Section 4.1).

8.2.3 Fire dimensioning

The charring rates determined in Section 7.2 of Volume 1 with increased charring for PUR-glued internal layers were confirmed according to Klippel, 2016.

8.2.4 Lateral pressure

Pressing transverse to the panel plane is regulated in ÖNORM B 1991-1-1 with deviating $k_{c,90}$ values and the actual pressing area is used as the effective contact area.

Beside the current scientific discussion on the subject of lateral pressure, the verification of lateral pressure is described according to the current status of standards in this volume. In addition to that, Section 9.2 discusses the calculative determination of the deformations of CLT panels under compression perpendicular to grain.

8.2.5 Load distribution at the panel strip

The assumptions on load distribution stated in Section 11.2.3 of Volume 1 did not yet consider the load-bearing effect of panels. For determination of the internal forces, effective widths can be applied, as they are described in Section 4.5.2 in the present volume.

8.2.6 Local load application into walls

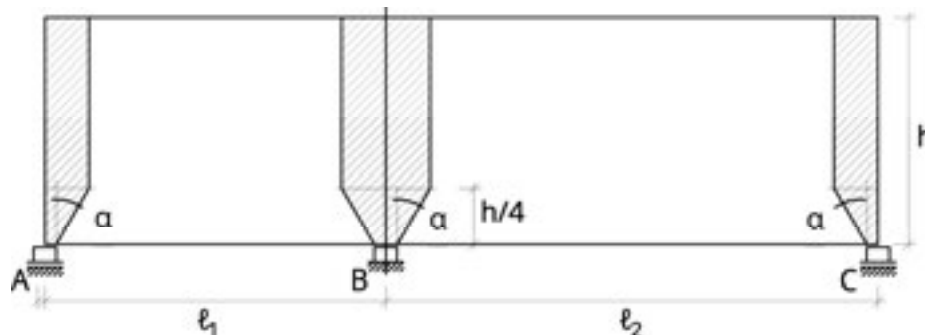


Figure 8.1 Load propagation in diaphragms according to Volume 1

The described model for load propagation in walls was adapted with results from theoretical examinations. It was confirmed within the limits described in Section 6.2 in the present volume.

9 In-depth considerations

9.1 Determination of the shear correction coefficient

As stated in Volume 1, the two calculation methods – the extended gamma method according to Schelling and the calculation as a shear-flexible beam according to Timoshenko – result in equivalent results, when slenderness conditions are present in construction practice and the loads are distributed in a relatively uniform fashion.

For floors, which continuously run alternatingly across long and short spans, with short cantilevers or concentrated loads, the shear-flexible beam results in more realistic results, since the results according to the gamma method with compact cross-sections lie strongly on the safe side.

For modelling as a two-dimensional structure, the model according to Reissner-Mindlin or a general grillage of members with shear and torsional flexibility shall be applied. For that, knowledge of the shear correction factor is required, in order to be able to correctly consider the shear deformation portions.

The application of the shear-flexible beam was compiled by Jöbstl for CLT elements of board layers with constant thickness and generally described in Schickhofer et al., 2010. In the annex of Volume 1, the analytical calculation was edited for a tabular calculation.

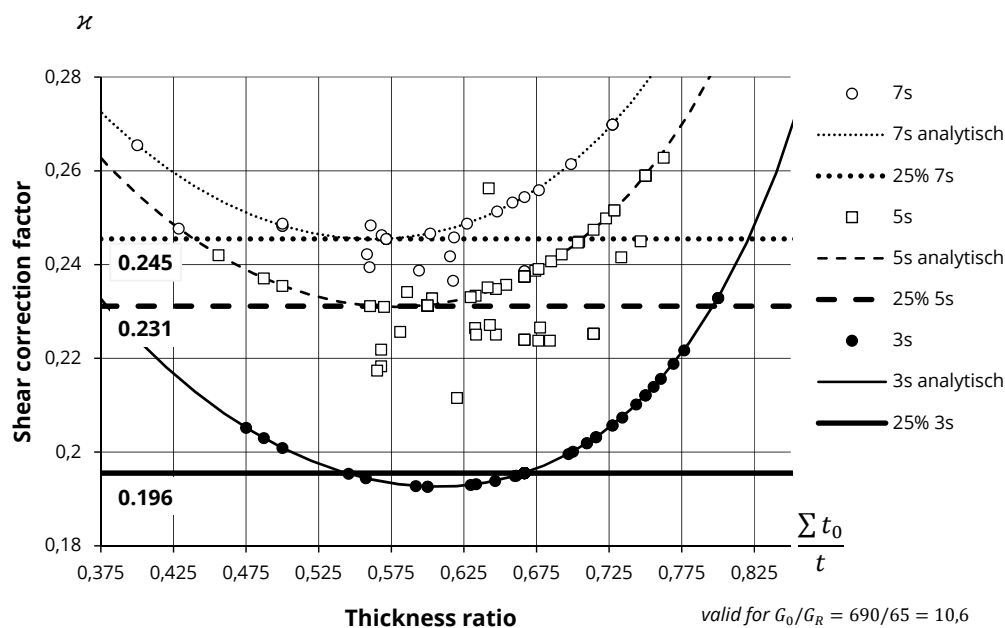


Figure 9.1 Shear correction factors for common CLT elements with 25 % quantiles

In Figure 9.1, the shear correction coefficients for common CLT layups were determined with the characteristic building material values stated in Section 3.1 and represented depending on the ratio of the sum of the longitudinal layer thicknesses ($\sum t_0$) to the overall thickness (t). For three, five and seven layers, that 25 % quantile value was

respectively determined, which is undercut by a quarter of the elements only. The shear correction coefficients thus determined are slightly below the shear correction coefficients of Jöbstl and consequently, being on the safe side, result in slightly larger deformations from shear.

For manual approximate dimensioning or control calculations, using the values from Table 9-1 is recommended. Normally, the shear correction coefficients can be retrieved from the product documents of the individual manufacturers.

Table 9-1 Standard values of the shear correction coefficients for CLT

	1 layer	3 layers	5 layers	7 layers	9 layers
Shear correction coefficient (25 % quantiles)	0.833	0.196	0.231	0.245	0.250

Example 9.1 Tabular calculation of the shear correction coefficient

The shear correction coefficient for a floor made of a CLT panel 150 5s (30l-30w-30l-30w-30l) is to be determined. To the characteristic building material properties apply the determinations according to Section 3.1.

Subsequently, the deflection w_{inst} for the floor uniaxially stressed across a span of $\ell = 4$ m is to be determined with a uniformly distributed load of $q_k = 5$ kN/m².

Tabular calculation

Calculation of the extensional stiffness EA and the position of the centre of gravity z_s

Layer	d [mm]	Orientation [°]	E [N/mm ²]	G [N/mm ²]	z_0 [mm]	EA [N]	$EA \cdot z_0$ [Nmm]
1	30	0	11,550	690	15	$3.465 \cdot 10^8$	$5.198 \cdot 10^9$
2	30	90	0	65	45	0	0
3	30	0	11,550	690	75	$3.465 \cdot 10^8$	$2.599 \cdot 10^{10}$
4	30	90	0	65	105	0	0
5	30	0	11,550	690	135	$3.465 \cdot 10^8$	$4.678 \cdot 10^{10}$
Σ	150					$1.040 \cdot 10^9$	$7.796 \cdot 10^{10}$

The position of the centre of gravity results from

$$z_s = \frac{EA \cdot z_0}{EA} = \frac{7.796 \cdot 10^{10}}{1.040 \cdot 10^9} = 75 \text{ mm}$$

Calculation of the bending stiffness EI and the shear stiffness GA

<i>Layer</i>	<i>d</i>	<i>Orient.</i>	<i>z</i>	<i>EI_{intrinsic}</i>	<i>EA e²</i>	<i>G · A</i>
	[mm]	[°]	[mm]	[Nmm ²]	[Nmm ²]	[N]
1	30	0	-60	$2.599 \cdot 10^{10}$	$1.247 \cdot 10^{12}$	$2.070 \cdot 10^7$
2	30	90	-30	0	0	$1.950 \cdot 10^6$
3	30	0	0	$2.599 \cdot 10^{10}$	0	$2.070 \cdot 10^7$
4	30	90	30	$0.000 \cdot 10^{00}$	0	$1.950 \cdot 10^6$
5	30	0	60	$2.599 \cdot 10^{10}$	$1.247 \cdot 10^{12}$	$2.070 \cdot 10^7$
	150			$7.796 \cdot 10^{10}$	$2.495 \cdot 10^{12}$	$6.600 \cdot 10^7$
				$2.573 \cdot 10^{12}$		

The bending stiffness and the shear stiffness, without consideration of the shear correction factor, result in:

$$EI_y = 2.573 \cdot 10^{12} \text{ Nmm}^2 = 2.573 \text{ kNm}^2 = 2.573 \text{ MNm}^2$$

$$GA = 6.6 \cdot 10^7 \text{ N} = 66000 \text{ kN} = 66 \text{ MN}$$

Calculation of the shear correction coefficient

Layer <i>i</i>	<i>d</i>		<i>E</i>	<i>z</i>	$[E \cdot S]_{z_{k,o}}^{z_{k,u}}$	$\sum_{k=1}^{i-1} [E \cdot S]_{z_{k,o}}^{z_{k,u}}$	$\int_{z_{i,o}}^{z_{i,u}} [E \cdot S]^2$	$\frac{\int [E \cdot S]^2}{G \cdot b}$
	[mm]	[°]	[N/mm ²]	[mm]				
	<i>a</i>	<i>b</i>	<i>c</i>	<i>d</i>	<i>e</i>	<i>f</i>	<i>g</i>	<i>h</i>
1	30	0	11,550	-75	$-2.079 \cdot 10^{10}$	$-2.079 \cdot 10^{10}$	$4.8895 \cdot 10^{21}$	$7.0863 \cdot 10^{15}$
				-45				
2	30	90	0	-15	0	$-2.079 \cdot 10^{10}$	$1.2967 \cdot 10^{22}$	$1.9949 \cdot 10^{17}$
3 top	30	0	11,550	0	$-1.299 \cdot 10^9$	$-2.2089 \cdot 10^{10}$	$7.0371 \cdot 10^{21}$	$1.0199 \cdot 10^{16}$
3' bottom				0	$-1.299 \cdot 10^9$	$-2.2089 \cdot 10^{10}$	$-7.0371 \cdot 10^{21}$	$-1.0199 \cdot 10^{16}$
4	30	90	0	15	0	$-2.079 \cdot 10^{10}$	$-1.2967 \cdot 10^{22}$	$-1.9949 \cdot 10^{17}$
				45				
5	30	0	11,550	75	$-2.079 \cdot 10^{10}$	$-2.079 \cdot 10^{10}$	$-4.8895 \cdot 10^{21}$	$-7.0863 \cdot 10^{15}$
Σ	150						Σ per half	$4.335 \cdot 10^{17}$

In that, the values of column *e* are calculated from:

$$[E \cdot S]_{z_{k,o}}^{z_{k,u}} = E_k \cdot b \cdot \left(\frac{z_{k,u}^2}{2} - \frac{z_{k,o}^2}{2} \right)$$

e.g. with values for cell *e* / 1

$$[E \cdot S]_{z_{k,o}}^{z_{k,u}} = E_k \cdot b \cdot \left(\frac{z_{k,u}^2}{2} - \frac{z_{k,o}^2}{2} \right) = 11550 \cdot 1000 \cdot \left(\frac{-45^2}{2} - \frac{-75^2}{2} \right) = -2.0790 \cdot 10^{10}$$

The values of column f are obtained by summation of the lines of column e from the upper or the lower, resp., cross-sectional edge up to the centre of gravity.

The values of column g are respectively obtained by evaluation of the polynomial

$$\int_{z_{i,0}}^{z_{i,u}} [E \cdot S]^2 = \frac{b^2 \cdot E_i^2}{60} (3 z_{i,u}^5 - 10 z_{i,0}^2 z_{i,u}^3 + 15 z_{i,0}^4 z_{i,u} - 8 z_{i,0}^5) +$$

$$+ \sum_{k=1}^{i-1} [E \cdot S]_{z_{k,0}}^{z_{k,u}} \cdot \frac{b \cdot E_i}{60} (20 z_{i,u}^3 - 60 z_{i,0}^2 z_{i,u} + 40 z_{i,0}^3) + \left\{ \sum_{k=1}^{i-1} [E \cdot S]_{z_{k,0}}^{z_{k,u}} \right\}^2 (z_{i,u} - z_{i,0})$$

For example, with values for cell $g / 3$ above, the following is obtained as an interim result:

$$\int_{z_{i,0}}^{z_{i,u}} [E \cdot S]^2 = \frac{1000^2 \cdot 11550^2}{60} (3 \cdot 0^5 - 10 \cdot (-15)^2 \cdot 0^3 + 15 \cdot (-15)^4 \cdot 0 - 8 \cdot (-15)^5) - 2.0790 \cdot 10^{10}$$

$$\cdot \frac{1000 \cdot 11550}{60} (20 \cdot 0^3 - 60 \cdot (-15)^2 \cdot 0 + 40 \cdot (-15)^3) + \{-2.0790 \cdot 10^{10}\}^2 (0 - (-15))$$

$$= 1.3507 \cdot 10^{19} + 5.4028 \cdot 10^{20} + 6.4834 \cdot 10^{21} = 7.0371 \cdot 10^{21}$$

$$\int_{z_{i,0}}^{z_{i,u}} [E \cdot S]^2 = 7.0371 \cdot 10^{21}$$

Ultimately, the values of column h are obtained by division of the values of column g by $G_i \cdot b_i$. The integral $\frac{\int [E \cdot S]^2}{G \cdot b}$ is determined by summation of column h from the two sides of the cross-section up to the centre of gravity. Using the shear and bending stiffnesses already determined further above, the shear correction coefficient can be calculated therefrom:

$$\varkappa_z = \frac{GA}{EI_{y,net}^2} \cdot \frac{\int [E \cdot S]^2}{G \cdot b} = \frac{6.6 \cdot 10^7}{(2.573 \cdot 10^{12})^2} \cdot 4.335 \cdot 10^{17} = 4.322$$

and the shear correction factor

$$\varkappa_z = \frac{1}{\varkappa_z} = \frac{1}{4.322} = 0.231$$

determined.

According to Table 9-1, an identical value of $\varkappa = 0.231$ results as an estimate of the shear correction factor for the five-layer panel.

The effective shear stiffness GA_s of the cross-section thus results in:

$$GA_s = \varkappa \cdot GA = 0.231 \cdot \frac{6.6 \cdot 10^7}{1000} = 152\,658 \text{ kN}$$

The deformation for the single-span beam under a uniformly distributed load results in

$$w = \frac{5 q \ell^4}{384 EI} + \frac{q \ell^2}{GA_s} = \frac{5 \cdot 5 \cdot 4^4}{384 \cdot 2573} \cdot 1000 + \frac{5 \cdot 4^2}{152658} \cdot 1000 = 6.48 + 0.524 = 7.0 \text{ mm}$$

The portion of shear deformation in the overall deformation is in this case around 7.5 %.

9.2 Deformation with local loads

In Section 4.5 local load applications are discussed. For completion purposes, in this section, the deformation determination is derived with the approach of linear load propagation.

9.2.1 Compression upon general stress distributions

For the stress distribution from concentrated loads, it is assumed that the contact area is square and the stresses propagate uniformly in both directions of the CLT panel at an angle of 35° . For lateral pressure stresses at the elastic level, the value of 35° (inclination of the load propagation 1:0.7) results from a 2/3 portion for the longitudinal layers with 45° (inclination 1:1) and a 1/3 portion for the transverse layers with 15° (1:0.268).

One approach for the calculation of indentations of sills – i.e. rod-shaped structural elements – was derived by Pischl, 2007. According to Van der Put, 2008, the actual stress distribution is more complex and does not allow for simple integration. The assumption of a linear increase in stresses, however, represents a good approximation. The shape of the stress propagation is a square frustum of height t with the side length c_1 at the load application point and the side length c_2 at the base, as shown in Figure 9.2. The point load $F_{c,90,k}$ acts in each horizontal section uniformly distributed onto the sectional area.

The shape of the stress-effective volumes depends on the load situation. In case of force passages, it is two symmetrical frustums of height $t = d/2$ with their base in the central plane of the panel of thickness d . In case of force applications without bottom support, the depth of the stress-effective volume shall be assumed with $0.4 \cdot t$.

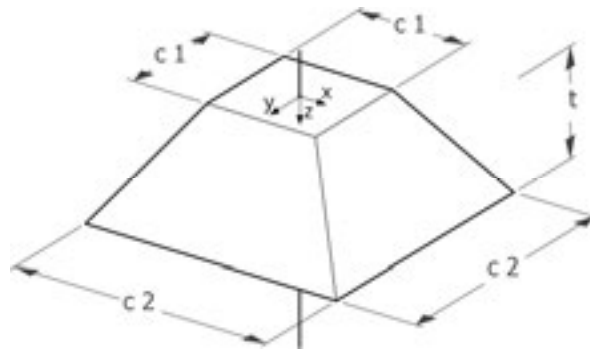


Figure 9.2 Stress-effective volume with a square contact area and equal propagation in both directions

For the square frustum as the stress-effective volume results:

Square frustum

Equation for the side length depending on coordinate z.

$$c(z) = c_1 - \frac{(c_1 - c_2) \cdot z}{t} \tag{9.1}$$

The deformation is obtained by integration of the frustum

$$w_{el} = \int_{z=0}^t \frac{F_{c,90,k}}{E_{90,mean} \cdot A(z)} dz = \int_{z=0}^t \frac{F_{c,90,k}}{E_{90,mean} \cdot c(z)^2} dz \tag{9.2}$$

$$w_{el} = \frac{F_{c,90,k} \cdot t}{E_{90,mean}} \cdot \frac{1}{c_1 \cdot c_2} \tag{9.3}$$

For the rectangular frustum as the stress-effective volume results:

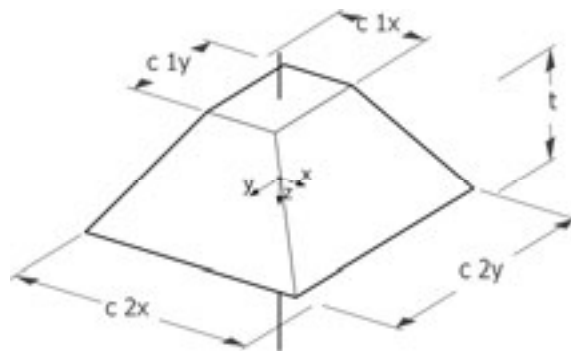


Figure 9.3 Stress-effective volume with rectangular contact area and unequal propagation in both directions

Rectangular frustum

Equation for the side lengths in x-direction and y-direction depending on coordinate z.

$$c_x(z) = c_{1x} - \frac{(c_{1x} - c_{2x}) \cdot z}{t} \tag{9.4}$$

$$c_y(z) = c_{1y} - \frac{(c_{1y} - c_{2y}) \cdot z}{t} \tag{9.5}$$

The deformation is obtained by integration of the frustum

$$w_{el} = \int_{z=0}^t \frac{F_{c,90,k}}{E_{90,mean} \cdot A(z)} dz = \int_{z=0}^t \frac{F_{c,90,k}}{E_{90,mean} \cdot c_x(z) \cdot c_y(z)} dz \tag{9.6}$$

$$w_{el} = \frac{F_{c,90,k} \cdot t}{E_{90,mean}} \cdot \frac{\ln\left(\frac{c_{1x} \cdot c_{2y}}{c_{2x} \cdot c_{1y}}\right)}{(c_{1x} \cdot c_{2y} - c_{2x} \cdot c_{1y})} \tag{9.7}$$

9.2.2 Deformation of panel due to load transfer column-panel-column

By applying the Formula 9.3 for supports in the panel's interior and in the corner or Formula 9.7 for supports at the edge, resp., the elastic compressions of the panel can be estimated.

Figure 9.4 shows the relation of panel thickness to compression strain for the force passage from a support above the CLT panel to a support below the panel with the cross-sectional dimensions of 14×14 cm each. As compressive stress in the contact area of the supports, $\sigma_{c,90,k} = 3$ N/mm² was assumed on both sides. This corresponds to a characteristic value of the superimposed load of $F_k = 58.8$ kN. The modulus of elasticity perpendicular to the grain was considered with $E_{90,mean} = 450$ N/mm².

Due to the better stress distribution, thicker floors show a lower compression strain related to their thickness. Even with thin floors, the calculated compression strain upon reaching the characteristic value of compressive strength is about 0.5 %.

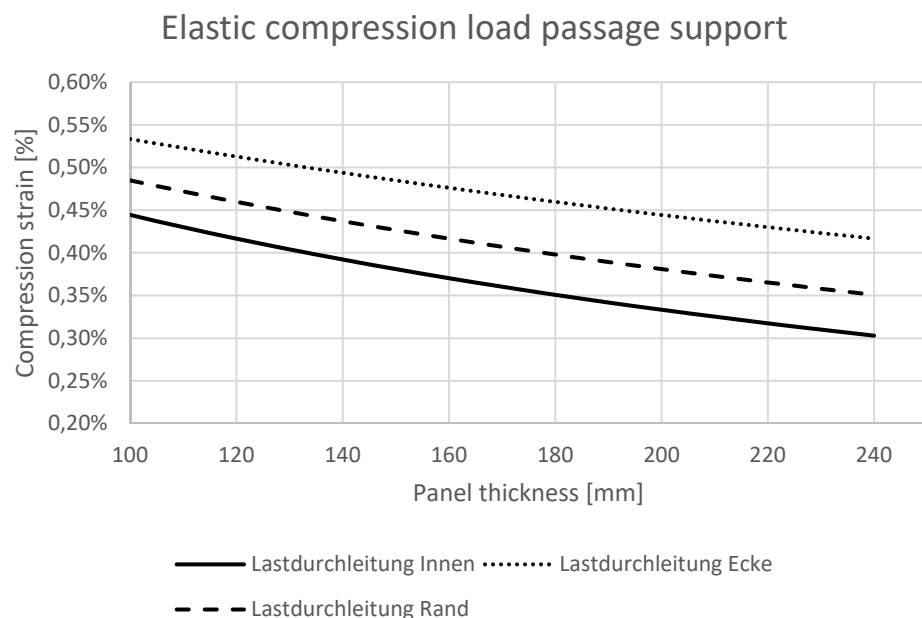


Figure 9.4 Compression strain of the CLT panel due to load transfer column-panel-column.

9.2.3 Deformation of panel due to load transfer wall-panel-wall

For linear loads, it shall be assumed that the load propagation is possible in one direction only. The body for the assumed stress distribution then corresponds to a prism, as shown in Figure 9.5.

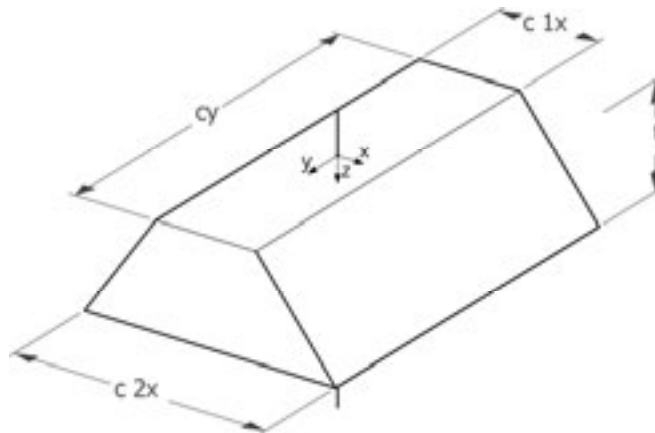


Figure 9.5 Stress distribution due to load transfer wall-panel-wall

Figure 9.6 shows the relation of panel thickness to compression strain for the force passage from a wall at the upper side of the panel to a wall at the lower side with the respective wall thickness of 14 cm. As compressive stress in the contact area of the wall, $\sigma_{c,90,k} = 3 \text{ N/mm}^2$ was assumed on both sides. This corresponds to a characteristic value of the superimposed load of $F_k = 420 \text{ kN/m}$. The of elasticity perpendicular to the grain was considered with $E_{90,mean} = 450 \text{ N/mm}^2$.

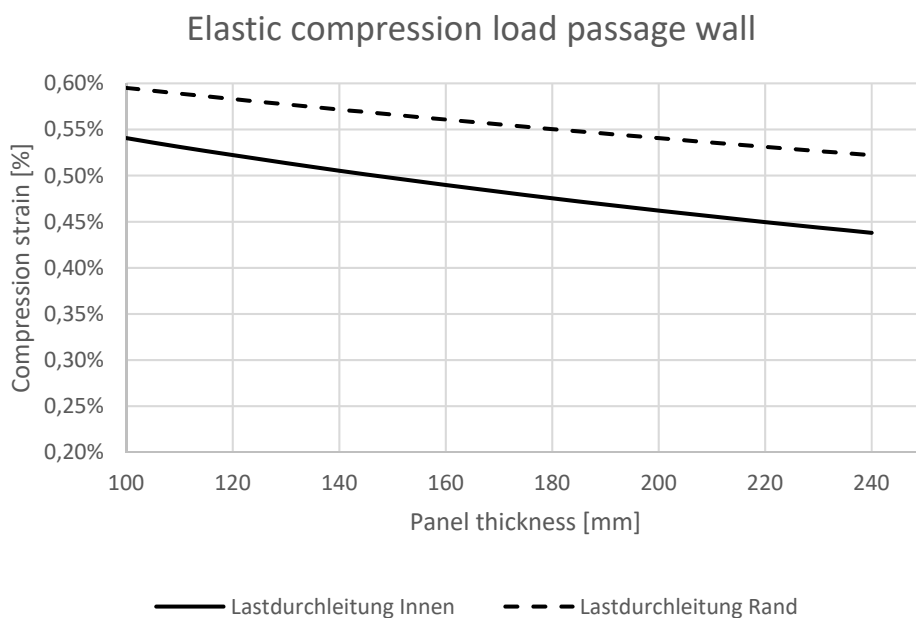


Figure 9.6 Compression strain of the CLT panel due to load transfer wall-panel-wall

9.3 Modelling as general grillage

Since the load-bearing performance of panels decisively depends on their torsional stiffness, the torsional stiffness shall also be correctly considered upon modelling the panel as a grillage of members. The classic grillage with rigid, but completely torsionally flexible members shall be expanded into a general grillage by considering the torsional stiffness and the shear stiffness of the members. For conversion of the panel's torsional stiffness of cross-laminated timber into the stiffnesses of individual member cross-sections of a grillage, the relations from Girkmann, 1968 and Bareš et al., 1968 can be used in the form of differential equations.

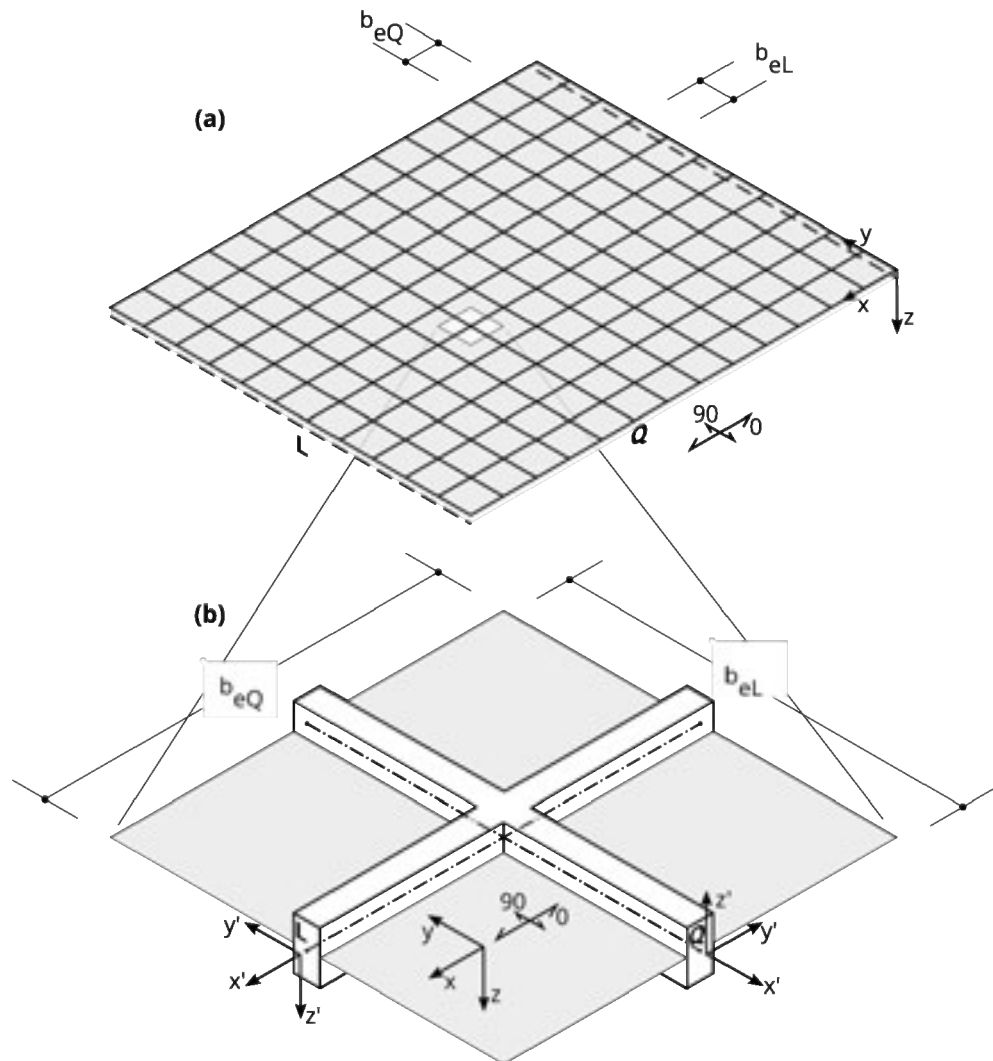


Figure 9.7 Cross-laminated timber plane (a) as grillage model (b) with longitudinal members (L) and transverse members (Q)

9.3.1 Comparison of differential equations

The load-bearing performance of orthotropic plates can be formulated by the differential equation of the bending area. If the cross-sectional stiffnesses of the individual beams in the grillage are related to the length unit, then the grillage turns into an equivalent orthotropic plate.

Bareš and Massonnet show in Bareš et al., 1968, that the differential equation has the following structure in both cases:

$$K_x \frac{\partial^4 w}{\partial x^4} + 2H \frac{\partial^4 w}{\partial x^2 \partial y^2} + K_y \frac{\partial^4 w}{\partial y^4} = p(x, y) \quad (9.8)$$

The difference between orthotropic panels and grillages lies in the determination of the stiffnesses, as compared to one another in Table 9-2. The associated dimensions can be retrieved from Figure 9.7.

Table 9-2 Stiffnesses for panel and grillage

		Orthotropic panels	Grillages
K_x	Bending stiffness in x-direction	$K_x = E I_{0,net}$	$K_x = E \frac{I_{yL}}{b_{eL}}$
K_y	Bending stiffness in y-direction	$K_y = E I_{90,net}$	$K_y = E \frac{I_{yQ}}{b_{eQ}}$
$2H$	Term for the torsional portions	$2H = (K_x \mu_y + K_y \mu_x) + 4C$	$2H = G \frac{I_{TL}}{b_{eL}} + G \frac{I_{TQ}}{b_{eQ}}$
	Torsional stiffness of the plate	$2C = 2K_{xy}$	

For panels of cross-laminated timber, the coefficients of transverse expansion μ are normally equated to zero, and from the terms for the torsional portions $2H$, the torsional moments of inertia of the members can be calculated from the panel stiffnesses K_{xy} according to the Formula (7.1).

$$I_{TL} = 2 b_{eL} \frac{K_{xy}}{G} \cdot \frac{2 b_{eQ}^2}{b_{eQ}^2 + b_{eL}^2} \quad (9.9)$$

$$I_{TQ} = 2 b_{eQ} \frac{K_{xy}}{G} \cdot \frac{2 b_{eL}^2}{b_{eQ}^2 + b_{eL}^2} \quad (9.10)$$

For square-meshed grillages (i.e. $b_e = b_{eL} = b_{eQ}$), the torsional moments of inertia are simplified to:

$$I_{TL} = 2 b_e \frac{K_{xy}}{G} = 2 b_e \cdot I_{xy} = 2 \cdot k_D \cdot \frac{b_e \cdot d^3}{12} \quad (9.11)$$

$$I_{TQ} = 2 b_e \frac{K_{xy}}{G} = 2 b_e \cdot I_{xy} = 2 \cdot k_D \cdot \frac{b_e \cdot d^3}{12} \quad (9.12)$$

with k_D according to Formula (7.2)

All remaining stiffnesses of the members can be obtained directly from the stiffnesses of the CLT panel by multiplying them with the distance associated with the respective

direction of the member. Normally, reference values are chosen for modulus of elasticity and shear modulus and associated cross-sectional values of the members stated.

For the cross-sectional areas consequently results:

$$A_{xL} = b_{eL} A_{0,net} \quad (9.13)$$

$$A_{xQ} = b_{eQ} A_{90,net} \quad (9.14)$$

The shear areas for the members L and Q not stated in the above differential equation can also be determined from the known panel stiffnesses and mapped via a shear-flexible member model:

$$A_{zL} = b_{eL} A_{z0,net} \quad (9.15)$$

$$A_{zQ} = b_{eQ} A_{z90,net} \quad (9.16)$$

In order to map the shear stiffness of the plate, the shear areas are respectively calculated in the local y-directions of the members L and Q:

$$A_{yL} = b_{eL} \frac{5}{6} A_{0,net} \quad (9.17)$$

$$A_{yQ} = b_{eQ} \frac{5}{6} A_{90,net} \quad (9.18)$$

The moments of inertia of the members L and Q for bending about the y-axes result in:

$$I_{yL} = b_{eL} I_{0,net} \quad (9.19)$$

$$I_{yQ} = b_{eQ} I_{90,net} \quad (9.20)$$

The moments of inertia for bending about the local z-axes, i.e. bending in the plate plane, are:

$$I_{zL} = \frac{b_{eL}^3 d_{0,net}}{12} = \frac{b_{eL}^3 A_{0,net}}{12} \quad (9.21)$$

$$I_{zQ} = \frac{b_{eQ}^3 d_{90,net}}{12} = \frac{b_{eQ}^3 A_{90,net}}{12} \quad (9.22)$$

Thus, all six cross-sectional values of the members are determined for the model as general spatial grillage.

9.3.2 Model for the calculation as a grid of members

With the stiffnesses stated above, the biaxial load-bearing effect of diaphragms as well as the load-bearing effect as a plate of two-dimensional structures can be mapped as a member model. For calculation, any software for spatial frameworks is required. Consideration of the shear flexibility of the members is desirable. The correct determination of the torsional stiffness, however, is more essential.

For the grid division – similar to the recommendations for the FEM method – a grid width of size $a = 15$ cm or a multiple thereof can be used as a smallest dimension. A comparison between a calculation using the FEM method and a general grillage showed

very good accordance, since the torsional stiffness was correctly mapped in the grillage, as shown in Figure 9.8 and Figure 9.9.

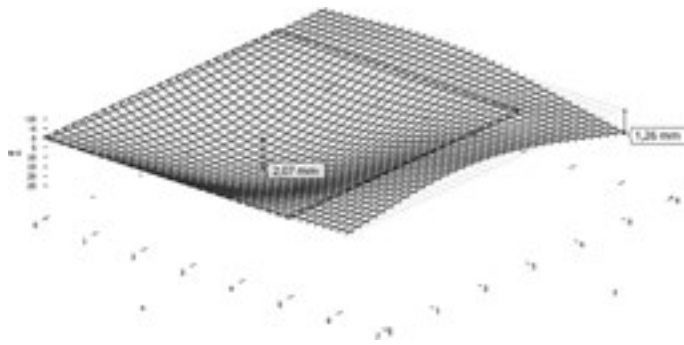


Figure 9.8 Deformed shape grillage calculation

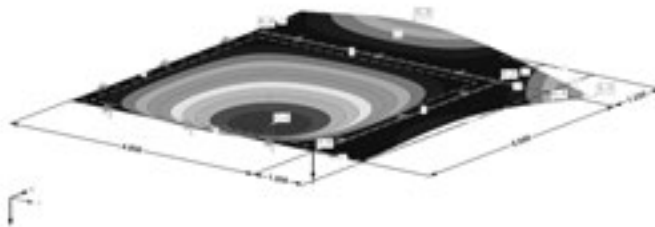


Figure 9.9 Result of the finite element calculation

9.3.3 Panels supported on three sides

The load-bearing performance of panels supported on three sides – as they occur, for example, with balconies – depends to a great extent on their torsional stiffness.

Initially considering a panel supported at two opposite edges – i.e. uniaxially stressed – under uniformly distributed load, the maximum deflection will occur along a line in the centre between the two supports. The two free edges deflect in a parabolic shape. By introducing a third support as a panel supported on three sides, this deflection is eliminated along the newly supported edge.

In that, with high torsional stiffness, the deformations as a whole decrease, since torsional moments are effective in load distribution. In case of relatively torsionally flexible panels, however, the flexural load-bearing effect dominates. By lifting the third edge, the originally horizontal line of the maximum deflections is lifted on one side and twisted. In that, the opposite edge is lowered and the deflection at the free edge of the torsionally flexible panel supported on three sides becomes higher than that of the panel supported on two sides.

A variation of the torsional stiffness, as shown in Figure 9.10, shows that cross-laminated timber normally lies in the torsionally flexible range. Thus, with panels over the same rectangular layout, the deflections with panels uniaxially stressed in the main direction of load-bearing capacity become lower than with support on three sides.

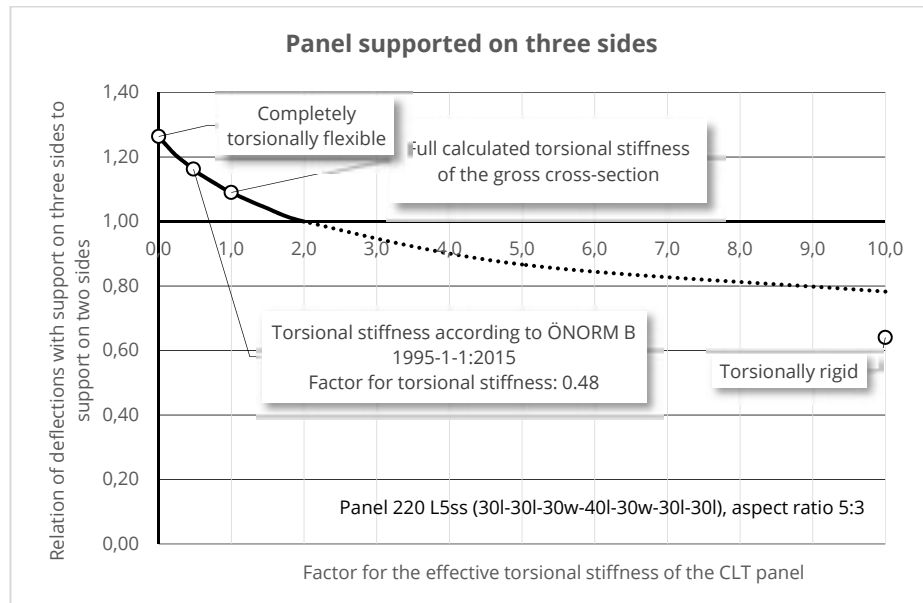


Figure 9.10 Influence of torsional stiffness on deflection

10 Sources

10.1 Standards

EN 1990:2013	Eurocode 0: Grundlagen der Tragwerksplanung (konsolidierte Fassung) Published: 2013-03-15
ÖNORM B 1995-1-1:2015	Eurocode 5: Bemessung und Konstruktion von Holzbauten - Teil 1-1: Allgemeines - Allgemeine Regeln und Regeln für den Hochbau - Nationale Festlegungen zur Umsetzung der ÖNORM EN 1995-1-1, nationale Erläuterungen und nationale Ergänzungen. Published: 2015-06-15
EN 1995-1-1:2015	Eurocode 5: Bemessung und Konstruktion von Holzbauten - Teil 1-1: Allgemeines - Allgemeine Regeln und Regeln für den Hochbau (konsolidie Fassung). Published: 2015-06-15

10.2 Literature

- Augustin et al., 4/2017 Augustin, Flatscher, Tripolt, Schickhofer: Messung der Vorkrümmungsamplituden von planmäßig mittig gedrückten BSP-Elementen zur Festlegung des Imperfektionsbeiwertes für den Knicknachweis, Bericht 03_2017 der holz.bau forschungs GmbH, Graz. Manuskript der Verfasser.
- Augustin et al., 3/2017 Augustin, Thiel: Proposal for the determination of the effective width and the verification of ribbed plates. Research report 02_2017 holz.bau forschungs GmbH, Graz. Manuskript der Verfasser.
- Bareš et al., 1968 Richard Bareš, C.E. Massonnet: Analysis of Beam Grids and Orthotropic Plates by the Guyon-Massonnet-Bareš Method. London: Lockwood, 1968.
- Blaß, 2004 Hans Joachim Blaß, Rainer Görlacher: Compression perpendicular to the grain
Proceedings of the 8th World Conference on Timber Engineering, Lahti, Finland. WCTE 2004. Vol. 2
- Bogensperger et al., 2014T. Bogensperger, M. Augustin: Lasteinleitung in Wandscheiben aus Brettsperrholz, Forschungsbericht der holz.bau forschungs GmbH, Technische Universität Graz. Eigenverlag: Graz, 2014
- Ciampitti, 2013 Alessandro Ciampitti: Untersuchung ausgewählter Einflussparameter auf die Querdruckkenngößen von Brettsperrholz, Masterarbeit, Institut für Holzbau, Institut für Holzbau und Holztechnologie, Graz, Technische Universität, 2013
- DAfStb, 1988 Deutscher Ausschuss für Stahlbeton DAfStb [Hrsg.]: Heft 240, Hilfsmittel zur Berechnung der Schnittgrößen und Formveränderungen von Stahlbetontragwerken nach DIN 1045, Ausgabe Juli 1988
- Girkmann, 1968 Karl Girkmann: Flächentragwerke: Einführung in die Elastostatik der Scheiben, Platten, Schalen und Faltwerke. 6. Auflage. Wien: Springer, 1968
- Halili, 2008 Ylli Halili: Versuchstechnische Ermittlung von Querdruckkenngößen für Brettsperrholz, Diplomarbeit, Institut für Holzbau, Institut für Holzbau und Holztechnologie, Graz, Technische Universität, 2008
- Jöbstl, 2007 Robert Jöbstl: Praxisgerechte Bemessung von Brettsperrholz. - in: Ingenieurholzbau Karlsruher Tage, Forschung für die Praxis. Karlsruhe am: 04.10.2007
- Klippel, 2016 Michael Klippel, Andrea Frangi: Brandverhalten von Brettsperrholz. In Bautechnik, Ausg. 93 von August 2016, Seiten 567-573. Berlin: Ernst und Sohn
- Leonhardt, 1973 F. Leonhardt, E. Mönning: Vorlesungen über Massivbau, Band 1. Springer: Berlin, Heidelberg, New York, 1973
- Leijten et al., 2012 Leijten, A. J. M., & Jorissen, A. J. M. (2012). The local bearing capacity perpendicular to grain of structural timber elements. Construction and Building Materials, 27(1), 54-59

- Mestek, 2011 Peter Mestek: Punktgestützte Flächentragwerke aus Brettsperrholz (BSP) – Schubbemessung unter Berücksichtigung von Schubverstärkungen, Dissertation TU, München, 2011
- Petersen, 1992 Christian Petersen: *Statik Und Stabilität Der Baukonstruktionen: Elasto- und plasto-statische Berechnungsverfahren druckbeanspruchter Tragwerke; Nachweisformen gegen Knicken, Kippen, Beulen*. Braunschweig [u.a.]: Vieweg, 1992.
- Pischl, 2007 Richard Pischl: Bemessung Im Holzbau: Zum Einfluss nachgiebiger Anschluss- und Stoßausbildungen auf Statik und Stabilität von Holztragwerken. Graz: proHolz Austria, 2007
- Polónyi, 1987 Polónyi, Stefan: mit zaghafter Konsequenz – Aufsätze und Vorträge zum Tragwerksentwurf, 1961-1987. Braunschweig: Fr. Vieweg, 1987.
- Pürgstaller, 2008 Andreas Pürgstaller: Tornadoshelters: an application for timber massive construction / of Andreas Pürgstaller. Graz, Technische Universität, Institut für Holzbau und Holztechnologie, Diplomarbeit, 2008
- Rombach, 2015 Rombach, Günter: Anwendung Der Finite-Elemente-Methode im Betonbau - Fehlerquellen und ihre Vermeidung. Berlin: Ernst, Wilhelm & Sohn, 2015
- Schickhofer et al., 2010 Gerhard Schickhofer, Thomas Bogensberger, Thomas Moosbrugger: BSPhandbuch, Holz Massivbauweise in Brettsperrholz: Nachweise auf Basis des neuen europäischen Normenkonzepts. Graz: Verlag der Technischen Universität Graz, 2010
- Silly, 2010 Gregor Silly: Numerische Studien zur Drill- und Schubsteifigkeit von Brettsperrholz (BSP). Graz, Technische Universität, Institut für Holzbau und Holztechnologie. Diplomarbeit, 2010
- Van der Put, 2008 T. A. C. M. van der Put: Derivation of the bearing strength perpendicular to the grain of locally loaded timber blocks. In Holz als Roh- und Werkstoff: European Journal of Wood and Wood Products, 66 (6). Springer, 2008
- Wallner-Novak et al., 2013 Markus Wallner-Novak, Josef Koppelhuber, Kurt Pock: Brettsperrholz Bemessung, Grundlagen für Statik und Konstruktion nach Eurocode. Wien: ProHolz Austria, 2013
- Winter, 2008 Stefan Winter: Holzbau der Zukunft: Teilprojekt 15. Stuttgart: Fraunhofer-IRB-Verlag, 2008

